

---

# **Optimal design of solar photovoltaic and concentrated solar power system for coal-fired power plants in NSW**

---

Mojtaba Jabbari Ghadi, Li Li, Jiangfeng Zhang

University of Technology Sydney

Project Number: RDE493-36

Final report

## ACKNOWLEDGEMENT

1. This project has been funded by the Department of Regional NSW through the Coal Innovation NSW Fund, which is administered by the Minister for Regional NSW, Industry and Trade.
2. Any views expressed herein do not necessarily reflect the views of Coal Innovation NSW, the Department of Regional NSW, the Minister for Regional NSW, Industry and Trade, or the NSW Government.
3. Some of the data used in this project are provided by Vales Point Power Station.
4. Particularly we would like to thank Dr James Knight (Coal Innovation NSW), Mr Thomas Gao (previously with Coal Innovation NSW, and now with Office of NSW Chief Scientist and Engineer), Mr Anthony Callen (Vales Point Power Station) and Mr Peter Loneragan (Research Office, UTS) for their kind help and support.

## EXECUTIVE SUMMARY

During recent years, the capability of concentrated solar thermal (CST) technology to use sunlight for heat generation has attracted significant attention from researchers and governments. CST technologies employ mirrors (also called heliostats) to focus a large area of sunlight into a focal location, producing high temperatures. This heat is captured using a molten salt (or oil) working fluid, to be used for heating water and generating steam to run a turbine and produce electricity, also referred to as concentrated solar power (CSP). Moreover, the captured heat can be stored in thermal energy storage tanks for up to 12 hours with little loss of energy. Then, electricity generated by the CSP system can be dispatched even during the night when there is no sunlight. There are more than 100 utility-scale CST plants operating worldwide, mostly in the US and Spain, however, large-scale CST is yet to be introduced in Australia.

On the other side, the Australian electricity generation system was founded on centralised, carbon-intensive coal-fired generation. About three-quarters of coal-fired power stations in Australia are operating beyond their original design life, and some have had extensive refits. It is expected that 14 GW of coal-fired power plants (CFPPs) will reach the end of their technical life and retire by 2040, while the electrical facilities of power plants are still useable if steam required for running turbines could be provided using renewable energies. Such an approach will help to reach the maximum exploitation of the current power stations after retirement, whilst, the integration of renewable energies into the coal power plants may reduce the current share of coal-burning to meet the existing load demand.

In this regard, this project aims at the coal consumption minimisation problem at CFPPs by the application of solar photovoltaic (PV), CSP, and energy storage systems. This project will optimally design the capacity and size of PV, CSP, and storage systems for the Vales Point CFPP so that this solar-coal hybridisation technology can reduce the coal consumption (by the CSP and PV) and use PV as the reserve system. Such renewable designs at CFPPs will assist NSW to optimise the electricity grid with a balanced energy portfolio in the near future. In the long run, these solar technologies could also help a traditional CFPP to be converted into a solar thermal power plant. In this final report, a comprehensive literature review

is presented to firstly investigate the current situation of power generation and emission from CFPP in Australia and NSW. Then, CSP applications, either sole operation or joint applications with different technologies of power generation, are analysed. The next section provides the detailed formulation on CSP systems (parabolic trough and central tower) as well as PV farm. Finally, three scenarios are presented for the joint operation of Vales Point CFPP with the proposed CSP and PV technologies. Detailed technical and financial parameters are considered in the planning procedure.

Based on the simulation results and also considering maturity and technical specifications of different technologies, parabolic solar power tower (SPT) and trough collector (PTC) are potential CSP technologies for the coupled operation with the trial CFPP in NSW. SAM software is utilised to calculate a realistic estimation of the capital cost as it can provide detailed and valid technical/financial models of renewable energies. Based on the obtained results, SPT technology can provide nearly 84% more energy than PTC, while its capital cost is around 20% higher than PTC. In the case of the joint operation with Vales Point Power Station, an emission reduction of 5% and 3% is expected for a 100 MW SPT and 100 MW PTC, respectively. Both technologies can provide steam temperature and pressure suitable for the integration with the Rankine cycle. While the PTC is appropriate for integrating into preheat water and entrance of the boiler, the capability of SPT to generate steam with the temperature around 550°C can deliver the opportunity of integration into high and intermediate pressure turbines. The optimal capacity for PV farm for the reserve market and internal use is 30 MW with a battery storage capacity of 6 MWh. Employing the CSP technology seems to be more suitable than the application of PV system in this case study because it may cut costs through utilisation of the existing CFPP turbine; however, the presence of an electrical battery system coupled with a PV unit can offer a very fast response in the case of sudden load changes, which can prevent continuous variations of generation level at CFPPs.

#### **INDEX TERMS**

Australian Energy Market, Solar thermal, Concentrated heat power, Photovoltaic, Thermal storage, Coal-fired power plant, System Advisor Model

## LAY SUMMARY

The Australian electricity generation system was founded on centralised, carbon-intensive coal-fired generation so that nearly one-third of the emission in Australia is produced in the electricity sector. Around one-third of coal-fired power plants (CFPPs) in Australia were closed during 2012–2017, and most of the remainder are exposed to closure over the coming decades. Present investments in generation capacity are primarily in the form of alternative clean powers, especially wind and solar. Since Australia has the highest average solar radiation per square meter among all the continents in the world, solar energy is a potential substitute for electricity generation while reducing emissions.

Concentrating solar thermal (CST) technology, also known as concentrated solar power (CSP), uses mirrors to concentrate a large area of sunlight into a targeted location, producing high temperatures. The high temperatures heat up a fluid known as the heat transfer fluid. Then, the heated fluid is pumped to another region to either produce steam from water that drives a turbine connected to a generator or to be stored in a thermal tank for utilisation during the night when there is no sunlight. Another superiority of CSP technology lies in its ability for the joint operation with CFPP, so that the steam produced by CSP can be fed into power blocks of the existing CFPP to reduce the current level of coal burning.

In this regard, the potential of parabolic trough collector (PTC) and solar power tower (SPT), as two mature technologies of CSP, for the coupled operation with a trial CFPP (Vales Point Power Station) in NSW is investigated in this project. Moreover, a photovoltaic (PV) system equipped with an electrical battery bank is designed as the reserve and for internal use of the power station. The simulation results show that SPT technology can provide nearly 84% more energy than PTC, while its capital cost is around 20% higher than PTC. In the case of the joint operation with the Vales Point Power Station, an emission reduction of 5% and 3% is expected for a 100 MW SPT and 100 MW PTC, respectively. The presence of an optimally designed 6 MWh electrical battery system coupled with a 30 MW PV unit can offer a very fast response in the case of sudden load changes, which can prevent continuous variations of the CFPP generation level.

## ABBREVIATIONS

ANSTO	Australian Nuclear Science Technology Organisation
ARENA	Australian Renewable Energy Agency
CAES	Compressed air energy storage
CCP	Coal combustion products
CCS	Carbon capture and storage
CER	Clean Energy Regulator
CFPP	Coal-fired power plant
CSIRO	The Commonwealth Scientific and Industrial Research Organisation
CSP	Concentrating solar power
DEE	Department of the Environment and Energy
DNI	Direct normal irradiation
ERF	Emissions Reduction Fund
EPA	Environment Protection Authority
HTF	Heat transfer fluid
LCOE	Levelised cost of energy
LFR	Linear Fresnel reflectors
METSTAT	Meteorological/statistical
NEM	National Electricity Market
NSRDB	National solar radiation database
PTC	Parabolic trough collector
RES	Renewable energy source
RET	Renewable Energy Target
SACPG	Solar-aided coal-fired power generation
SAPG	Solar-aided power generation
SEI	Stockholm Environment Institute
SPT	Solar power tower
SWIS	South-West Interconnected System
TES	Thermal energy storage
TMY	Typical meteorological year

## TABLE OF CONTENTS

<b>1 Introduction.....</b>	<b>16</b>
1.1 Electric power supply in Australia.....	16
1.2 Coal-fired power stations in Australia .....	16
1.2.1 Other states.....	18
1.3 Emissions from electricity generation.....	18
<b>2 Encouraging and applying policies for emission reduction in Australia .....</b>	<b>21</b>
2.1 Committing to the Paris agreement.....	21
2.2 Climate policy of the Australian government .....	21
<b>3 A literature review on concentrating solar power technology .....</b>	<b>23</b>
3.1 Solar parabolic-dish technology.....	26
3.2 Parabolic-trough collector.....	28
3.3 Central receiver/ solar power-tower.....	32
3.4 Linear Fresnel-reflector.....	35
<b>4 Overview of CSP developments .....</b>	<b>39</b>
4.1 CSP technology in different countries .....	39
4.2 Drivers and barriers for the deployment of CSP.....	47
4.3 CSP options for hybridisation with thermal power plants .....	48
<b>5 Overview of solar photovoltaic development in different countries.....</b>	<b>50</b>
5.1 Photovoltaic technology in different countries .....	50
5.2 Hybrid PV based power plants.....	53
<b>6 CSP hybrid options, data preparation .....</b>	<b>56</b>
6.1 Solar aided CFPP .....	56
6.1.1 Optimal integration point .....	56
6.1.2 Small and medium scale hybrid power plants.....	57
6.1.3 Large-scale power plant hybridisation .....	58
6.2 Typical meteorological year.....	59

6.3 CFPP configuration.....	61
<b>7 Formulation and mathematical modeling of CSP based power plants .....</b>	<b>63</b>
7.1 CSP system formulation.....	64
7.1.1 Objective function.....	64
7.1.2 Constraints .....	66
7.2 PV system formulation.....	68
7.2.1 Objective function.....	68
7.2.2 Constraints .....	69
7.3 Whole system formulation.....	71
7.3.1 Constraints .....	71
<b>8 Simulation and results .....</b>	<b>72</b>
8.1 Scenario 1: Parabolic trough CSP.....	78
8.1.1 Specifications of the solar field.....	78
8.1.2 Specifications of collector.....	79
8.1.3 Specifications of receiver.....	80
8.1.4 Power cycle specifications .....	80
8.1.5 Storage system specifications .....	82
8.1.6 System costs.....	82
8.1.7 Multi-objective analysis.....	82
8.1.8 Results.....	84
8.2 Scenario 2: Power tower CSP-molten salt .....	85
8.2.1 Design point parameters.....	86
8.2.2 Heliostat field.....	86
8.2.3 Tower and receiver.....	87
8.2.4 Power cycle specifications .....	87
8.2.5 Storage system specifications .....	88
8.2.6 System costs.....	88



8.2.7 Multi-objective analysis.....	88
8.2.8 Results.....	90
8.3 Scenario 3: Photovoltaic integration.....	91
8.3.1 Module type.....	91
8.3.2 Inverter type.....	94
8.3.3 PV farm sizing.....	94
8.3.4 Battery system.....	96
8.3.5 Capital costs.....	96
8.3.6 Multi-objective analysis.....	97
8.3.7 Results.....	99
<b>9 Conclusions.....</b>	<b>101</b>
<b>References.....</b>	<b>105</b>
<b>Appendices.....</b>	<b>111</b>
<b>Sign off.....</b>	<b>112</b>

## LIST OF FIGURES

Fig. 1. Electricity generation for the year 2018, by fuel type, by states [GWh] [6] .....	18
Fig. 2. ACT greenhouse gas emissions profile, March 2019 [8] .....	19
Fig. 3. Aging profile and projections of power stations in Australia [7] .....	19
Fig. 4. Various concentrated solar power technologies along with their installed ratios [17] .....	24
Fig. 5. Concentrated solar power projects around the world [18].....	24
Fig. 6. Main sections of a concentrated solar power plant and their components [19].....	25
Fig. 7. A schematic of parabolic-dish concentrated solar power .....	27
Fig. 8. The schematic of a parabolic trough collector system [31].....	29
Fig. 9. A schematic of the solar power tower system [31].....	34
Fig. 10. A schematic of the linear Fresnel reflector system [43] .....	38
Fig. 11. Direct sun irradiation in Australia [65].....	44
Fig. 12. An illustration typical meteorological year modeling for a full year .....	59
Fig. 13. A detailed configuration of a coal-fired power plant (Vales Point power station).....	60
Fig. 14. Overview of a solar aided coal-fired power plant .....	61
Fig. 15. Hourly global irradiance recorded in the meteorological station .....	73
Fig. 16. Hourly beam irradiance recorded in the meteorological station.....	73
Fig. 17. Hourly diffuse irradiance recorded in the meteorological station .....	73
Fig. 18. Hourly wind speed recorded in the meteorological station .....	74
Fig. 19. Hourly dew point temperature recorded in the meteorological station .....	74
Fig. 20. Monthly irradiance recorded in the meteorological station.....	75
Fig. 21. Monthly heat map of dry-bulb temperature recorded in the meteorological station .....	75
Fig. 22. Monthly wind speed and wind direction recorded in the meteorological station.....	76
Fig. 23. Monthly profile of different irradiances recorded in the meteorological station.....	76
Fig. 24. Duration curve of different irradiances and wind speed in the meteorological station .....	77
Fig. 25. Bi-objective Pareto front solutions for levelised cost of energy and annual emission reduction (parabolic trough CSP) .....	83
Fig. 26. Bi-objective Pareto front solutions for levelised cost of energy and capital cost (parabolic trough CSP).....	84
Fig. 27. Bi-objective Pareto front solutions for capital cost and annual emission reduction (parabolic trough CSP) .....	84
Fig. 28. Bi-objective Pareto front solutions for levelised cost of energy and annual emission reduction (polar tower CSP) .....	89

Fig. 29. Bi-objective Pareto front solutions for levelised cost of energy and capital cost (polar tower CSP).....	90
Fig. 30. Bi-objective Pareto front solutions for total capital cost and annual emission reduction (polar tower CSP).....	90
Fig. 31. Battery connected to AC side of photovoltaic system.....	96
Fig. 32. Bi-objective Pareto front solutions for levelised cost of energy and annual emission reduction (photovoltaic).....	97
Fig. 33. Bi-objective Pareto front solutions for levelised cost of energy and capital cost (photovoltaic) .....	98
Fig. 34. Bi-objective Pareto front solutions for capital cost and annual emission reduction (photovoltaic) .....	98

## LIST OF TABLES

Table 1. Electricity generation mix in Australia, Oct 2018 [3].....	16
Table 2. Active CFPPs in New South Wales [4] .....	17
Table 3. Active CFPPs in Queensland [4] .....	17
Table 4. Active CFPPs in Victoria [4] .....	17
Table 5. Active CFPPs in Western Australia [4] .....	17
Table 6. Characteristics of concentrated solar power technologies [20-22] .....	25
Table 7. Technical characteristics of parabolic-dish concentrated solar power plants [31] .....	28
Table 8. Detailed characteristics of parabolic trough collector plants worldwide, except the USA and Spain – Part 1 [31] .....	30
Table 9. Detailed characteristics of parabolic trough collector plants worldwide, except the USA and Spain – Part 2 [31] .....	30
Table 10. Details of parabolic trough collector plants in Spain [31] .....	31
Table 11. Details of parabolic trough collector in the USA [31] .....	33
Table 12. Operational, under-construction and under-development solar power tower plants [31].....	36
Table 13. Linear Fresnel reflector plants [31]. .....	37
Table 14. Specifications of Australian concentrated solar power projects (Part 1) [67] .....	45
Table 15. Specifications of Australian concentrated solar power projects (Part 2) [67] .....	46
Table 16. Specifications of Australian concentrated solar power projects (Part 3) [67] .....	47
Table 17. Specifications of NSW Gosford Narara meteorological Research Center .....	72
Table 18. Average annual value of meteorological parameters.....	77
Table 19. Objective parameters for parabolic trough collector optimisation.....	78
Table 20. Specifications of solar field (parabolic trough collector) .....	79
Table 21. Specifications of selected heat transfer fluids (parabolic trough collector).....	79
Table 22. General specification of solar field (parabolic trough collector) .....	79
Table 23. Detailed technical characteristics of selected collector types (parabolic trough collector) ...	80
Table 24. Detailed technical characteristics of selected receiver types (Part 1) - (parabolic trough)....	81
Table 25. Detailed technical characteristics of selected receiver types (Part 2) – (parabolic trough) ...	81
Table 26. General specification of thermal storage (parabolic trough collector) .....	82
Table 27. Costs of system (parabolic trough collector) .....	82
Table 28. Possible range of operating for solar power tower .....	86
Table 29. Parameters of solar power tower design point.....	86
Table 30. Specifications of heliostats (solar power tower).....	87

Table 31. Detailed specification and parameters of tower and receiver (solar power tower).....	87
Table 32. General specification of thermal storage (solar power tower).....	88
Table 33. Costs of system (solar power tower).....	88
Table 34. Possible range of operating for photovoltaic farm.....	92
Table 35. Module specifications (Type 1) – Photovoltaic.....	92
Table 36. Module specifications (Type 2) – Photovoltaic.....	93
Table 37. Module specifications (Type 3) – Photovoltaic.....	93
Table 38. Inverter specifications (Type 1) – Photovoltaic.....	94
Table 39. Inverter specifications (Type 2) – Photovoltaic.....	95
Table 40. Inverter specifications (Type 3) – Photovoltaic.....	95
Table 41. Costs of PV system – Photovoltaic.....	97
Table 42. Comparison of scenarios.....	102
Table 43. Recommended joint PV-CSP practice.....	102

## PROJECT AIM, OBJECTIVES, MILESTONES AND PERFORMANCE MEASURES

This project aims at the coal consumption minimisation at CFPPs by the application of solar PV, CSP and energy storage systems. The provided optimal design determines technologies for Vales point CFPP to reduce the coal consumption (by the CSP and PV) and the spinning reserve cost (by PV). Besides, utilisation of these solar technologies will help traditional CFPPs to be converted into solar thermal power plants. Note that the generation units of Vales point CFPP are very big, two Toshiba 660 MW. These big units present a great challenge for them to be integrated with CSPs which are often less than 100 MW due to various technical and economic reasons.

It is also important to note that current power plants often have generators running on standby to deliver reserves for potential increase of power demand, and this is typically called spinning reserve. The relevant spinning reserve can be met, fully or partially, by the power from PV and/or the corresponding energy storage systems, and therefore, the coal consumption for spinning reserve can be significantly reduced if the PV and energy storage sizes are properly designed. Hence, this project investigates the optimal sizing problem for PV, CSP and the corresponding energy storages for the hybrid solar and coal-fired power plant by considering solar irradiance, investment, life cycle cost, payback period, power demand, generation capacity, and uncertainties of solar energy. An optimal trade-off between generation capacity, economic investment, life cycle cost, and carbon reduction is achieved.

ID	Task/Strategy	Timeframe		Performance Measure	Status
Task ID	Milestone	Start date	Completion date	Relevance to the project and achievement.	
M1	The state-of-the-art research progress on the applications of PV and CSP in coal-fired power plants and relevant policies investigation	01/01/2019 (Q1)	28/2/2019 (Q1)	A draft report on relevant research about the application of PV and CSP in coal-fired plants was prepared;	100%
	Collection of data from a trial NSW coal-fired power plant on system specifications and power generation;			Trial NSW coal-fired power plant was identified and visited for data collection purpose.	100%

M2	Collection and analysis of the other databases on PV, CSP and energy storage; a preliminary report preparation.	01/01/2019 (Q1)	31/3/2019 (Q1)	One report consisting of a review on the state-of-the-art research progress on the applications of PV and CSP in coal-fired power plants, the relevant policy, and system overview of a trial NSW coal-fired power plant was delivered;	100% (seminar cancelled)
				A conference paper was accepted entitled "A Review on the Development of Concentrated Solar Power and its Integration in Coal-Fired Power Plants" in an IEEE conference.	100%
M3	A system configuration study of a trial coal-fired power plant;	01/04/2019 (Q2)	31/5/2019 (Q2)	A draft report consisting of key system characteristics of the trial coal-fired plant was prepared;	100%
	Identification of possible choices of CSP design for the coal-fired power plant.			CSP available choices were prepared;	100%
M4	Identification of global optimal design objectives to include PV, CSP and energy storage at the power plant.	01/04/2019 (Q2)	30/6/2019 (Q2)	An interim report consisting of key system characteristics of the trial coal-fired power plant, available choices of CSP design; and the global optimal design objectives for PV, CS, and energy storage was delivered;	100%
				One public seminar on the above findings was delivered on 28 <sup>th</sup> of Jun 2019, at UTS.	100%
M5	Modelling the interactive system constraints at the power plant to assist the global optimal design.	01/05/2019 (Q2)	31/7/2019 (Q3)	Interactive system constraints, such as power generation requirement and PV, CSP, energy storage, and solar irradiance, were modelled. One conference was attended.	100%
M6	Completing the global optimal design model for PV, CSP and energy storage at the power plant by September 2019.	01/06/2019 (Q3)	30/9/2019 (Q3)	Interim results were communicated to the power plant and CINSW to seek feedback.	100% (seminar replaced by conference presentation)
M7	Solving and validating the optimal design model for PV, CSP and energy storage.	01/09/2019 (Q3)	31/10/2019 (Q4)	Computer simulation for the optimal design solution was completed and analysed. The studied coal-fired power plant in NSW provided with a list of investment solutions with the corresponding coal savings and emission reductions. The coal savings, and also emission reductions, was around 7% when the necessary amount of investment on PV and CSP systems was in place.	100%
M8	Calibrating the optimal design model for PV, CSP and energy storage following peer-review feedbacks; Final report is prepared.	01/11/2019 (Q4)	31/12/2019 (Q4)	A final project report was delivered to CINSW; One public seminar was delivered.	100%

## 1 INTRODUCTION

This section presents an outline of Australia’s energy markets and the influence of coal-fired power plants (CFPPs) to power provision, and then explores commitments of Australia in terms of the Paris Agreement and the impact that de-commitment of CFPPs can have in meeting these obligations.

### 1.1 Electric power supply in Australia

The two largest electric power markets in Australia include the Western Australia's South-West Interconnected System (SWIS) and National Electricity Market (NEM). Eastern and south-eastern coasts of Australia are covered by the NEM which includes the states of Australian Capital Territory, Victoria, New South Wales, Queensland, South Australia, and Tasmania, while the south-west part of Western Australia is covered by SWIS [1]. In total, about 94% of the electricity market is covered by the NEM (i.e., 86% of the market demand) and SWIS (8% of the market demand). Currently, up to 74% of electric power generation of NEM is provided by CFPPs (both black and brown coal, while coal made up 44% of the capacity of the NEM in 2018) which shows the dominance of this type of power plant. Table 1 details Australia's electricity generation mix based on data provided by the Australian Energy regulator [2].

TABLE 1. ELECTRICITY GENERATION MIX IN AUSTRALIA, OCT 2018 [3]

Fuel	Capacity (Percent of total generation)	Output (Percent of total generation)
Black coal	36.6	53.6
Brown coal	9.4	18.1
Gas	19.4	7.1
Hydro	16.4	10.7
Wind	10.7	8.9
Liquid	2.2	0
Solar	3.4	0.9
Battery	0.3	0
Other	1.7	0.5

### 1.2 Coal-fired power stations in Australia

Currently, there are 20 active CFPPs operating in Australia. A list of active CFPPs in Australia is shown in Table 2 to Table 5 [4]. However, some states of Australia including Tasmania, Northern Territory, Australian Capital Territory, and South Australia mostly rely on other types of energy generation [5].



TABLE 2. ACTIVE CFPPS IN NEW SOUTH WALES [4]

Power station	Commission Year	Max. Capacity (MW)	Turbines	Coal Type	Conveyance	Mine type	Cooling Water
Bayswater	1982	2,640	4	Bituminous	Conveyors, rail	Open cut	Fresh
Eraring	1982	2,880	4	Bituminous	Rail, truck	Underground	Salt
Liddell	1971	2,000	4	Bituminous	Conveyors, rail	Open cut	Fresh
Mt Piper	1993	1,400	2	Bituminous	Road, conveyor	Underground	Fresh
Vales Point B	1978	1,320	2	Bituminous	Conveyors	Underground	Salt

TABLE 3. ACTIVE CFPPS IN QUEENSLAND [4]

Power Station	Commission Year	Max. Capacity (MW)	Turbines	Coal Type	Conveyance	Mine Type	Cooling Water
Callide B	1989	700	2	Bituminous	Conveyor	Open cut	Fresh
Callide C	2001	810	2	Bituminous	Conveyor	Open cut	Fresh
Gladstone	1976	1,680	6	Bituminous	Rail	Open cut	Seawater
Kogan Creek	2007	750	1	Bituminous	Conveyor	Open cut	Dry cooled
Millmerran	2002	852	2	Bituminous	Conveyor	Open cut	Dry cooled
Stanwell	1993	1,445	4	Bituminous	Rail	Open cut	Fresh
Tarong	1984	1,400	4	Bituminous	Conveyor	Open cut	Fresh
Tarong North	2002	443	1	Bituminous	Conveyor	Open cut	Fresh

TABLE 4. ACTIVE CFPPS IN VICTORIA [4]

Power Station	Commission Year	Max. Capacity (MW)	Turbines	Coal Type	Conveyance	Mine Type	Cooling Water
Loy Yang A	1984	2,200	4	Lignite	Conveyors	Open cut	Fresh*
Loy Yang B	1993	1,050	2	Lignite	Conveyors	Open cut	Fresh*
Yallourn Power Station	1975	1,480	4	Lignite	Conveyors	Open cut	Fresh*

\* uses fresh cooling tower

TABLE 5. ACTIVE CFPPS IN WESTERN AUSTRALIA [4]

Power Station	Commission Year	Max. Capacity (MW)	Turbines	Coal Type	Conveyance	Mine Type	Cooling Water
Collie	1999	340	1	Bituminous	Conveyor	Open cut	Fresh
Muja	1981	854	4	Bituminous	Conveyor	Open cut	Fresh
Bluewaters	2009	416	2	Bituminous	Conveyor	Open cut	Fresh
Worsley Alumina	1982	107	4	Bituminous	Rail	Open cut	Fresh

### 1.2.1 Other states

- ✓ Hydroelectricity is the dominant power generation in Tasmania with natural gas as the backup while there is no functioning CFPP in this state.
- ✓ The Northern Territory primarily relies on natural gas and various renewable energy sources (RESs) as alternative options. Similarly, there are no functioning CFPPs in this state.
- ✓ Despite the governmental investment in the Australian Capital territory in RESs, this state is defined as a part of NSW in the NEM, and its consumption is calculated in the total electricity demand of NSW.
- ✓ There were a number of CFPPs in South Australia formerly; however, the last to be closed were the Playford B and Northern power plants.

Generation and load demand in different states of Australia are depicted in Fig. 1.

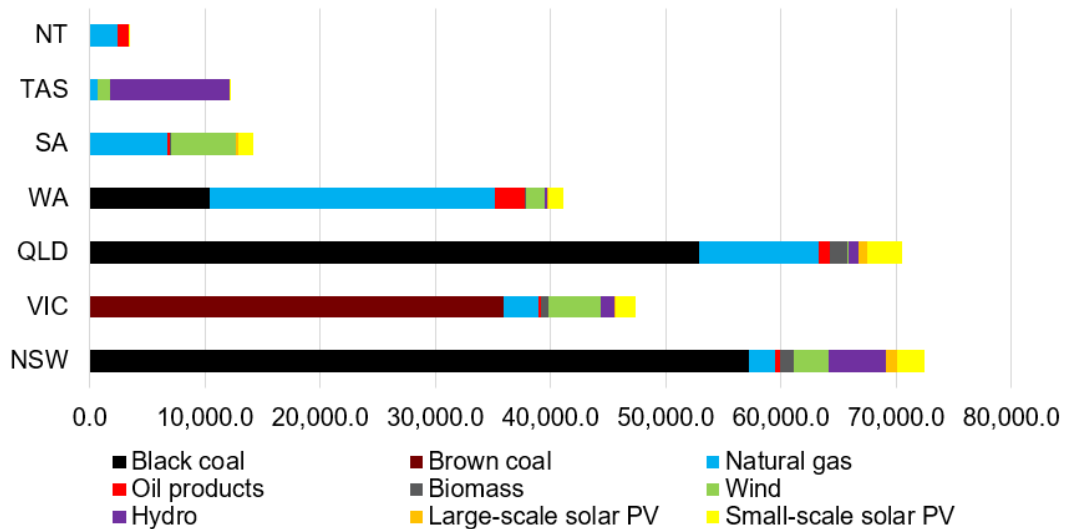
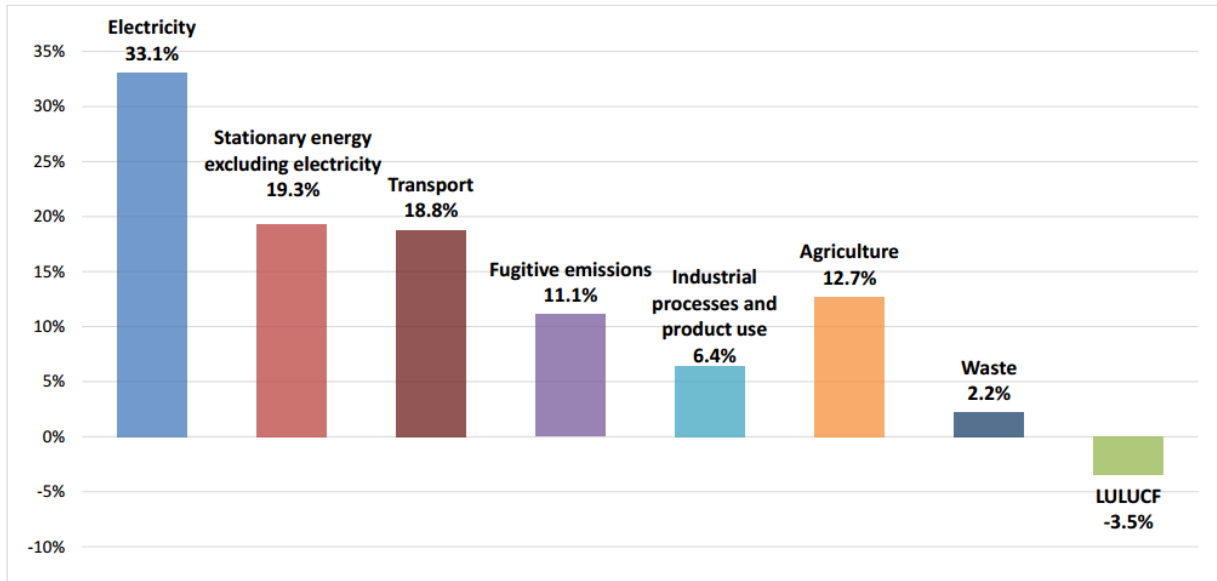


Fig. 1. Electricity generation for the year 2018, by fuel type, by states [GWh] [6]

### 1.3 Emissions from electricity generation

Based on the Clean Energy Council report, as it can be seen in Fig. 2, roughly a third of the emissions in Australia are contributed by the electricity sector, and it is highly likely for this trend to continue up to the year 2025. Australia's electricity market is a carbon-intensive CFPP based system, and this sector is the major contributor to the emission of greenhouse gases [7].



Source: Department of the Environment and Energy

Fig. 2. ACT greenhouse gas emissions profile, March 2019 [8]

Additionally, brown coal based CFPPs are the most emission-intensive type among different categories of power plants, followed by black coal and gas. The overall emissions of each fuel are a function of two factors: first, the share of the fuel from total generation and second, the emissions intensity of the fuel type. Approximately 66.5% of generation emissions in the NEM are produced by coal (i.e., 50% from black and 16.5% from brown coal). This situation is worse in the case of aging CFPPs, as shown Fig. 3 [9].

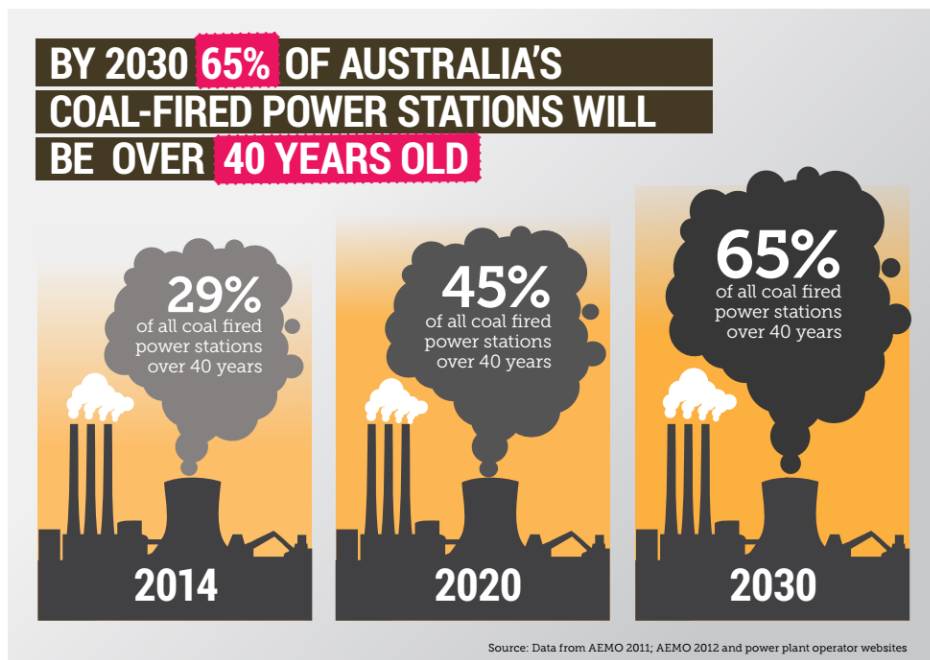


Fig. 3. Aging profile and projections of power stations in Australia [7]

As the Climate Council stated in its annual report, a major part of Australia's CFPPs are old and highly inefficient; therefore, they are very unlikely to be retrofitted with carbon capture and storage (CCS) technologies. Such a situation is happening when more than half of Australia's CFPPs will be over 40 years old within a decade and also a number of them will be operating when reaching 60 years old and still utilising subcritical coal technology [7]. In this regard, brown coal based CFPPs are at the top of the carbon dioxide emitters in Australia. However, black coal fed CFPPs in Queensland and NSW are polluting about 30-40% less than those in Victoria, based on Environment Victoria [10].

## **2 ENCOURAGING AND APPLYING POLICIES FOR EMISSION REDUCTION IN AUSTRALIA**

### **2.1 Committing to the Paris agreement**

Australia committed to the Paris Agreement on April 22, 2016, which is intended to reinforce the United Nations Framework Convention of Climate Change (UNFCCC). Countries which pursue the Paris Agreement agree to apply definite criteria to prevent negative impacts on climate changes [11], such as:

1. The rise of average global temperature must be maintained below 2 °C above preindustrial stages, knowing that this would considerably decrease the threats and influences of climate change.
2. Boosting the capability to adjust the negative impacts of climate change as well as to increase the resiliency of the climate to reach a lower emissions level of greenhouse gas, while not threatening food production.
3. Making finance flows consistent with the path to low greenhouse gas emissions and climate-resilient development.

On November 10, 2016, both the Doha Amendment to the Kyoto Protocol and Paris Agreement were ratified by the Australian Government, after the recommendation of the Joint Standing Committee. These agreements defined 2020 and 2030 targets for Australia towards emissions reduction [12]. To this end, signatory countries of the Paris Agreement have also planned for the de-commissioning of CFPPs to meet agreed climate goals. To date, the Netherlands, Denmark, Austria, Canada, France, and the United Kingdom have all started or completed the closure of CFPPs in their electric power markets.

### **2.2 Climate policy of the Australian government**

Towards commitments of the Paris Agreement, the Australian Government has targeted to reduce 26–28% emissions below 2005 levels by 2030. It has been stated by the Department of the Environment and Energy (DEE) that the adopted target represents a 50–52% decrease in emissions per capita, while it will also provide a 64–65% decline in the emissions intensity of the economy by 2030 in comparison to 2005 [13]. The DEE notes that this amount of decline, when considering an emission intensity basis and measured

per person, will surpass countries such as Canada, Korea, Japan, the European Union, and even the United States. However, it is still challenging for Australia to reach the target of keeping global warming below two degrees above preindustrial level. Moreover, the initial target of Australia for the reduction by 2030 is insufficient comparing with other economies.

The Australian Renewable Energy Target (RET) [14] policy aims to decrease greenhouse gas discharges from the electric power sector as well as to encourage further electricity generation from renewable and sustainable sources. RET includes two operating schemes as follows:

- The small RES Scheme, which is responsible for supporting small-scale RES (solar hot water systems and household solar panels) installations.
- The large RES Scheme, which is responsible for supporting the investment in large-scale RES power plants to reach an additional 33,000 GWh of RES generation by 2020.

The Australian Emissions Reduction Fund (ERF) aims to offer incentives for individuals and organisations to adopt new technologies and practices to decrease their emissions. A contributor must be registered with the ERF, establish a safe contract with the Australian Government through an auction, implement the project based on the chosen scheme, report the results back to ERF, and finally, they can gain Australian carbon credit units for the achieved reductions and sell them. This system (which is described as a safeguard mechanism) is employed by ERF as an exchange outline for CO<sub>2</sub> emissions.

### 3 A LITERATURE REVIEW ON CONCENTRATING SOLAR POWER TECHNOLOGY

Global electricity consumption is growing quickly because of urbanisation, industrialisation, and growth in population. As fossil fuel reserves are diminishing while the usage of fossil fuel continues to cause environmental and health problems, it is urgent but challenging for the world to provide sustainable and clean energy supply in mass levels. Currently, fossil fuels (e.g. natural gas, liquid petroleum, and coal), as the depleting energy sources, supply 80% of the major global energy, and are the main causes of greenhouse-gas emissions like CO<sub>2</sub>. It is estimated that utilisation of RES will reduce CO<sub>2</sub> emission by about 30% by 2050, compare to the emissions in 2012 [15]. Due to the characteristics of being low-cost and sustainable, solar energy is broadly known as a promising alternative among different types of renewable energy.

Within the solar technologies, concentrating solar power (CSP) technology has the capability of large-scale dispatchable power provision when it is equipped with thermal energy storage (TES) in hybrid operations [16]. Mirrors and lenses are used in CSP systems to concentrate a large area of sunlight onto a small area to absorb solar heat. Then, electricity is generated when produced heat drives a steam turbine coupled with an electric generator. Generally, there are several components in CSP plants including electrical generator, steam turbine, receiver, and concentrators.

Currently, four industrial types of CSP technology are available in the market based on receiver type: 1) linear Fresnel reflectors (LFR), 2) solar power tower (SPT), 3) parabolic trough collectors (PTC), and 4) solar parabolic dishes (SPD) [17]. An outline of CSP technologies and their corresponding installation ratios are shown in Fig. 4. It can be seen that PTC has the highest global establishment. CSP plants are also categorised into under development, under construction, and operational. The current instalment of CSP projects around the world is shown in Fig. 5 [18]. The CSP technologies employ concentrators to focus sunlight onto a receiving system, which transfers a heated high temperature working fluid into a conventional steam turbine to drive the turbine and generator.

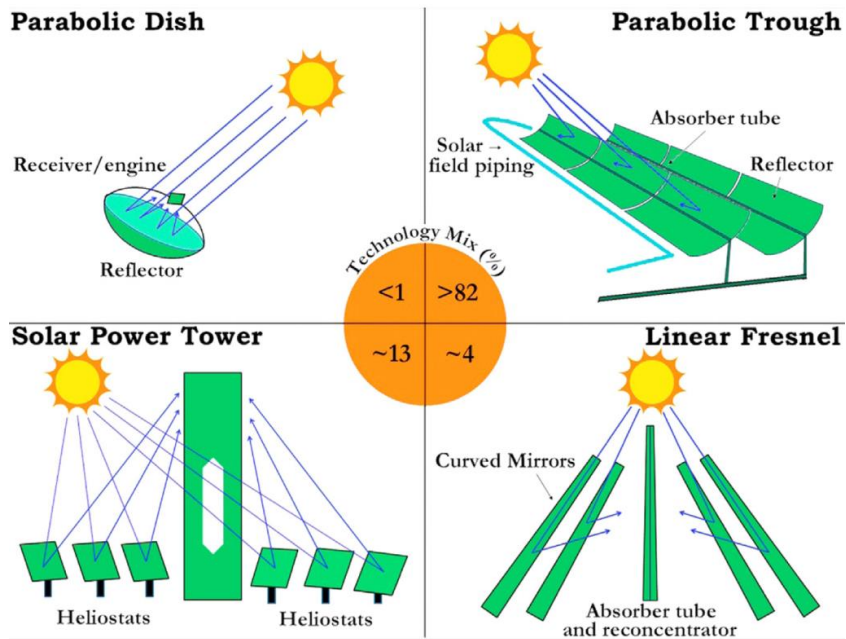


Fig. 4. Various concentrated solar power technologies along with their installed ratios [17]

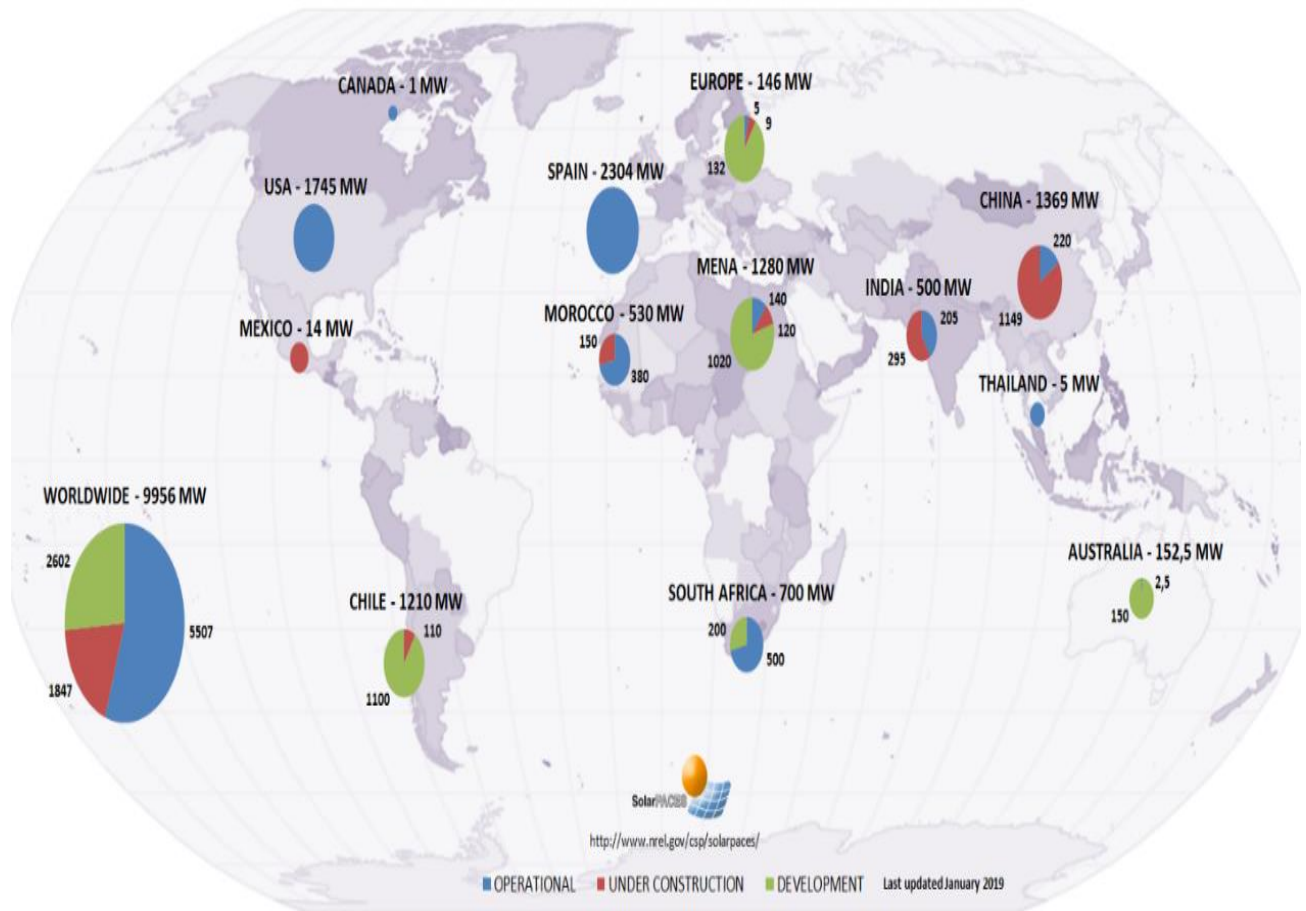


Fig. 5. Concentrated solar power projects around the world [18]



Moreover, a CSP operator may store heated-up fluid in a TES (i.e. a tank) to schedule a continuous operation on cloudy days or during the night. TESs does not exist in all CSP plants due to the relevant cost implications. As an illustration, only about 40% of all Spanish CSP plants (50 plants) have TES [19]. Major elements of a CSP plant are shown in Fig. 6.

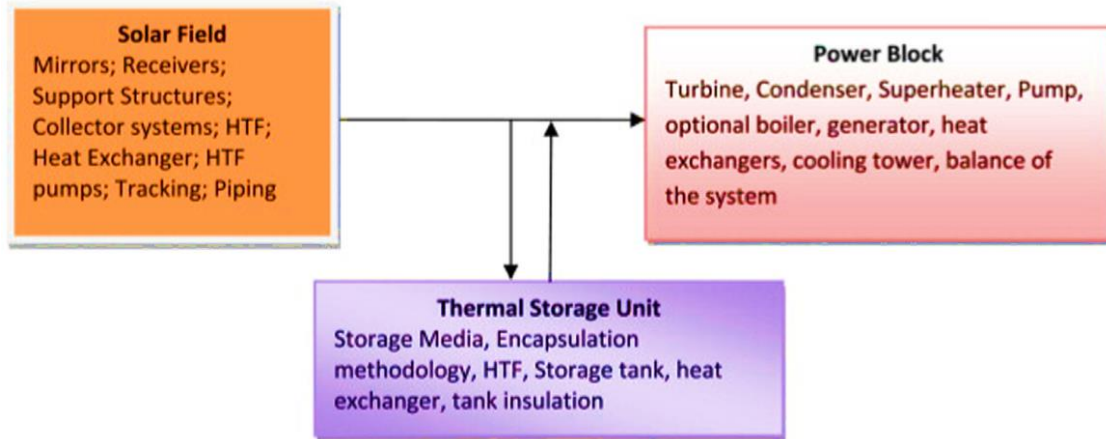


Fig. 6. Main sections of a concentrated solar power plant and their components [19]

Table 6 details the major characteristics of all CSP technologies.

TABLE 6. CHARACTERISTICS OF CONCENTRATED SOLAR POWER TECHNOLOGIES [20-22]

	SPD	SPT	LFR	PTC
Potential capacity (MWe)	0.01–0.4	10–150	10–200	10–200
Concentration ratio	1,000–3,000	300–1,000	70–80	25–100
Specific power (W/m <sup>2</sup> )	200	300	–	300
Optical efficiency	High	Medium	Low	Medium
Annual solar-to-electric efficiency	20–35%	20–35% (concepts)	8–20%	15%
Solar efficiency max.	29% (demonstrated)	20% (demonstrated) 35% (expected)	21% (demonstrated)	20% (expected)
Thermal efficiency (%)	30–40	30–40	–	30–40
Plant peak efficiency (%)	~ 30	23–35	~ 18	14–20
Collector concentration	> 1,300 suns	> 1,000 suns	> 60 suns (depends on secondary reflector)	70–80 suns
Site solar characteristics/solar radiation required	Generally, sites with an annual sum of direct normal irradiation (DNI) larger than 1,800 kWh/m <sup>2</sup>			
Operating temperature of the solar field (°C)	800	250–650	250–390, possible up to 560° C	290–550

Receiver/absorber	Absorber attached to the collector, moves with collector	External surface or cavity receiver, fixed	Fixed absorber, no evacuation, secondary reflector	Absorber attached to the collector, moves with the collector, complex design
Land requirement	Small	Medium	Medium	Large
Area requirement (m <sup>2</sup> /MWh)	30–40	8–12	6–8	4–6
Typical shape of the solar plant	Rectangular	Sector of a circle/rectangular	Rectangular	Rectangular
Capital cost (US\$/kW)	12,578	4,000+	–	3,972
Capital cost (US\$/m <sup>2</sup> )	–	476	234	424
Operation and maintenance cost (US\$/kW h)	0.21	0.034	0.011	0.012 – 0.02
Suitability for air cooling	Best	Good	Low	Low to good
Water cooling (L/MW h)	–	2,000 or dry	3,000 or dry	3,000 or dry
Water requirement (m <sup>3</sup> /MW h)	0.05–0.1 (mirror washing)	2–3 (wet cooling), 0.25 (dry cooling) and 0.3–1 (hybrid)	3 (wet cooling) and 0.2 (dry cooling)	3 (wet cooling), 0.3 (dry cooling) and 0.4–1.7 (hybrid)
Storage possibility	Depends on plant configuration	Depends on plant configuration	Yes, but not yet with DSG	Yes, but not yet with direct steam generation (DSG)
Possibility for storage with molten salt	Possible, but not proven	Commercially available	Possible, but not proven	Commercially available
Storage system	No storage, chemical storage under development	Direct 2-tank molten salt at 550 °C ( $\Delta T = 300$ °C)	Short-term pressurised steam storage (< 10 min)	indirect 2-tank molten salt at 380 °C ( $\Delta T = 100$ °C) or Direct 2-tank molten salt at 550 °C ( $\Delta T = 300$ °C)
Heat transfer fluid	Air, hydrogen, helium	Water/steam, molten salt, air (demonstration)	Water/steam	Synthetic oil, water/steam (DSG), molten salt (demonstration), air (demonstration)
Steam conditions (°C/bar)	Not applicable	540/100 to 160	260/50	380 to 540/100
Annual CF (%)	25–28	55 (10 h TES)	22–24	25–28 (no TES), 29–43 (7 h TES)
Grid stability	Low	High (large TES)	Medium (back-up firing possible)	Medium to high (TES or hybridisation)
Possible backup/hybrid mode	Yes, but in limited cases	Yes	Yes	Yes
Development status	Demonstration	Mature	Demonstration	Most proven
Technology development risk	Medium	Medium	Medium	Low
Outlook for improvement	Through mass production	Very significant	Significant	Limited

### 3.1 Solar parabolic-dish technology

Solar parabolic-dish technology uses a dish formed parabolic concentrator that reflects solar radiation onto a receiver at the focal point. A two-axis tracking system makes it capable of following the sun. A Stirling/Brayton engine is located at the focal point to effectively convert thermal energy into kinetic energy

[23]. The pressure and temperature of the working fluid may reach around 200 bar and 700–750 °C at the focal point of the SPD if a dish with a concentration ratio of roughly 2,000 is used [21, 23-25]. In general, SPDs have a diameter between 5-10 m which gives an internal surface area of around 40–120 m<sup>2</sup>. The surface of SPDs is coated with aluminum or silver to construct a shiny surface while the body is made of plastic or glass. One of the best performances is obtained when a glass body (with a certain percentage of iron to improve reflection) and a silver coated surface (thickness of 1 µm) are adopted [26], in which a solar reflection of 90–94% may be achieved. The electric capacity of a single SPD with such a configuration can vary between 0.01-0.5 MW [26].

Inside the Stirling engine, heat collected from solar energy flows from the hot point to a cold sink to operate it. This then runs an electric generator to generate electricity. Stirling engine based SPD technology has an efficiency of between 25-30% [26, 27]. This system has one of the highest efficiencies among all solar-to-electric conversion technologies. The reason is that the curved mirrors utilised in this technology always point straight to the sun, while there are cosine losses in cases of SPT and PTC technologies [16, 28]. On an equal configuration basis, solar-to-electric efficiency of SPD may approximately be 50–100% higher than SPT and PTC systems [29]. SPT has a great advantage over other types in that it is readily applicable in small isolated and remote networks [30]. Fig. 7 shows a schematic of parabolic-dish CSP.

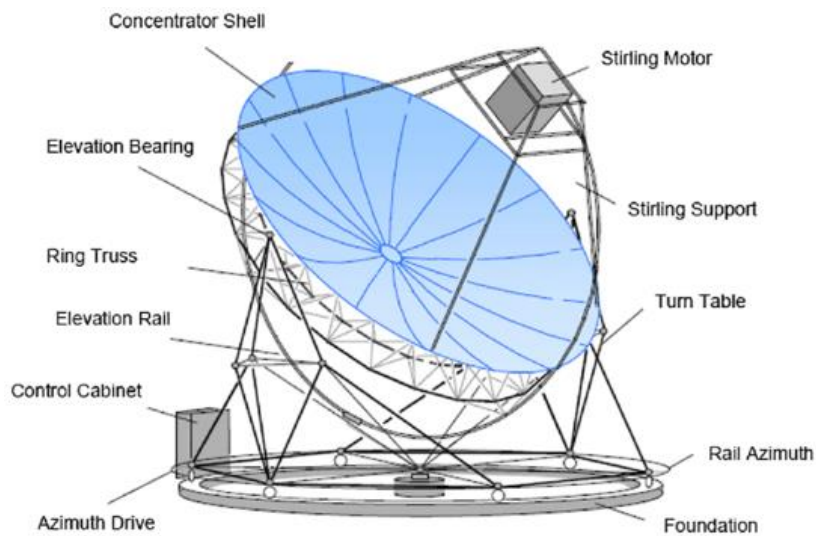


Fig. 7. A schematic of parabolic-dish concentrated solar power

This technology can be combined with CFPPs to offer a more reliable source of electric power. The technical characteristics of two highlighted SPDs are given in Table 7 [31].

TABLE 7. TECHNICAL CHARACTERISTICS OF PARABOLIC-DISH CONCENTRATED SOLAR POWER PLANTS [31]

Name	Tooele army depot	Maricopa solar project (Maricopa)
Location	Tooele, Utah, United States	Peoria, Arizona, United States
Project type	Commercial	Demonstration
Start year	2013	2010
Capacity	1.5 MW	1.5 MW
Latitude/longitude (location)	40°30' 4.0" North, 112°22' 25.0" West	33°33' 31.0" North, 112°13' 7.0" West
Land area (acres)	17	15
Number of dishes	429	60
Engine type	Stirling	Stirling
Dish aperture area	35 m <sup>2</sup>	–
Heat-transfer fluid type	Helium	Hydrogen
Type of Storage	None	None
Method of cooling	Closed-loop cooling system	Only water used for washing mirrors.
Annual solar-to-electricity efficiency	–	26%

### 3.2 Parabolic-trough collector

Giant U-shaped mirrors are employed in PTC technology to reflect solar radiation onto the receiver. Generally, there are several hundreds of trough mirrors in a PTC collector field which are aligned on a north/south axis and are configured in parallel rows. To track the sun from east to west during a day, a single-axis configuration is adopted in PTC to ensure solar radiation is constantly absorbed by pipes of the receiver [31]. A coloured absorption tube or receiver is utilised in PTCs to reach maximum absorption with the minimum heat losses. The working fluid, which is circulated in the focal point of troughs, can be molten salt (with different percentage of potassium nitrate, potassium, or sodium nitrate), Helium or oil. The working temperature of the fluid may reach 400 °C depending on some parameters like flow rate, solar intensity, and concentration ratio [32]. As an illustration, working temperature of 350–550 °C with solar-to-electric efficiency of 15% can be achieved using a PTC with the radiation concentration ratio of 70–100 times [33].

In the direct steam configuration of this technology, a steam-turbine power unit is added to the collector field in which steam needed to run the turbine is provided by using a heat exchanger. Besides the steam

provision, the rest of the configuration is very similar to the conventional thermal generators. In order to increase the efficiency of the system, similar to traditional steam turbines, low pressure and low temperature steam from the outlet of the turbine will be cooled and recycled to repeat the process [34]. In order to support CSP plant during low solar radiation periods, supplementary coal-fired or natural-gas-fired plants are joined with the power generation system [31].

It is noteworthy that the PTC is more advanced and has higher maturity compared to other types of CSP [27]. A simplified structure of PTC is shown in Fig. 8.

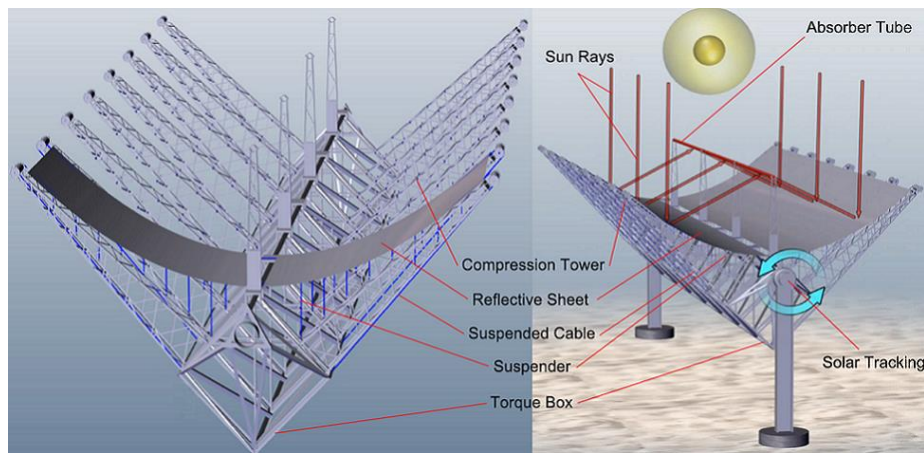


Fig. 8. The schematic of a parabolic trough collector system [31]

The first PTC was constructed in 1912 in Cairo, Egypt [21]. Currently, more than 70 PTCs are operational globally, mostly located in the USA and Spain. Some technical characteristics of a number of PTC plants (except in the USA and Spain) are detailed in Table 8 and Table 9.

Spain has more PTC plants than any other country in the world. The capacity of turbines ranges from 22.5 MW to 50 MW. The solar radiation source in this country is estimated to be 2,136 kWh/m<sup>2</sup>, with an electricity production estimate of approximately 158,000 MWh/year [31]. Up to 2016, Spain reaches a total installed capacity of 1,871.9 MW operational PTC. Table 10 summarises the details of PTC plants in Spain.

TABLE 8. DETAILED CHARACTERISTICS OF PARABOLIC TROUGH COLLECTOR PLANTS WORLDWIDE, EXCEPT THE USA AND SPAIN – PART 1 [31]

No.	Country	Project	Location (climate data point)	Net turbine capacity (MW)	Solar resource (kWh/m <sup>2</sup> /yr)	Average daily solar radiation over a year – horizontal (kWh/m <sup>2</sup> /day)	Electricity generation (MWh/yr)
1	Morocco	Airlight Energy Ait-Baha Pilot Plant	Agadir/Inezgane	3	2,200	5.55	2,390
2	Morocco	ISCC Ain Beni Mathar	-	20	-	-	55,000
3	Italy	Archimede	-	4.72	1,936	-	9,200
4	Italy	ASE Demo Plant	Perugia	-	1,527	3.75	275
5	South Africa	Bokpoort	-	50	-	-	230,000
6	South Africa	KaXu Solar One	-	100	-	-	330,000
7	Canada	City of Medicine Hat ISCC Project	Medicine Hat Airport	1.1	-	4.04	1,500
8	India	Godawari Solar Project	-	50	-	-	118,000
9	India	Megha Solar Plant	Anantapur	50	-	5.34	110,000
10	India	National Solar Thermal Power Facility	-	1	-	-	-
11	Algeria	ISCC Hassi R'mel	-	20	-	-	-
12	Egypt	ISCC Kuraymat	Cairo H.Q.	20	2,431	5.31	34,000
13	United Arab Emirates	Shams 1	-	100	1,934	-	210,000
14	Thailand	Thai Solar Energy 1 (TSE1)	Kanchanaburi	5	-	4.88	8,000

TABLE 9. DETAILED CHARACTERISTICS OF PARABOLIC TROUGH COLLECTOR PLANTS WORLDWIDE, EXCEPT THE USA AND SPAIN – PART 2 [31]

No.	Project type	Land area (m <sup>2</sup> )	Specific land area – net (m <sup>2</sup> /kW)	Cost (approximately)	Working/heat transfer fluid	Thermal storage description	Thermal storage capacity (h)
1	Pilot plant	240,000	80	-	Air at ambient pressure	Packed-bed of rocks	5
2	Commercial	-	-	-	Therminol VP-1	None	-
3	-	80,000	16.95	-	Molten salts	Molten salts	8
4	Demonstration	30,000	-	-	Molten salt	Molten salt	-
5	Commercial	1,000,000	20	US\$ 565 million	Dowtherm A	Molten salts	9.30
6	Commercial	-	-	US\$ 860 million	Thermal oil	Molten salts	2.50
7	Demonstration	-	0	US\$ 9 million	Xceltherm@SST	None	-
8	Commercial	1,500,000	30	-	Dowtherm A	None	-
9	Commercial	2,420,000	48.40	Rs 848 Crore	Xceltherm@MK1	None	-
10	Demonstration	-	-	-	Therminol VP-1	None	-
11	Commercial	640,000	32	Euros 315 million	Thermal oil	None	-
12	Commercial	-	-	-	Therminol VP-1	None	-
13	Commercial	2,500,000	25	US\$ 600 million	Therminol VP-1	None	-
14	Commercial	1,100,000	220	-	Water/Steam	None	-

TABLE 10. DETAILS OF PARABOLIC TROUGH COLLECTOR PLANTS IN SPAIN [31]

Project	Gross Turbine Capacity (MW)	Net Turbine Capacity (MW)	Electricity generation (MW h/yr)	Project type	Land area (m <sup>2</sup> )	Specific land area – net (m <sup>2</sup> /kW)	Cost (million Euro)	Working fluid	Thermal storage description	Thermal storage capacity (h)
Andasol-1 (AS-1)	50	49.9	158 k	*Com	2,000 k	40.08	–	Thermal Oil	Molten salts	7.5
Andasol-2 (AS-2)	50	49.9	158 k	*Com	2,000 k	40.08		Dowtherm A	Molten salt	7.5
Andasol-3 (AS-3)	50	50	175 k	–	2,000 k	40	315	Thermal Oil	Molten salts	7.5
Arcosol 50 (Valle 1)	49.9	49.9	175 k	–	2,300 k	46.09	270	Diphenyl/Diphenyl Oxide	Molten salts	7.5
Arenales	50	50	166 k	*Com	2,200 k	44	–	Diphenyl	Molten salts	7
Aste 1A	50	50	170 k	*Com	1,800 k	36	–	Dowtherm A	Molten salts	8
Aste 1B	50	50	170 k	*Com	1,800 k	36		Dowtherm A	Molten salts	8
Astexol II	50	50	170 k	*Com	1,600 k	32	–	Thermal Oil	Molten salts	8
Borges Termosolar	25	22.5	98 k	*Com	960 k	42.67	153	Thermal Oil	None	–
Casablanca	50	50	160 k	*Com	2,000 k	40	–	Diphenyl/Biphenyl oxide	Molten salts	7.5
Enerstar	50	50	100 k	*Com	2,140 k	42.8	–	Thermal Oil	None	–
Extresol-1	50	0	158 k	*Com	2,000 k		–	Diphenyl/Biphenyl oxide	Molten salts	7.5
Extresol-2	49.9	49.9	158 k	*Com	2,000 k	40.08	–	Diphenyl/Biphenyl oxide	Molten salts	7.5
Extresol-3	50	50	158 k	*Com	2,000 k	40	–	Diphenyl/Biphenyl oxide	Molten salts	7.5
Guzmán	50	50	104 k	*Com	2,000 k	40	–	Dowtherm A	None	–
Helioenergy 1	50	50	95 k	*Com	1,100 k	22	–	Thermal Oil	None	–
Helioenergy 2	50	50	95 k	*Com	1,100 k	22	–	Thermal Oil	None	–
Helios I	50	50	97 k	*Com	2,600 k	52	–	Thermal Oil	None	–
Helios II	50	50	97 k	*Com	2,600 k	52	–	Xceltherm®MK1	None	–
Ibersol Ciudad Real (Puertollano)	50	50	103 k	–	1,500 k	30	200	Diphenyl/Biphenyl oxide - Dowtherm A	None	–
La Africana	50	50	170 k	*Com	2,520 k	50.4	387	–	Molten salts	7.5
La Dehesa	49.9	49.9	175 k	–	2,000 k	40.08	–	Diphenyl/Biphenyl oxide	Molten salts	7.5
La Florida	50	50	175 k	–	2,000 k	40	–	Diphenyl/Diphenyl oxide	Molten salts	7.5
La Risca	50	50	105.2 k	–	1,350 k	27	–	Biphenyl/Diphenyl oxide	None	–
Lebrija 1	50	50	120 k	–	1,880 k	37.6	–	Therminol VP1	None	–
Majadas I	50	50	104.5 k	–	1,350 k	27	–	Biphenyl/Diphenyl oxide	None	–
Manchasol-1	49.9	49.9	–	*Com	2,000 k	40.08	–	Diphenyl/Diphenyl oxide	Molten salts	7.5
Manchasol-2	50	50	2,208	*Com	2,000 k	40	–	Diphenyl/Diphenyl oxide	Molten salts	7.5
Morón	50	50	100 k	*Com	1,600 k	32	295	Thermal Oil	None	–

Olivenza 1	50	50	100 k	*Com	1,600 k	32	284	Thermal Oil	None	–
Orellana	50	50	118 k	*Com	1,860 k	37.2	240	Thermal Oil	None	–
Palma del Río I	50	50	114.5 k	–	1,350 k	27	–	Biphenyl/Diphenyl oxide	None	–
Palma del Río II	50	50	114.5 k	–	1,350 k	27	–	Biphenyl/Diphenyl oxide	None	–
Solaben 1	50	50	100 k	*Com	1,100 k	22	–	Thermal Oil	None	–
Solaben 2	50	50	100 k	*Com	1,100 k	22	–	Thermal Oil	None	–
Solaben 3	50	50	100 k	*Com	1,100 k	22	–	Thermal Oil	None	–
Solaben 6	50	50	100 k	*Com	1,100 k	22	–	Thermal Oil	None	–
Solacor 1	50	50	100 k	*Com	1,100 k	22	–	Thermal Oil	None	–
Solacor 2	50	50	100 k	*Com	1,100 k	22	–	Thermal Oil	None	–
Termesol 50 (Valle 2)	-	49.9	-	–	2,300 k	46.09	270	Diphenyl/Diphenyl Oxide	Molten salt	7.5
Termosol 1	-	50	-	*Com	2,000 k	40	–	Thermal Oil	Molten salt	9
Termosol 2	-	50	-	*Com	2,000 k	40	–	Thermal Oil	Molten salt	9

\*Com: Commercial type

As of 2016, the USA had reached a total installed capacity of 1,255.8 MW of operational PTC. As opposed to Spain in which capacity of CSPs is limited to 50 MW due to government restrictions, there are the largest CSP units with capacity around 250 MW in the USA such as the Solana Generating Station, Mojave Solar Project, and Genesis Solar Energy Project. In the USA, the estimated CSP electricity production is 944,000 MWh/year, and the highest solar irradiation is 64.7497 m<sup>2</sup>/kW among all operational CSP plants in this country [31]. Some characteristics of the PTC plants in the USA are shown in Table 11.

Based on the analysis software of RETScreen Clean Energy, it is estimated that the average daily solar irradiation (for CSP located cities) in the USA and Spain is 4.8–5.78 kWh/m<sup>2</sup>/day, and 5.13–4.63 kWh/m<sup>2</sup>/day, respectively. It shows the higher potential of Spain for solar systems. China is another country which is heavily invested in PTC plants (six plants with a total capacity of 414 MW).

### 3.3 Central receiver/ solar power-tower

In the SPT technology, a large number of flat mirrors, known as Heliostats, are employed to reflect solar irradiations onto a receiver located at the top of a tower [31]. The tower is built of high-temperature tolerant materials like noble metals and ceramics to have high stability against elevated temperatures. Considering



TABLE 11. DETAILS OF PARABOLIC TROUGH COLLECTOR IN THE USA [31]

Project	Land area (m <sup>2</sup> )	Specific land area – net (m <sup>2</sup> /kW)	Net turbine capacity (MW)	Electricity generation (MWh/year)	Solar resource (kWh/m <sup>2</sup> /yr)	Cost in millions of US\$ (approximately)
Genesis solar energy project	7,891,370	31.57	250	580,000	–	–
Holaniku at Keahole Point	12,140.60	6.07	2	4,030	–	–
Martin next generation solar energy center	2,023,430	26.98	75	155,000	–	476.3
Mojave solar project	7,142,702	28.57	250	600,000	–	1,600
Nevada solar one	4,000,000	55.56	72	134,000	2,606	266
Saguaro power plant	64,749.70	64.75	1	2,000	2,636	6
Solana generating station	7,800,000	31.20	250	944,000	–	2,000
Solar electric generating station I (SEGS I)	–	0	13.8	–	2,725	–
Solar electric generating station II (SEGS II)	–	0	30	–	2,725	–
Solar electric generating station III (SEGS III)	–	0	30	–	2,725	–
Solar electric generating station IV (SEGS IV)	–	0	30	–	2,725	–
Solar electric generating station V (SEGS V)	–	0	30	–	2,725	–
Solar electric generating station VI (SEGS VI)	–	0	30	–	2,725	–
Solar electric generating station VII (SEGS VII)	–	0	30	–	2,725	–
Solar electric generating station VIII (SEGS VIII)	–	0	80	–	2,725	–
Solar electric generating station IX (SEGS IX)	–	0	80	–	2,725	–
Stillwater geo-solar hybrid plant	84,984	42.49	2	3,000	–	–

high average flux imposed on the receiver of SPTs ( $200 \text{ kW/m}^2$  to  $1,000 \text{ kW/m}^2$ ), the temperature of the working fluid can reach up to  $700 \text{ }^\circ\text{C}$  [28], which is high enough to produce the steam directly (or through a heat exchanger) for a running turbine and electricity generation. Air, liquid sodium, molten salt, and water/steam are options which can be used as the working liquid in the tower to reach high capacities of 100–200 MW [35]. The structure of an SPT plant is depicted in Fig. 9.

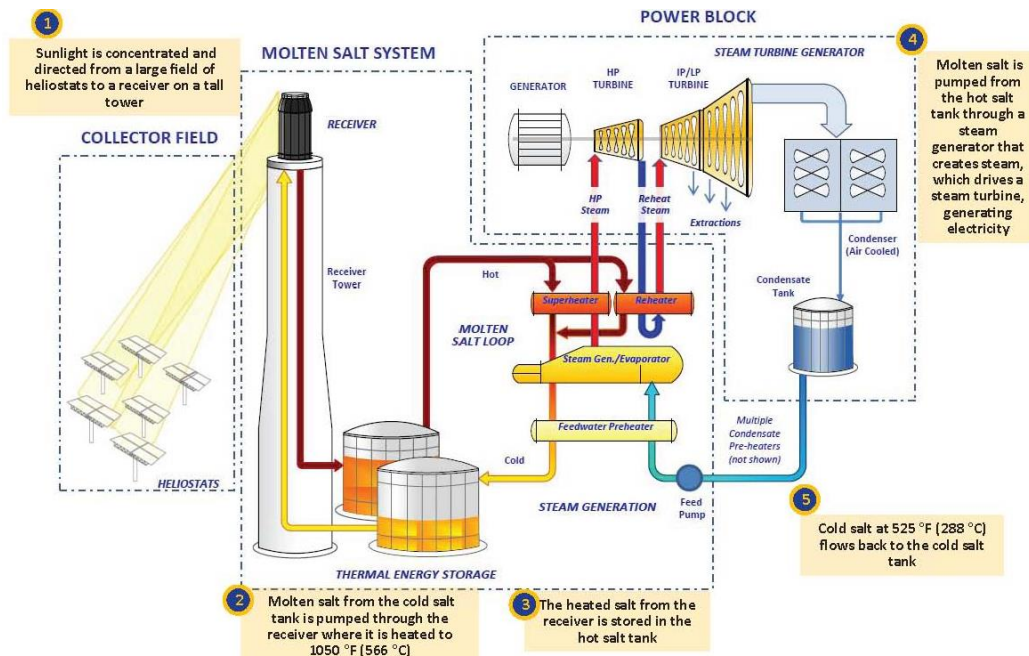


Fig. 9. A schematic of the solar power tower system [31]

SPT technology has been demonstrated by the United States Department of Energy in California in the 1980s as a potential CSP to provide electricity for continuous 24h operation at the utility-scale. It is noteworthy that the major cost of SPT construction is in the heliostats [36]. An automatic computer-based system controls the heliostat to reach the highest sun reflection. Whilst water can be used as the working fluid (e.g., Sierra Sun Tower plant), molten salt is widely utilised in the solar tower plants in the USA because it is non-toxic, non-flammable, and has a higher heat capacity than water. Water circulated in the tower changes into superhot/high-pressure steam in the receiver of the tower. A minor part of this steam is stored in the TES tank whilst the remainder, similar to PTC, is sent to an electric power block to run a turbine and generate electricity. TES permits the system operator to use stored steam during hours with insufficient sunlight to maintain continuous operation. However, during the hours with high sunlight, the

cold molten salt (i.e., stored in the cold tank), which still has a temperature around 300 °C, will be heated up to around 550-600 °C to be stored in the hot TES tank. The heat exchanger is responsible for transferring heat from the hot molten salt to water and turning it into the high-pressure steam which can run the steam turbine. Moreover, exhausted steam is pumped into a heat exchanger after a level of condensing [37]. The capacity of a TES is an important factor for the continuous operation of CSP. Based on the state-of-the-art study in [38], TES can be planned to provide sufficient heat for up to 13 hours of operation. Considering current advances in SPT technology, utility-scale power can be generated from this type of CSP (30-400 MWe), while efficiency can vary between 20-35% [39]. Similar to other technologies, SPT also needs a considerable amount of water. Cleanliness of the mirrors, accuracy of the mirror tracking system and optical characteristics of the heliostats are other factors which significantly affect the efficiency of the SPT. Being of sufficient scale (50–100 MW) is another characteristic of SPT required for it to be profitable and economically viable [40]. It is advised that commercial SPT with a capacity of less than 30 MW can be jointly operated with a CFPP, oil-fired Rankine plant or natural gas combined-cycle to reduce the financial risks [41]. Some investors prefer to hybridise a SPT CSP with solar PV due to its lower capital costs. Some under-development, under-construction and operational SPT units in the world are detailed in Table 12.

### **3.4 Linear Fresnel-reflector**

In LFR technology, an array of linear mirrors plays the role of reflectors. Similar to the other CSP plants, there is a generator, steam turbine, structural systems, tracking system, and receivers. The working principle of the collectors, as the most important component of the system, is the same as the Fresnel lens. The Fresnel collectors focus the solar irradiation onto the linear tower, in which a long cylinder as the main receiver contains several water-carrying tubes. This water is then turned into high pressure/temperature steam under high radiation, which runs the turbine to generate electricity [42, 43]. Major components of an LFR CSP are depicted in Fig. 10. The capital cost of LFR is lower than other types like PTC due to lower price of reflectors; however, the efficiency of LFR is also lower [28]. Their capacity may vary between 10-200 MW with solar-to-electric efficiency between 8–10% [43].

TABLE 12. OPERATIONAL, UNDER-CONSTRUCTION AND UNDER-DEVELOPMENT SOLAR POWER TOWER PLANTS [31].

Project	Country	Status	Gross turbine capacity (MW)	Net turbine capacity (MW)
ACME solar tower	India	Operational	2.50	2.50
Crescent Dunes solar energy project (Tonopah)	United States	Operational	110	110
Dahan power plant	China	Operational	1	1
Gemasolar thermosolar plant	Spain	Operational	19.90	19.90
Greenway CSP Mersin tower plant	Turkey	Operational	1.40	1
Ivanpah solar electric generating system	United States	Operational	392	377
Jemalong solar thermal station	Australia	Operational	1.10	–
Jülich solar tower	Germany	Operational	1.50	1.50
Khi solar one	South Africa	Operational	50	50
Lake Cargelligo	Australia	Operational	3	3
Planta solar 10	Spain	Operational	11.02	11
Planta solar 20	Spain	Operational	20	20
Sierra SunTower	United States	Operational	5	5
Ashalim Plot B	Israel	Under Construction	121	121
Atacama-1	Chile	Under Construction	110	110
Golmud	China	Under Construction	200	200
NOOR III	Morocco	Under Construction	150	150
Sundrop CSP project	Australia	Under Construction	1.50	1.50
Supcon solar project	China	Under Construction	50	50
Copiapó	Chile	Under Development	260	260
Delingha Qinghai tower project	China	Under Development	135	135
Dunhuang project	China	Under Development	100	100
Golden tower project	China	Under Development	100	100
Hami 50 MW CSP project	China	Under Development	50	50
Qinghai Gonghe CSP plant	China	Under Development	50	50
Redstone solar thermal power plant	South Africa	Under Development	100	100
Shangyi tower CSP project	China	Under Development	50	50
Yumen 100 MW tower CSP project	China	Under Development	100	100
Yumen 50 MW CSP project	China	Under Development	50	50

A summary of the characteristics of the LFR CSP in the world is provided in Table 13.

TABLE 13. LINEAR FRESNEL REFLECTOR PLANTS [31].

Project	Status	Country	Gross turbine capacity (MW)	Net turbine capacity (MW)	Electricity generation (MWh/yr)	Solar resource (kWh/m <sup>2</sup> /yr)	Project type	Land area
Augustin Fresnel 1	Operational	France	0.25	0.25	–	–	–	–
Dhursar	Operational	India	125	125	280,000	–	–	–
Kimberlina solar thermal power plant	Operational	United States	5	5	–	–	Demonstration	12 acres
Liddell power station	Operational	Australia	9	9	13,550	–	Commercial	–
Puerto Errado 1 thermo-solar power plant	Operational	Spain	1.4	–	2,000	2,100	Prototype	5 ha
Puerto Errado 2 thermo-solar power plant	Operational	Spain	30	30	49,000	2,095	Commercial	70 ha
Rende-CSP plant	Operational	Italy						
Alba Nova 1	Under construction	France	12	12	25,000	1,800	Demonstration	23 ha
IRESN 1 MWe CSP-ORC pilot project	Under construction	Morocco	–	–	–	–	–	–
Dacheng Dunhuang 50 MW molten salt Fresnel project	Under development	China	50	50	–	–	–	–
Urat 50 MW Fresnel CSP project	Under development	China	50	50	–	–	–	–
Zhangbei 50 MW CSG Fresnel CSP project	Under development	China	50	50	–	–	–	–
Zhangjiakou 50 MW CSG Fresnel project	Under development	China	50	50	–	–	–	–

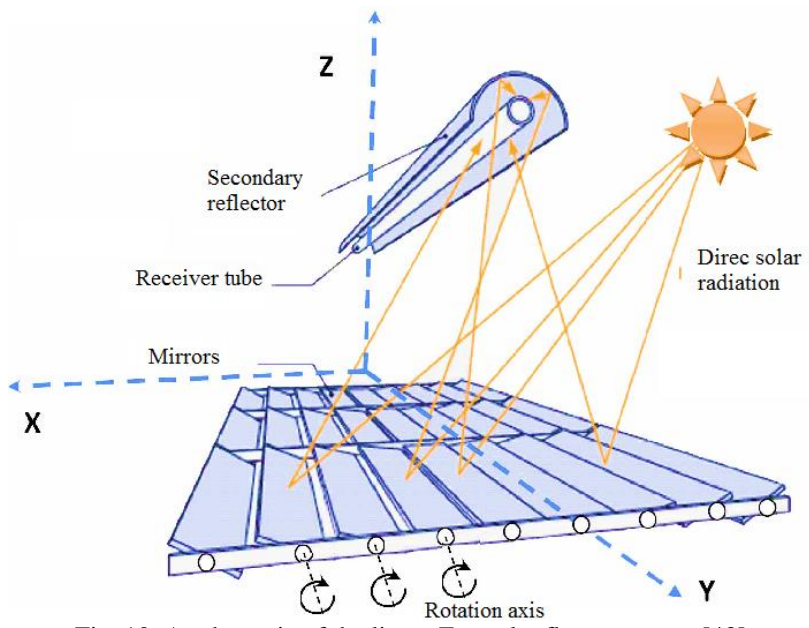


Fig. 10. A schematic of the linear Fresnel reflector system [43]

## 4 OVERVIEW OF CSP DEVELOPMENTS

### 4.1 CSP technology in different countries

Long-term capacity expansion of power systems is a multi-objective task to improve economic factors, reduce environmental effects, meet the security and reliability standards, and improve social outcomes [44]. During recent years, high integration of renewable technologies into electricity distribution networks has imposed severe additional obstacles for power system planners [45, 46]. However, the deeper awareness of the negative environmental influences of fossil fuel consumption has started a revolution towards establishing renewable energy schemes. The Paris Agreement, which has been signed by some developed countries, is limiting the greenhouse gas emissions in all sectors of the economy [47, 48]. As a promising electricity generation technology, CSP tackles this problem with a modest future cost [49]. In this regard, some countries have started to accomplish the implementation of their extensive research programs on renewable energy. This section presents an overview of studies to facilitate the CSP study of this project.

**CSP review in Chile:** Ref. [50] presents a review of the integration impacts of CSP equipped with TES in the electric power systems of Chile. The study is an extensive long-term capacity expansion planning model to establish CSP-TES operation. The proposed method defines an investment approach for the assets of the transmission-generation system over a 20-year planning period considering capital costs, load growth, and fuels cost. The proposed model studies the operating dynamics of the grid by considering multiple representative days for each investment period. Influences of TES on CSP operation, different situations of carbon tax levels and capital costs are studied for two major CSP-TES technologies available on the market.

**CSP review in Libya:** An exploration of the possible applications of CSP plants in Libya is reviewed in [51, 52]. The current energy situation, as well as socio-economic framework of Libya for various kinds of CSP plants, are presented. In addition, a detailed evaluation of CSP plant construction parameters including solar irradiation, water resources, land topography, and grid connections are provided. Furthermore, a simulation to investigate the thermo-economic performance of a 50 MW PTC unit is

performed. The simulation uses Andasol-1 in Spain as the reference plant and meteorological data of the Solar Energy Research and Studies Center in Tajoura city to evaluate the obtained outcomes.

**CSP review in Nigeria:** A study with a focus on the applicability of TES and hybridisation of CPS with liquid fuel based power plants in Nigeria is presented in [53]. Considering technology progress and a high level of DNI in this country, the authors consider CSP as a high potential solar technology for electric power generation at the commercial level in Nigeria. Then, current CSP technologies are investigated under different social, environmental and operational scenarios in Nigeria based on desktop-survey data to define the most appropriate configuration for solar thermal electric power plants.

**CSP review in India:** India is another country that has been the target of case studies on CSP development. Technology growth of renewable power generation is treated by [54] as an initiative to decrease the forthcoming climatic crisis. CSP technology is evaluated in this piece of research as a worthy investment option with the capacity of providing electricity for about 7% of the total electric power demand of the world by the year 2030. States of Rajasthan and Gujarat, India, are identified as the potential locations for extensive CSP applications. In [55], the authors mention that India has massive solar power potential with more than 300 clear sky days in a year and solar radiation of 1,700–1,900 kWh per square metre. The Indian Government set a target of 100,000 MW additional solar-based generation for the period 2011-2022.

**CSP review in Serbia:** In [20], current solar power activities and future projects, potentials of solar energy (especially CSP technology) in Serbia, and Serbian Government solar initiatives are presented. Then, long-term meteorological data are utilised to examine the potential of CSP in Serbia. It states that Serbia has around 30% higher potential of biomass and solar irradiation than Middle Europe. Some international and Serbian CSP plants are compared to validate the feasibility of the planning results, where horizontal and vertical solar irradiations, as well as the diffuse ratio to global DNI, are considered.

**CSP review in China:** An extensive overview and pre-feasibility evaluation of the CSP technology in China, as well as some costs estimation methods, are provided in [56, 57]. These studies note that CSP technologies are useful in locations where the annual direct solar radiation is over 1,800 kWh/m<sup>2</sup>, and there is also the availability of high-voltage electricity transmission. Then a solar irradiation map of China for



some specific regions is adopted as the base data for determination of potential solar energy harvesting using four types of CPS technologies. Finally, the results of the feasibility investigation are utilised to show the massive CSP technology potential in the Chinese market.

**CSP review in Iran:** Ref. [58] illustrates that economy of fossil fuel-dependent countries like Iran requires promising paths towards renewable energy development. It also mentions that the availability of large desert lands with abundant solar irradiation which could encourage the growth of solar/solar-thermal units for both electricity generation and thermal power provision. The paper extensively investigates the status, potential, and perspective of solar thermal projects in Iran. In the end, current initiatives and distinctive considerations of the Iranian Government for supporting solar energy are drawn.

**CSP review in Malaysia:** Ref. [23] provides a comprehensive report on current solar technologies and their associated challenges to allow the evaluation of the downsides and benefits of CSP implementation in Malaysia. The paper paves the way for planners of both solar photovoltaic (PV) and CSP systems in this country while reviewing the different electricity and heat applications of these solar systems. In the case of residential water heating, three major collectors including flat-plate, evacuated-tube solar, and compound PTC are investigated. Finally, the paper justifies some of the limitations and barriers for full-scale exploitation and promotion of solar energy in Malaysia.

**CSP review in Turkey:** According to [25], wide wastelands with ample solar irradiations are extensively available in the southeastern and western regions of Turkey. Besides, there is strong support from the Turkish Government to develop solar projects involving CSP technologies, and this makes Turkey an appropriate location for CSP utilisation. Following a review of generation-consumption patterns in the country, [25] illustrates that natural gas and thermal power plants form the major source of electric power production in Turkey, which has raised considerable concerns for the fuel-dependent energy sector of this country. Turkey generally imports petroleum products from India (11.12%), Iraq (17.08%), Iran (18.37%), and the Russian Federation (25.21%). Crude oil and diesel oil form more than 89% of Turkey's petroleum product imports. After evaluation of the solar energy resources in Turkey, investigation of the land cover and land use for CSP equipment is undertaken. Other siting factors are also considered such as land slope

(i.e., preferably less than 1%, while up to 3% is also acceptable with higher construction cost), water availability (at a Rankine steam CSP plant, water is required for the cooling tower, mirror washing, and the steam cycle) and the suitability of dry cooling systems.

**CSP review in the United States:** The studies in [59, 60] show that the world's largest CSP plants are the Mojave Solar Project (i.e., PTC technology, 354 MW) and Ivanpah Solar Power Facility (i.e., PTC technology, 392 MW) in the United States. To achieve more profit, the size of CSP plants should increase. While regulatory restrictions adopted in Spain limit CSP projects to 50 MW, the CSP capacities in the United States and some other countries are often 150–500 MW. In 2016, PTC technology reached a total capacity of 1,255.8 MW in the United States. The project Solar Electric Generating Station I (SEGS I) as the first PTC project in the United States has a capacity of 13.8 MW and was established in 1984, while the most expensive project of this country, named Solana Generating Station, was installed in 2013 with a cost of US\$ 2 billion. In this regard, California with 15 CSP plants has the largest number of CSP plants of all the states in the USA.

**CSP review in Spain:** With the total CSP capacity of 2.3 GW in operation, Spain is a leader in this technology [61, 62]. Moreover, Spain with 50 CSP projects during the five years from 2008 was the biggest in Europe. While 90% of these projects utilise PTC technology, three of these 50 projects are SPT CSP and two of them are LFR CSP with the total capacity of 50 MW and 31.4 MW, respectively. From the earliest CSP projects, TES facilities were involved in the generation systems, where Andasol, as the first CSP project in Europe, uses a TES with 7.5 hours storage capacity, and Termasol project in Spain (completed before the year 2012) uses a 9-hour TES. Spain owes its rapid progress in the CSP sector to a series of regulations adopted between 2004 and 2013.

**CSP projects in Australia:** Australia possesses one of the highest DNI resources in the world. It is expected that by mid-2020 there will be 1.8 GW of cumulative solar capacity (85% PV and 15% CSP) available compared to less than 200 MW in 2012 [63]. Ref. [63] states that the capacity for electric power generation in Australia can reach more than 50 GW from all energy source, and it further demonstrates that adding up to 15 GW additional capacity of CSP technology to the system only requires a modest extension

of the grid. There are five major CSP projects in Australia: Sundrop CSP project, Liddell power station, Lake Cargelligo, Jemalong solar thermal station, and Aurora solar energy projects. However, there have been several trial CSP projects as well. A comprehensive study on economic and technical factors involved in design procedures for CSP systems in Australia is also presented in [63]. Moreover, requirements for the integration of CSP systems in different markets with different roles are explored.

It is worth mentioning that the highest solar radiation is achieved in the central and northwest of the continent which are mostly desert regions. The Australian Energy Resource Assessment provides supplementary data about solar resources as well as the influencing factors for the adoption and development of the various energy resources to 2030 [64]. Average yearly solar radiation received in Australia is 58 million PJ which is around 1,000 times its total load demand. At present, only about 5% of total power generation in Australia is based on solar power, although the capacity of solar energy in this country is much higher (i.e., having the highest average solar radiation in the world). DNI of the sun in Australia is shown in Fig. 11. The Australian government aimed to increase the solar power utilisation in two rounds. The first round (i.e., Mandatory Renewable Energy Target (MRET)) was formed between years 2001-2010 which was aimed to provide 9,450 GWh annual production from RESs. Then, the second round started in year 2009 while the previous plan adopted during the first round has been renamed (as RET) and targeted at additional 45,000 GWh per year by 2020 (i.e., approximately 20% of the total electricity demand of Australia). The Australian Renewable Energy Agency (ARENA) was established in July 2011 with approximately \$ 3.2 billion grant funding to support and develop new RES research. In July 2012, carbon taxation of \$ 23 (by 5% increase per year, abolished from 1 July 2014) per tonne for CO<sub>2</sub> emission was introduced for major industrial emitters that use fossil fuels.

For CSP technology, the CSIRO was responsible for leading an \$ 87 million research program to decrease the cost of CSP generation from 25 to 10-12 cents per kWh. As a result, CSP projects of Liddell, Lake Cargelligo and Kogan Creek Solar Boost (to be coupled with CFPPs) were started. However, two small projects of Lake Cargelligo and Liddell are no longer in operation and the project Kogan Creek

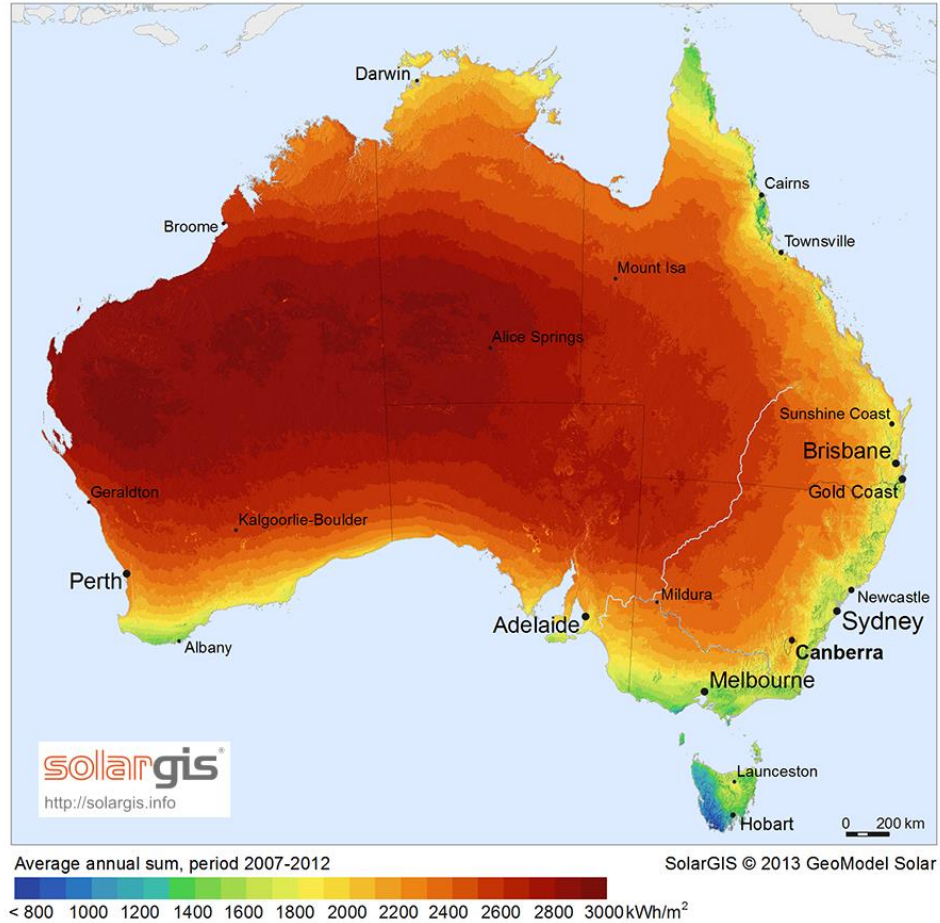


Fig. 11. Direct sun irradiation in Australia [65]

was cancelled in 2016 [66].

From the year 2016, several new promising projects started, for example, Sundrop farms tower CSP project (i.e., to supply onsite electrical demand, heat provision for greenhouses at night, desalinate the seawater for tomato crops) was started in Port Augusta with the capacity of 36.6 MW. Pilot project Jemalong with a capacity of 1 MW and 3 hours of liquid sodium TES is another operational project. The most prominent project under development is established in Port Augusta, where SolarReserve won a tender with a bid to replace a decommissioned CFPP with a 150 MW tower CSP project by 2020 at a world record contract price of AU\$ 78 /MWh (i.e., the lowest cost in the world). Specifications of five CSP plants in Australia are detailed in Table 14 -Table 16 [67].

TABLE 14. SPECIFICATIONS OF AUSTRALIAN CONCENTRATED SOLAR POWER PROJECTS (PART 1) [67]

## Aurora Solar Energy

Status Date:	October 23, 2017
<b>Background</b>	
Technology:	Power Tower
Status:	Under Development
Location:	SA Australia
Region:	Port Augusta
Lat/Long Location:	
Electricity Generation:	500,000 MWh/yr (Expected)
Break Ground Date:	2018
Start Production Date:	2020
Cost (approx):	650 million AU\$
PPA/Tariff Date:	August 14, 2017
PPA/Tariff Rate:	78 AU\$/MWh
PPA/Tariff Period:	20 years
Incentives:	AU\$110 million federal loan

### Participants

Developer(s):	Solar Reserve
---------------	---------------

### Plant Configuration

#### Solar Field

Heat-Transfer Fluid Type:	Molten Salt
---------------------------	-------------

#### Power Block

Turbine Capacity (Gross):	150 MW
Turbine Capacity (Net):	135 MW
Output Type:	Steam Rankine
Cooling Method:	Dry Cooling

### Thermal Storage

Storage Type:	2-tank direct
Storage Capacity:	8 hours
Storage Description:	Molten salt

## Jemalong Solar

Status Date:	November 24, 2017
<b>Background</b>	
Technology:	Power Tower
Status:	Operational
Location:	Jemalong NSW Australia
Lat/Long Location:	33° 24' 0.00" South, 148° 6' 0.00" East
Land Area:	10 hectares
Electricity Generation:	2,200 MWh/yr
Break Ground Date:	April 2014
Start Production Date:	2017
Cost (approx):	21 AU\$ million
Project Type:	Pilot project
Incentives:	AU\$8.89 million from ARENA

### Participants

Developer(s):	Vast Solar
Operator(s):	Vast Solar
Generation Offtaker(s):	Essential Energy

### Plant Configuration

#### Solar Field

Receiver Manufacturer:	Vast Solar
Heat-Transfer Fluid Type:	Liquid sodium
Heliostat Solar-Field Aperture	
Area:	15,000 m <sup>2</sup>
# of Heliostats:	3,500
Heliostat Manufacturer:	Vast Solar
Heliostat Description:	Standard Azi/Ele
Tower Height:	30 m
Receiver Inlet Temperature:	270 C
Receiver Outlet Temperature:	560 C

#### Power Block

Turbine Capacity (Gross):	1.1 MW
Output Type:	Steam Rankine
Cooling Method:	Dry Cooling
Cooling Method Description:	MACCSOL Air Cooled Condenser
Fossil Backup Type:	None

### Thermal Storage

Storage Type:	2-tank direct
Storage Capacity:	3 hours
Storage Description:	Liquid sodium

TABLE 15. SPECIFICATIONS OF AUSTRALIAN CONCENTRATED SOLAR POWER PROJECTS (PART 2) [67]

## Lake Cargelligo

Status Date:	March 20, 2017
<b>Background</b>	
Technology:	Power Tower
Status:	Currently Non-Operational
Location:	Lake Cargelligo New South Wales Australia
Lat/Long Location:	33° 18' 42.00" South, 146° 24' 35.00" East
Start Production Date:	May 2011
Project Type:	Demonstration
Incentives:	AUD 5\$ million grant as a part of AEST Program

### Participants

Developer(s):	Lloyd Energy Systems Pty Ltd
EPC Contractor:	Comet Windmills
Operator(s):	Graphite Energy
Generation Offtaker(s):	Australian National Energy Market

### Plant Configuration

#### Solar Field

Receiver Manufacturer:	Lloyd Energy Systems Pty Ltd
Heat-Transfer Fluid Type:	Water/Steam
Heliostat Solar-Field Aperture Area:	6,080 m <sup>2</sup>
# of Heliostats:	620
Heliostat Aperture Area:	9.8 m <sup>2</sup>
Receiver Type:	Graphite solar storage receiver
Receiver Inlet Temperature:	200 C
Receiver Outlet Temperature:	500 C

#### Power Block

Turbine Capacity (Gross):	3 MW
Turbine Capacity (Net):	3 MW
Output Type:	Steam Rankine
Power Cycle Pressure:	50 bar

### Thermal Storage

Storage Type:	Other
Storage Description:	Core graphite thermal storage technology

## Liddell Power Station

Status Date:	March 20, 2017
<b>Background</b>	
Technology:	Linear Fresnel reflector
Status:	Currently Non-Operational
Location:	Liddell Australia
Region:	New South Wales
Lat/Long Location:	32° 22' 34.00" South, 150° 58' 48.00" East
Electricity Generation:	13,550 MWh/yr
Generation Data Explanation:	thermal megawatts-hour
Break Ground Date:	2011
Start Production Date:	October 2012
Project Type:	Commercial
Incentives:	\$9.25 million from the NSW Government Climate Change Fund Renewable Energy Development Program

### Participants

Developer(s):	Novatec Solar
EPC Contractor:	Novatec Solar
Operator(s):	Macquarie Generation
Generation Offtaker(s):	Australian National Electricity Market

### Plant Configuration

#### Solar Field

Solar-Field Aperture Area:	18,490 m <sup>2</sup>
# of Lines:	4
Line Length:	403 m
Collector Manufacturer:	Novatec Solar Nova-1
Collector Description:	Fresnel
Mirror Manufacturer:	Novatec Solar
Receiver Manufacturer:	Novatec Solar
Heat-Transfer Fluid Type:	Water/Steam
Solar-Field Inlet Temp:	140°C
Solar-Field Outlet Temp:	270°C

#### Power Block

Turbine Capacity (Gross):	3 MW
Turbine Capacity (Net):	3 MW
Turbine Description:	The 9 MWth solar boiler feeds steam into the existing 2000 MW coal-fired power station
Power Cycle Pressure:	55 bar
Cooling Method:	Dry cooling
Cooling Method Description:	Air-cooled condensers
Design-Point Conditions:	270°C, 55 bar, 9.3 MWth peak thermal output

### Thermal Storage

Storage Type:	None
---------------	------

TABLE 16. SPECIFICATIONS OF AUSTRALIAN CONCENTRATED SOLAR POWER PROJECTS (PART 3) [67]

## Sundrop CSP Project

Status Date:	October 26, 2016
<b>Background</b>	
Technology:	Power Tower
Status:	Operational
Location:	Port Augusta Australia
Lat/Long Location:	32° 35' 38.00" South, 137° 51' 21.00" East
Electricity Generation:	1,700 MWh/yr
Break Ground Date:	October 12, 2015
Start Production Date:	October 6, 2016

### Participants

Developer(s):	Aalborg CSP
EPC Contractor:	John Holland

### Plant Configuration

#### Solar Field

Heat-Transfer Fluid Type:	Water/Steam
Heliostat Solar-Field Aperture	
Area:	51,505 m <sup>2</sup>
# of Heliostats:	23,712
Heliostat Manufacturer	
(Model):	eSolar (SCS5)
Tower Height:	127 m

#### Power Block

Turbine Capacity (Gross):	1.5 MW
Turbine Capacity (Net):	1.5 MW
Output Type:	Steam Rankine

### Thermal Storage

Storage Type:	None
---------------	------

## 4.2 Drivers and barriers for the deployment of CSP

The ability of joint-operation of different renewable energy technologies with solar resources to mitigate its intermittency for bulk power generation is a major factor for the CSP technology to receive significant attention among researchers [68, 69]. However, there are a large number of barriers and drivers for the CSP deployment in different countries. Based on a study conducted in the European Union [70], reluctant and uncertain policies of governments in addition to high costs of CSP establishment are two top barriers compared to other types of renewable energy and conventional power plants. Such barriers are more intense when there is a plan to construct a CSP in a desert or remote region. Furthermore, there are other challenges

for the optimal determination of heat-transfer fluid, receiver, TES subsystems, environmental impacts, and water consumption [65, 71].

### **4.3 CSP options for hybridisation with thermal power plants**

The benefit of energy dispatchability of CSPs through thermal storage is obvious, and there are some plants in the world equipped with these storage units for power generation during hours without solar irradiation, which can cope with load variations and also make the intermittent solar resource dispatchable [72]. Although TES would give CSP plants an exceptional superiority over PV, TES is currently an expensive technology, and cost-competitive TES is not available yet. Also, it has limited capacity only providing up to 13 hours storage which not enough to cover prolonged weather events, for example. Therefore, it is a logical solution to use CSP systems as a steam generator for joint operation with traditional thermal power plants, while waiting for more cost competitive TESs to be developed. In this regard, identification of the most appropriate CSP technology for hybridisation with the Rankine cycle of fossil fuel-based conventional thermal plants (e.g., coal) and also nonconventional fuels (e.g., waste materials and biomass) was evaluated by [73]. The authors' calculations, industry information, and literature review are employed to demonstrate the results. The scenarios for host power plants in [73] include coal, natural gas, waste materials, and biomass as the fuel, while several integration options are considered such as superheated steam for the high-pressure turbine, cold reheat line, and feed-water heating. Another review study on various strategies for CSP hybridisation is given in [74] considering wind, PV, geothermal, biofuels, natural gas, and coal. Based on the results of that paper, biofuel, natural gas, and coal, through hybridisation with CSPs, can provide valuable options to employ solar heat at various temperatures. However, these configurations are not purely renewable (except biofuels); they can offer flexibility, dispatchability, and reliability. Hybrid designs related to PV, wind, and geothermal are purely renewable, but they have also other issues to overcome. For instance, the power cycles limit the efficiency of hybrid designs of geothermal-CSP despite requiring low operation-temperature. Similarly, reviews of CSP hybrid configurations with geothermal, biomass, wind, natural gas, and coal are presented in [75, 76]. Based on



their renewable energy generation levels, the generation models include low, medium, and high-renewable hybrids.

Within high-renewable hybrid designs, CSP-geothermal, CSP-biomass, and CSP-wind have minimum adverse influences on the environment. However, some factors such as cost-effectiveness, capacity factor, solar-to-electricity efficiency, and energy efficiency of these systems need to be enhanced to be competitive. Within the medium-renewable hybrid designs, solar-thermal plants with natural gas as back-up supplies offer a high share of solar power but suffer mostly from high capital costs as well as low system-efficiency, which hinders their penetration into the market. Within the low-renewable hybrid configurations, solar-aided coal Rankine plants, solar-Brayton, and solar-combined cycles are technically mature enough to prove their superiority over the medium and high-renewable hybrids. Ref. [77] categorises possible options for CSP hybrids into strong, medium, and light hybrids while discussing the potential configurations of CSP with wind, geothermal, waste materials, biomass, natural gas, and coal. Then options for integrating CSP into various steam cycles including superheating steam, live steam, reheat steam, and feed-water heating have been investigated. The paper focuses on CSP-hybrid models for Australian data. Finally, [78] provides an extensive comparison method to review the thermal performance of 15 hybrid generation configurations of solar, fossil and other hybrid models. To this end, a power plant is divided into several parts and then, the modeling is carried out for each part. In the case of the solar plant, comprehensive modeling is carried out which includes the formation of heat losses from the piping, optics of the collector, and heat transfer in the receiver tube. Both steam and gas turbines are mathematically modeled for the given 15 hybrid configurations. Three reference conversion models of Rankine, Brayton, and combined cycles for PTC integration are also analysed in this study.

## 5 OVERVIEW OF SOLAR PHOTOVOLTAIC DEVELOPMENT IN DIFFERENT COUNTRIES

### 5.1 Photovoltaic technology in different countries

This section presents a brief explanation of photovoltaic development in different countries:

**PV review in Romania:** Authors in [79] present a review of PV energy developments in Romania, from the year 2011 onward. The paper illustrates that PV electricity generation in Romania (after hydro and wind with 35.7%) is less than 4%. By the end of the year 2018, 1,122 PV investments have been accomplished in Romania (including large grid-scale utilities and small roof-top) with the capacities ranging from a few Watts to 82 MW. The largest PV park of Romania in Ucea de Sus covers an area of about 200 ha and was commissioned in 2013.

**PV review in China:** China is a leader in the installation and utilisation of solar power. However, there are still several challenges towards the further development of PV generation throughout China. The economic harvest of PV Poverty Alleviation (PVPA) is analysed for China in [80]. Then chief strategies for PV and PVDM are summarised, new business methods for PV developments are studied and compared, obstacles in PVDM are presented, and the relevant tactics are proposed.

**PV review in Korea:** Ref. [81] provides fundamental analysis for policy implication and economic feasibility of PV systems in Korea. Moreover, it is shown that the present price of residential PV systems for cohousing, without subsidy, is financially reasonable which may positively raise acceptability of renewable energy. It is worth mentioning that currently the energy sector of Korea heavily relies on fossil fuels, which accounts for around 45% of total greenhouse gas emission.

**PV review in Spain:** Ref. [82] details several barriers for the development of Solar PV projects in Spain. After a thorough analysis on the prosumer penetration into the existing market of Spain, this reference proposes some strategies to speed up the growth rate of solar PV. The paper concludes that it is urgent to modernize the regulatory framework of the energy market to promote PV units. Besides, Ref. [83] presents an extensive performance review on six large-scale PV plants with different mounting topologies (e.g. dual-axis and single-axis tracking and fixed) over several years of operation. This study identifies some trends

in relation to location, size, and type of mounting system. In addition to the investigation of several mounting topologies, the effects of ambient temperature and wind speed are also considered.

**PV review in Slovakia:** Ref. [84] states that Slovakia could reach 17th position in the world in terms of PV capacity per capita. It analyses the effects of PV systems on spot market prices, and quantifies the observations based on hourly data using multivariate regression method.

**PV review in Brazil:** Authors in [85] consider government initiatives and incentives as the major factors for the realisation of energy transitions in Brazil. The growing contribution of PV generation in both environmental and socioeconomic dimensions is illustrated. The study presents an acute review on the functions of innovative systems, as well as several marketing recommendations. Another study for the Brazil case is accomplished in [86] aiming at the development of regulatory motivations to employ PV energy in Brazil and the characteristics and technologies of PV systems.

**PV review in Lebanon:** Ref. [87] studies energy generation using renewable resources with a focus on solar PV production in some of the developing countries (with a specific case study of Lebanon). This study compares long-term goals and current achievements of developing countries in terms of social, political and economic considerations. Investigated projects ranged from small-scale standalone networks such as mini/microgrids to the bulk-scale power stations. The paper shows that the development of solar PV systems in different countries is highly dependent on the living standards, national gross income, and the political position of the country.

**PV review in Africa:** In [88], a literature review of PV solar energy development in Africa is provided. Three key points are presented in this paper: performance, specificities, and current situation of PV solar. Another review paper on PV development in selected countries of sub-Saharan Africa is presented in [89]. The paper firstly points out the vast potential of renewable energy (specifically PV solar) in the sub-Saharan area. Then it presents some key features necessary for the study and growth of the PV generation systems in terms of renewable energy policies, solar radiation level, installed capacity, and percentage of solar PV in the future energy mix in the selected countries.

**PV review in Slovenia:** The principal objective of [90] is to review the current situation of PV

generation in Slovenia (European Union) and to analyse its performance compared to some developed countries. Analysis of different weather conditions and seasons are involved in the comparison study. Performance evaluation is calculated through a ratio between final yield and reference yield, which highly depends on the module temperature and intensity of solar radiation. Finally, the paper concludes that the performance of PV systems is largely influenced by snow, shadings, the azimuth angle, and correct inclination of the PV modules

**PV review in the USA:** Authors in [91] provide a reasonable range of future placement of PV capacity in the USA employing a supply-oriented technique based on supply-chain growth constraints, and a demand-oriented technique which minimises the overall cost of the electricity suppliers. Anticipated trends and previous experience are considered in these two techniques. Each technique is applied to two future scenarios: the first scenario simulates the situation in which the penetration of the PV market is finally controlled by the unrestrained variability of PV solar power, and the second one investigates the impact of low-cost energy storage to alleviate operational constraints. In the case of scenarios with energy storage at very low-costs, an average plausible range given by the two models for the capacity of PV generation in the USA could be 150 to 530 GW<sub>dc</sub> in 2030 and 260 to 810 GW<sub>dc</sub> in 2040.

**PV review in the Australia:** Authors in [92] demonstrate effective storage and transferring of PV power will confirm that this source of energy will create a substantial influence on the electricity grid supply of Australia in the future. Then, this country will reach the position to meet its increasing clean energy demand. The study shows the policies adopted by the Australian Government have been applied to some steps. Repayments offered for installations of residential PV decrease the cost of this technology and therefore boost its uptake. Several similar funds and solar flagship programs are discussed in this paper. In [93], authors explain that ‘rooftop’ or residential PV technology can play a significant role in more utilisation of renewable energy, thus reducing greenhouse gas emissions from generations based on fossil fuels. Also, it is mentioned that in Australia, support exists to boost the placement of residential PV in residential areas in the form of Feed-in Tariffs (FiTs) and Renewable Energy Certificates (RECs). The study delivers an extensive review of current works that measure renewable energy in Australia and carries out thoroughly a

non-commercial PV specific examination of existing data across the several criteria of market maturity, employment, installation, and influences of Australian policies for residential PV between 2001 and 2012. This study recognises general accomplishment in the case of deployment and environmental targets, and partial achievements towards the promotion of the renewable energy sector, that is lacking native manufacturing.

Ref. [94] aims to evaluate whether PV technology is indeed a sustainable choice for the energy transition in Australia. Additionally, an assessment on the lifecycle sustainability of a 1.2 MW roof-top PV (i.e., called UQ Solar) is conducted. The paper shows that, in environmental aspects, UQ Solar has an acceptable performance. It also discusses that the project is only economically feasible with the funding support by the Queensland Government.

## **5.2 Hybrid PV based power plants**

CSP and PV are the two current major solar systems in the world. There are several differences between CSP and PV in terms of performance, impact on the environment, and market operation. A comparison between these two technologies has been presented in [95]. Considering relatively similar assumptions, the impacts of the power station site and DNI on the performance of PV and CSP plants were determined. An analysis of hybrid solar-gas turbine system performance versus PV plant is accomplished in [96] based on a life-cycle analysis. The outcomes of the paper indicate that employing existing technologies, PV is a more environment-friendly choice, with green-house gas emission of 0.043 kg CO<sub>2eq</sub>/kWh.

Although replacing all of CFPPs by renewable energy is not a logical solution due to the reliability issue, some countries have started transition to 100% renewable generation. Based on data collected by the U.S. Energy Information Administration, some countries are in range or close to 100 percent renewable power: Denmark (69.4%), Brazil (75%), Austria (80%), Norway (98.5%), Costa Rica (99%), Iceland (100%), and Paraguay (100%). In this regard, [71] details policies for replacing CFPPs in the Portuguese electricity system with large PV systems. It has been stated in the paper that pumped-hydro coupled with PV units can reduce up to 56% of CO<sub>2</sub> emissions. However, the cost of PV systems with current technology is much

lower than traditional thermal power. Final conclusions of the paper illustrate that large-scale solar PV farms are less beneficial than local PV because of energy-transportation costs. Moreover, solar PV can support system operators by decreasing CO<sub>2</sub> emissions as well as reducing pressure on water reserves.

Hybridisation of conventional thermal power plants with solar PV units is another option that can provide significant advantages for power system planners and operators. A possible option for adding solar PV coupled with small-scale nuclear power plants is studied in [97]. Its proposed configuration converts the PV electricity into the heat that is used for the provision of nuclear-superheated steam. Molten salts in thermal storages are heated by means of electric heaters run by PV electricity. Because of the higher temperature in the inlet of the turbine, the hybrid configuration has higher efficiency than ordinary nuclear power plants. In order to investigate other options for hybridisation, a feasibility evaluation of the applications of the fuel cell (for example solid oxide and reversible), PV, gas turbine, electrical battery, and compressed air energy storage (CAES considering both economic and technical aspects) has been done in [98] to form a hybrid power plant. Utilisation of the storage systems is to reach higher generation reliability, while the ultimate objective of the paper is to reduce the waste of power generated by solar units; therefore, a water reservoir joined with air reservoir of the CAES is suggested by the authors to ensure a constant air supply pressure.

Based on the literature, hydropower is one of the most potent types of energy for hybridisation with PV generation. In this regard, an optimal day-ahead power production scheduling for a large hybrid power plant of PV and hydro is presented in [99]. The proposed robust model considers the uncertain generation of the PV system. Comparing the obtained results with those of separate operation of the hydro unit, there is a 1.9% increase in energy generation of the hybrid model as well as a 9.7% decrease in total online time of the hydro units. The main focus of [100] is to explore long-term operating rules of PV-hydro systems using a stochastic optimisation technique that tackles uncertainties of PV power and reservoir inflow. The paper presents a relatively linear correlation between reservoir storage and available energy. The joint operation of PV and hydro plants enables the application of battery banks and water reservoirs as potential substitutions for energy storage within a system. Similar scenarios are examined in [101] which analyses

the influence of various levels of energy resource complementarity on the performance of hydro PV plants. A further step in the planning of utility-scale PV power plant for joint operation with hydropower is studied in [102]. The world's largest hydro plant is selected to investigate the incorporation of a PV plant on this type of power generation. This study offers a model for optimal sizing of the PV farm to validate the feasibility of complementary PV-hydro operation. To satisfy the different levels of the load demands, three novel modes of operation are proposed. The objective of these operation modes is to maximise the lifetime net revenue of coupled operation. The impact of PV-hydro operation upon water resource allocation is also determined. Authors in [103] focus on large PV plants to show that the best-performing PV plants today excel medium-tier ones owing to the owners' operation and maintenance policies, the quality of the installation, the plant design, and reliability and quality of the components used.

In [104], CFPP is the objective of hybridisation with PV systems. The paper presents financial and operational results of three proposed CFPPs retrofitted with CO<sub>2</sub> capture and solar PV systems, such that six configurations with different economic, thermal and comprehensive performances are compared. Furthermore, a sensitivity analysis is done based on variations of three economic and three technical parameters. As expected, adding a renewable solar plant provides an improvement in the thermal efficiency and electricity income of the coupled plant.

## 6 CSP HYBRID OPTIONS, DATA PREPARATION

### 6.1 Solar aided CFPP

Coal consumption can be reduced as the result of integrating solar energy into CFPPs. Furthermore, solar augmentation will offer low-risk and low-cost substitutes to solar thermal plants in the stand-alone operation mode. Thus, a large number of studies have investigated different aspects of combining CSP with CFPP.

#### 6.1.1 Optimal integration point

Obviously, the first vital step is to find a suitable location for the integration of CSP into the thermal cycle. Ref. [105] focuses on formulation, investigation, and comparison of three hybrid models for CSP integration into conventional steam power plants. The integration models include the concepts of high-pressure turbines, cold reheat line, and feed-water preheating, in which an LFR CSP is employed for direct steam injection in parallel with the steam boiler. In the presented models, the steam coupling point of the solar thermal unit is the only difference among different structures. Obviously, the type and operating point of the solar field are a function of the steam injection point in each scenario. The results identify the maximum limit for solar share, the impacts of solar thermal units on the steam cycle (thermal load balance), and the overall performance of the generation system. To conclude, more solar steam may cause more imbalances in different sections of the turbine which makes a significant challenge in the design of the system. Besides, a hybrid design approach is required to maximise emission and fuel savings while having a high share of solar power. Therefore, optimisation on the design of the hybrid generation system is necessary based on the configuration of the existing power plant to achieve maximum possible solar share [105]. A similar study is accomplished in [106] with four schemes to integrate the low-or-medium temperature solar steam into conventional CFPPs, to compensate a share of the bled-off steam added to the recovering Rankine cycle for the preheat feed-water. A 200 MW CFPP in two operating modes of fuel saving and power boosting is analysed to validate the benefits of employing the solar-aided power



generation (SAPG) technology under several CSP incorporation scenarios to improve steam/fuel consumption rates and solar-to-power efficiency. It is demonstrated that the conversion efficiency of solar heat-to-power can reach 36.5% for solar heat at 260 °C, while this efficiency may be only 11% for a temperature below 100 °C.

### **6.1.2 Small and medium scale hybrid power plants**

An integration at higher steam temperature is presented in [107], where a 330 MW CFPP is hybridised, and the steam pulled out from the high-pressure turbine is replaced by solar heat to preheat the feed-water before entering the economizer. Annual and daily thermodynamic/ economic performances of a solar-aided coal-fired power generation (SACPG) under off-design operating situations are studied.

Another study of a mid-temperature (approximately 300 °C) SACPG 200 MW focused on the use of solar heat as a preheater for feed-water before it entering into the boiler [108]. In addition to an extensive economic feasibility analysis, a methodology for determination of a feed-in tariff is proposed in several financing scenarios based on area size, type of collector, and solar field cost. Similarly, in [107], a case study is undertaken on a typical 200 MW CFPP hybridised with PTC, where the heat generated by solar units (approximately 300 °C) is utilised for preheating of feed-water before entering the boiler. The objectives of [107] are (1) to evaluate the energy level of hybrid configurations for low- and medium-temperature CSPs, (2) to identify the impact of turbine internal efficiency on the conversion efficiency, (3) to present a new evaluation criteria for the SACPG, and (4) to use thermodynamic performance of a typical SACPG to validate the presented theoretical studies. Another study on a 300 MW SACPG test case is presented in [109] in which a PTC based solar field is integrated into the power plant. Yearly performance of a SACPG system (i.e., based on improved matrix thermal balance equation) is explored using an hourly methodology with different TES capacity, solar field sizes and load demand conditions. The capacity of TES and solar aperture area are also optimised at different loads. It can be concluded that the output of a CSP plant or SACPG system can be stabilised in the joint operation with a TES at different operating loads.

### 6.1.3 Large-scale power plant hybridisation

Some studies focus on CSP integration into larger thermal power plants. From the perspective of coupling properties and operational mechanism, authors in [110, 111] provide a methodology to include all possible mechanism of the SAPG. To this end, the operation of a supercritical CFPP hybridised with PTCs is modeled in the mode of fuel-saving employing MATLAB Simulink. The output power and efficiency for a low/intermediate/high-pressure cylinder are analysed when extraction steam is replaced by the steam provided by CSP in the feed-water heating system. A 600 MW supercritical CFPP joined with PTC as the solar technology is selected as the case study. In [112], the annual performance of another 600 MW SPT-aided CFPP is studied, and the impact of TES capacity on annual efficiency of solar-to-electric power as well as annual solar power generation is investigated. The target of TES capacity optimisation is to reach the lowest levelised cost of electricity (LCOE). Sensitivity analysis for several key economic factors is accomplished. Comparison of the obtained results with a traditional CFPP demonstrates that there is a reduction in the annual average coal consumption rate of the SPT-aided CFPP when DNI increases. Another study on a 600 MW SACPG for economic performance analysis under different TES capacities, aperture areas, and tracking modes is done in [113]. In that piece of work, hourly meteorological data are used to model the operation of a SAPG coupled with PTC technology, where feed-water is preheated by a solar field. Based on investigations of off-design and annual performances, some of the vital operating parameters of the given system including the ratio of row spacing to aperture width, solar multiple, and TES hours are optimised to reach the desirable economic and thermodynamic levels. To reach an optimised value for TES capacity, an economic sensitivity analysis similar to [112] is also performed. Ref. [114] examines the concept of CSP and CFPP combination, and calculations from their initial studies advise that a PTC could actually deliver 20% of the energy required for the steam cycle. The analysis concludes that it is economically beneficial to create an integrated solar steam cycle rather than using an isolated CSP.

Ref. [115] employs medium or low-temperature CSPs for SAPG (200-1,000 MW) purposes. Economic benefits of the SAPG with different capacities (1,000 MW and 600 MW ultra-supercritical, 600 MW subcritical, 300 MW and 200 MW typical) are evaluated. CSP with temperatures from 90 °C to 260 °C is

coupled with the aforementioned units in fuel-saving and power boosting operating modes.

## 6.2 Typical meteorological year

Typical meteorological year (TMY) data represent one-year of hourly (8,760) weather data values extracted from long-term (at a minimum, 10 years) data records [116]. TMY data are highly popular for researchers in the case of RES and building designers, since TMY can represent a concise estimated data for a typical year while representing characteristics of several years. Based on a procedure of concatenating the months from several years and weighting various weather parameters, TMY data sets are generated. For this reason, actual conditions at any given time or information of extreme events are not provided in TMY data set. Nevertheless, TMY data are effective for situations in which a RES planner intends to compare different technologies using a long-term modeling approach. Fig. 12 shows a simple sketch of TMY modeling. Although different techniques exist to generate TMY data sets, long-term weather records are utilised to create this data.

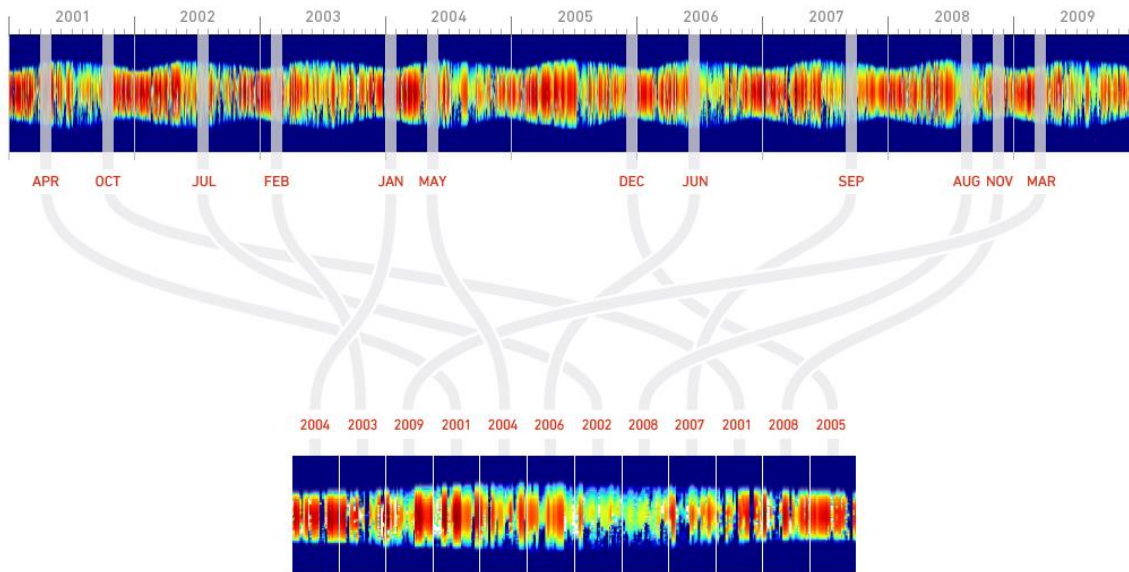


Fig. 12. An illustration typical meteorological year modeling for a full year

As detailed in [117], US national solar radiation database (NSRDB) is used to produce TMY32 data set employing an empirical method. Five weather parameters including wind speed, dew point temperature, dry bulb temperature, DNI, and global horizontal irradiance are selected for 12 months based on available

data recorded for 30 years. Considering the fact that the solar radiation parameters are assigned with the highest priority in the weighting procedure, a chosen typical month may not actually be typical for other parameters. Although TMY application for real projects is highly common and popular today, it should be mentioned that TMY data sets may have some missing points and shortages as well, for instance, extreme weather events are not included due to their low occurrence probability. In addition, TMY data are occasionally named as a P50 data set, which means that there is a 50% probability that the value of a parameter like global horizontal irradiance will exceed TMY data set. Normally, employing TMY data set, a system planner cannot investigate system performance for a mostly cloudy year or a year after some volcanic activities which affects surrounding areas. Another shortcoming of TMY data set happens in the case of missing data within the 30-year input data. As an illustration, measurement devices may be down for some hours/days or a station is closed during a maintenance period. Thus, TMY values may not characterise the true average of long-term values for a certain parameter at a given location. Even with these shortcomings, TMY is still the most popular and best available option for long-term system planners.

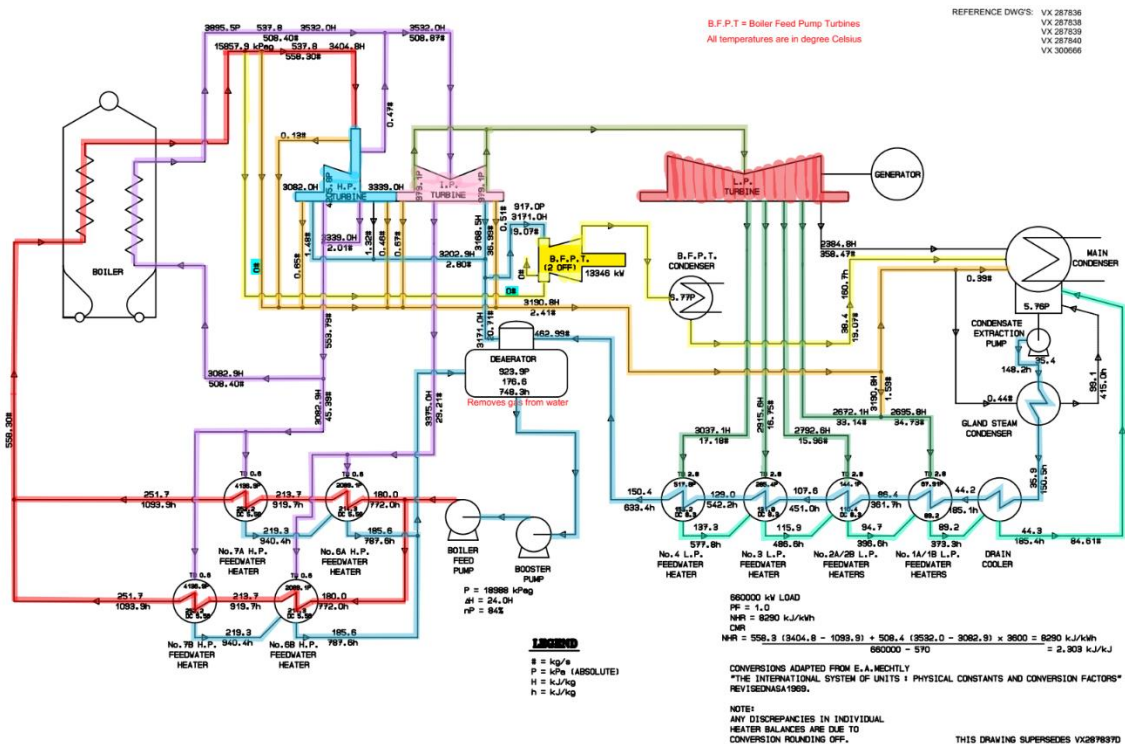


Fig. 13. A detailed configuration of a coal-fired power plant (Vales Point power station)

### 6.3 CFPP configuration

Electricity in traditional thermal power plants is produced utilising steam power. The high temperature steam turns turbines to generate electricity. A detailed configuration of a CFPP is depicted in Fig. 13. This project aims to reduce the generation costs and emissions of such a power plant using CSP and PV farm, while steam from the CSP unit will be fed into the steam cycle of the CFPP. Based on the temperature and pressure of the steam provided by the CSP unit, the joint point to the steam cycle needs to be identified. The summarised configuration of the aforementioned 600 MW CFPP integrated with solar energy is illustrated in Fig. 14.

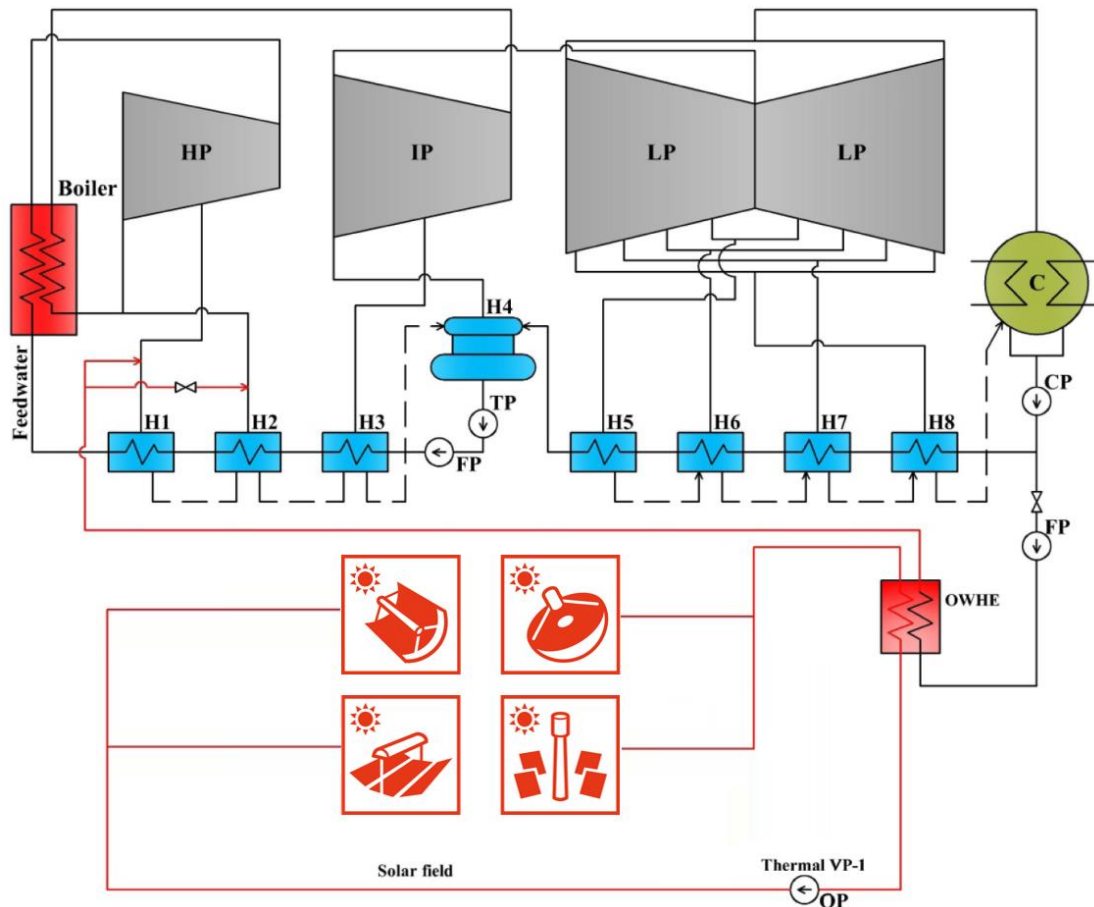


Fig. 14. Overview of a solar aided coal-fired power plant

The joint operation is to use the solar field to provide steam in order to increase temperature generated by CFPP. The SACPP configuration comprises two sub-systems: a solar collector field and CFPP. The boiler employed in CFPP is a 660 MW Toshiba. The heating sub-system for feedwater has three heaters for

high-pressure feedwater (H1-H3), a de-aerator (H4), and four heaters for low-pressure feedwater (H5- H8).

The solar collector field contains a feedwater pump (FP), an oil circulating pump (OP), two oil-water heat exchangers (OWHE), and a series of solar collectors. Additionally, there two heat exchangers (oil-water) which and thermal energy of collectors to feedwater in which oil is used as the heat transfer medium.

## **7 FORMULATION AND MATHEMATICAL MODELING OF CSP BASED POWER PLANTS**

In this project, the LCOE is considered as the main objective function, besides the project cost and emission reduction, for the preliminary assessment of the given energy-producing project. The LCOE is a fundamental factor to determine if it is financially efficient to move forward with the plan of a project or not. The LCOE index will reflect the status of a project that would be profitable or break even. In fact, one of the primary essential steps for analyzing the plane of an energy generation planning project is the LCOE calculation. A crucial reason for using LCOE is that calculation of this factor allows financial analysts to compare different energy-producing technologies (or different types of a specific power source) regardless of risks, sizes, capital costs, and unequal life spans of technologies used in a project. Since the per-unit cost of generated power is determined by LCOE, it can be considered as an average minimum selling price by which lifetime production revenue compensates primary investment costs in a defined payback period. In sum, similar to the concept of net present value (NPV), LCOE indicates how worthwhile a project is [3]. Whilst the LCOE is a common and widely-used metric in energy economics, the use of LCOE to compare non-dispatchable (e.g., wind, solar photovoltaic) and dispatchable (e.g., coal, gas-fired) generation technologies is fundamentally flawed as it assumes a single homogenous price for the marginal value of all electricity produced (\$/MWh). However, this point is not significantly highlighted in this project as the comparison is accomplished among different types of renewable solar technology (different types of CSP and PV). This objective is constrained to several operating and financial constraints in this project. Additionally, there are some practical constraints related to the site of CFPP (e.g., the level of solar radiation, or limitation on land availability for solar farm construction that is modeled by solar-multiple limitation). In order to reach an accurate financial estimation, a large number of technical constraints and modeling related to the technical operation of solar units (e.g., detailed specifications of solar collector and receivers, type of heat fluid in CSP units, capacity and type of thermal and electrical storage units, and joint point of solar technology into CFPP) need to be taken into account. A highlighted point about this project is the presentation of Pareto front solutions, instead of a single design point, for different objective

functions. In other words, a set of solutions indicating different planning points will assist the decision-makers in reaching possible options for investment.

## **7.1 CSP system formulation**

### **7.1.1 Objective function**

LCOE denotes the revenue per unit of produced electric power to recover the costs of constructing and operating a generating power plant during a pre-defined life-span. LCOE is frequently regarded as a suitable measure of the overall competitiveness of diverse producing technologies [4]. However, there are some flaws associated with this index. When two power generation technologies are being compared and they can provide the same services that a grid requires to function, such as frequency control and inertia, and can deliver 24/7 dispatchable power, this index works fine. However, the issue occurs when comparing one technology that has these services and one that does not. For example, one technology that can deliver power at nighttime and one that cannot. Without a value on grid services or dispatchability, the simple metric cannot include these in the calculations. In such a situation, the total system cost is the most useful metric to value a technology, as it looks at the whole electricity system across all timescales. It is important to remember that no power generation technology should be assessed in isolation if it is to be incorporated into the grid. There are three main points that total systems cost (TSC) addresses and distinguishes it from LCOE: 1) the value of a power generation technology depends on an existing grid, 2) energy supply is only one of several services that technologies bring to a grid, 3) aiming for intermediate emissions reduction targets without considering the long-term goals can lead to poor decisions.

The main factors to calculate LCOE include financing costs, variable and fixed operations and maintenance (O&M) costs, fuel costs, and capital costs. The importance of each factor may vary for different technologies and projects. Additionally, there are some uncertainties associated with these factors since the value of these parameters may change temporally and regionally due to the advancement of technologies and change of fuel prices. The first objective is to minimise LCOE, where the LCOE is calculated as follows by a simple method from [118].



$$\text{Min LCOE}^{CSP} = \frac{FCR^{CSP} \cdot TCC^{CSP} + FOC^{CSP}}{AEP^{CSP}} + VOC^{CSP} \quad (1)$$

where  $TCC$  is the total capital cost,  $FOC$  is fixed annual operating cost,  $VOC$  is variable operating cost,  $FCR$  fixed charge rate, and  $AEP$  is the annual electricity production. The second objective is to minimise the emission after the CSP integration into the CFPP:

$$\text{Min Em}^{CSP} = St^{CSP} * CR^{CFPP} * CRP^{CFPP} \quad (2)$$

where  $St^{CSP}$  is the annual steam provided by CSP,  $CR^{CFPP}$  is the coal consumption rate per steam unit, and  $CRP^{CFPP}$  is the price of the coal. Different terms of the first objective function are defined as follows:

$$\begin{aligned} TCC^{CSP} = & SF^{CSP} \cdot C_{SF}^{CSP} + SI^{CSP} \cdot C_{SI}^{CSP} + HTF^{CSP} \cdot C_{HTF}^{CSP} + HS^{CSP} \cdot C_{HS}^{CSP} \\ & + PP^{CSP} \cdot C_{PP}^{CSP} + BP^{CSP} \cdot C_{BP}^{CSP} \end{aligned} \quad (3)$$

where  $SF^{CSP}$  is the area required for installing the solar field,  $SI^{CSP}$  is the land area needed to be further invested for solar field (i.e., can be considered as the same as  $SF^{CSP}$  value),  $HTF^{CSP}$  is the area necessary for installing the heat transfer fluid pumps and piping,  $HS^{CSP}$  is the thermal capacity of heat storage,  $PP^{CSP}$  refers to the electrical capacity of power plant if there is a separate turbine-generator for power generation, and  $BP^{CSP}$  is the block gross capacity to account for additional costs (i.e., can be considered as the same as  $PP^{CSP}$  value). In this regard,  $C_{\theta}^{CSP}$ ,  $\forall \theta \in SF, SI, HTF, HS, PP, \text{ and } BP$ , refer to their corresponding costs which include the costs of equipment and the need to cover investment costs. An  $FCR^{CSP}$  multiplied by the total investment will determine the yearly revenue needed to support the investment. Detailed formulations of  $FCR^{CSP}$  are provided in pp. 22-24 of [119].

Parameters of  $FOC^{CSP}$  and  $VOC^{CSP}$  are the fixed and variable operation and maintenance costs, which are calculated as follows:

$$FOC^{CSP} = \sum_{n=1}^N C_{FCC}^{CSP} \cdot r^n \cdot PP^{CSP} \quad (4)$$

$$VOC^{CSP} = \sum_{n=1}^N C_{VOC}^{CSP} \cdot r^n \cdot AEP^{CSP} \quad (5)$$

where  $C_{FCC}^{CSP}$  is a fixed cost proportional to the system's rated or nameplate capacity and  $C_{VOC}^{CSP}$  is a fixed cost

proportional to the amount of electricity the system generated annually. The multiplier  $r$  is the inflation rate which is updated annually by a parameter  $n$  within operation period.  $AEP^{CSP}$  is optimised within the program to reach the highest value through scheduling of thermal/electrical generating units and thermal storage. Generally, two different types of technical and financial parameters are involved in simulations to calculate the objective function. In case of technical parameters, Sections 8.1.1-8.1.5 provide the detailed technical specifications of parabolic trough CSP, and Sections 8.2.1-8.2.5 present the relevant parameters for central tower CSPs. These parameters are used to evaluate technical performance of CSP systems and subsequently to evaluate the yearly energy production of solar plants. In addition, the financial parameters are detailed in Section 8.1.6 for parabolic trough CSP and Section 8.2.6 for central tower CSP. A 25-year period is considered as the lifespan of CSP units.

### 7.1.2 Constraints

This objective function is subject to the following constraints:

- **CSP solar multiple**

$$M_{Low}^{CSP} \leq SM^{CSP} \leq M_{High}^{CSP} \quad (6)$$

where  $SM^{CSP}$  is a value specified for solar multiple and is limited between two constant values of  $M_{Low}^{CSP}$  and  $M_{High}^{CSP}$ . The ratio between the produced thermal power of the solar field and the thermal power needed to run the power block at its nominal conditions is named the solar multiple. Solar multiple for CSP plants (specifically when operating on stand-alone mode) should always be a value bigger than one to reach nominal conditions on the power block. Nevertheless, the lack of thermal storage while having a large value for solar multiple leads to overproduction and waste of the produced thermal energy, while this situation will never happen in this study since all steam provided by CSP units can be fed into the power block of Vales Point CFPP. Therefore, the only limitations for increasing the solar multiple relate to firstly, the lack of space near the Vales Point power plant and secondly, design problems for the development of the huge solar field and solar receiver. Sizing the solar field of a CSP involves the determination of the optimal solar field aperture area for a system at a given location.

- **CSP capacity (MWe)**

$$Cap_{Low}^{CSP} \leq PP^{CSP} \leq Cap_{High}^{CSP} \quad (7)$$

where  $PP^{CSP}$  refers to the CSP system's rated size (i.e., limited between two user-defined value  $Cap_{Low}^{CSP}$  and  $Cap_{High}^{CSP}$ ) for the calculation of parameters related to capacity (e.g., estimated overall cost per net capacity amount of the capacity factor and system cost).

- **CSP thermal storage capacity (MWt)**

$$HS_{Low}^{TES,CSP} \leq HS^{CSP} \leq HS_{High}^{TES,CSP} \quad (8)$$

A TES system is used to store heat in the form of a liquid medium produced by the solar field, which can assist in turning the turbine during hours with no/low sun irradiation. A TES is valuable on numerous occasions where the peak of load demand happens after sunset. Within the optimisation procedure of finding optimal capacity for TES  $HS^{CSP}$ , it is limited to two boundary values of  $HS_{Low}^{TES,CSP}$  and  $HS_{High}^{TES,CSP}$ .

- **Total capital cost**

Similar to all planning projects, one of the most vital conditions for project establishment is the margin of investment. Therefore, the total investment amount of the project  $TCC$  is limited by low and upper bounds as follows.

$$TCC_{Low}^{CSP} \leq TCC^{CSP} \leq TCC_{High}^{CSP} \quad (9)$$

- **Solar collector assembly type**

$$SCA^{CSP} \in \{S_1, S_2, \dots, S_n\} \quad (10)$$

The solar collector assembly (SCA) describes some types of the collector (i.e.,  $S_1, S_2, \dots, S_n$ ) which are different in terms of the collector dimensions and optical characteristics. In this project, a number of predefined types of collectors are investigated which are diverse in SCA length, aperture, aperture reflective area, average focal length.

- **CSP receiver type**

$$HCE^{CSP} \in \{H_1, H_2, \dots, H_n\} \quad (11)$$

A heat collection element (HCE) is a metal pipe contained in a vacuum within a glass tube that runs through the focal line of the trough-shaped parabolic collector [120]. The HCE variable describes the

properties that can make up the solar field. In this project, a number of predefined types of the receiver (i.e.,  $H_1, H_2, \dots, H_n$ ) are investigated which are diverse in optical efficiency, heat loss factor, and level of absorption.

- **CSP injection point**

Finding an optimal point for CSP injection into the thermal steam cycle of the power plant is another vital issue which is investigated in this project. Considering the fact that steam provided by different types of CSP technology (i.e., including trough, tower, Fresnel, and dish) may have different levels of pressure and temperature, the connection point to the Rankine cycle can provide the opportunity to utilise different technologies with various operating specifications.

## 7.2 PV system formulation

### 7.2.1 Objective function

Similar to the CSP objective, the minimum LCOE is considered as the objective in this section for PV systems. In this project, PV systems will be used for spinning reserve and/or to supply the internal usage of the power plant. Similar to CSP modeling, the first objective function on LCOE is considered as follows:

$$\text{Min } LCOE^{PV} = \frac{FCR^{PV} \cdot TCC^{PV} + FOC^{PV}}{AEP^{PV}} + VOC^{PV} \quad (12)$$

where  $TCC$  is the total capital cost,  $FOC$  is fixed annual operating cost,  $VOC$  is variable operating cost,  $FCR$  is the fixed charge rate, and  $AEP$  is the annual electricity production. The second objective is to reduce emissions as the result of PV integration as follows:

$$Em^{PV} = Pt^{PV} * CR^{CFPP} * CRP^{CFPP} \quad (13)$$

where  $Pt^{PV}$  is the annual power provided by CSP,  $CR^{CFPP}$  is the coal rate consumption per MW power unit, and  $CRP^{CFPP}$  is the price of the coal.

Different terms of the first objective function are defined as follows:

$$\begin{aligned} TCC^{PV} = SF^{PV} \cdot C_{SF}^{PV} + SI^{PV} \cdot C_{SI}^{PV} + HTF^{PV} \cdot C_{HTF}^{PV} \\ + BS^{PV} \cdot C_{BS}^{PV} + PP^{PV} \cdot C_{PP}^{PV} \end{aligned} \quad (14)$$

where  $SF^{PV}$  is the area required for installation of the PV panels,  $SI^{PV}$  is the land area needed to be

improved for PV panels (i.e., can be considered as the same as  $SF^{CSP}$  value),  $HTF^{PV}$  is the area necessary for installation of converters,  $BS^{PV}$  is the capacity of electrical storage,  $PP^{PV}$  refers to the electrical capacity of PV power plant. In this regard,  $C_{\vartheta}^{PV}$ ,  $\forall \vartheta \in SF, SI, HTF, BS, \text{ and } PP$ , refer to their corresponding costs which include costs of equipment and amounts needed to cover investment costs.

Parameters of  $FOC^{PV}$  and  $VOC^{PV}$  are fixed and variable operation and maintenance costs, which are calculated as follows:

$$FOC^{PV} = \sum_{n=1}^N C_{FCC}^{PV} \cdot r^n \cdot PP^{PV} \quad (15)$$

$$VOC^{PV} = \sum_{n=1}^N C_{VOC}^{PV} \cdot r^n \cdot AEP^{PV} \quad (16)$$

where  $C_{FCC}^{PV}$  is a fixed cost proportional to system's rated or nameplate capacity ( $PP^{PV}$ ) and  $C_{VOC}^{PV}$  is a fixed cost proportional to the amount of electricity the system generates annually ( $AEP^{PV}$ ). The multiplier  $r$  is the inflation rate defined earlier.

Similar to CSP systems, two different types of technical and financial parameters are involved in simulations to calculate the objective function for the PV system. In case of technical parameters, Sections 8.3.1-8.3.4 provide the detailed technical specifications of the PV system. These parameters are used to evaluate the technical performance of PV solar units and subsequently to evaluate their yearly energy production. In addition, the financial parameters are detailed in Section 8.3.5. A 25-year period is considered as the lifespan of PV units as well.

## 7.2.2 Constraints

These objective functions are constrained by the following constraints:

- **PV solar multiple**

$$M_{Low}^{PV} \leq SM^{PV} \leq M_{High}^{PV} \quad (17)$$

where  $SM^{PV}$  is a value specified for solar multiple and is bounded by two constant values of  $M_{Low}^{PV}$  and  $M_{High}^{PV}$ . Similar to CSP system, sizing the solar field of a PV involves the determination of the optimal PV field aperture area for a system at a given location. Larger SM values mean larger land areas

occupied by PV panel and higher capital cost. An optimum value of solar multiple can optimise the utilisation of battery unit and more annual power provision which results in lower LCOE.

- **PV capacity (MWe)**

$$Cap_{Low}^{PV} \leq PP^{PV} \leq Cap_{High}^{PV} \quad (18)$$

PV system's rated size is limited between two user-defined values  $Cap_{Low}^{PV}$  and  $Cap_{High}^{PV}$  for the calculation of capacity-related parameters (e.g., capacity factor and the estimation of total cost per net capacity).

- **PV electrical storage capacity (MWe)**

$$BS_{Low}^{BS,PV} \leq BS^{PV} \leq BS_{High}^{BS,PV} \quad (19)$$

A battery storage system stores energy provided by PV. Within the optimisation procedure of finding optimal capacity for battery bank  $BS^{PV}$ , this value is limited to two boundary values of  $BS_{Low}^{BS,PV}$  and  $BS_{High}^{BS,PV}$ .

- **Total capital cost**

Similar to all CSP plants, one of the most important limitations is to have the margin for PV investment. Therefore, the total PV investment amount of the project is bounded by a higher limit as follows.

$$TCC_{Low}^{PV} \leq TCC^{PV} \leq TCC_{High}^{PV} \quad (20)$$

- **PV panel module**

$$SCA^{PV} \in \{A_1, A_2, \dots, A_n\} \quad (21)$$

The PV panel type describes some types of the PV module (i.e.,  $A_1, A_2, \dots, A_n$ ) which are different in the optical characteristics and output power of the panels. In this project, a number of predefined types of PV panels are investigated.

- **PV inverter type**

$$PIT^{PV} \in \{I_1, I_2, \dots, I_n\} \quad (22)$$

In this project, a number of predefined types of the receiver (i.e.,  $I_1, I_2, \dots, I_n$ ) are investigated which are diverse in electrical efficiency, power loss factor, and demanded ambient efficiency.

### 7.3 Whole system formulation

The objective functions for the whole system including both CSP and PV are the same as those defined for CSP and PV systems, thus not repeated here (i.e., all the objectives for independent CSP and PV will be included for the whole system design).

#### 7.3.1 Constraints

In addition to constraints defined for each of PV and CSP technologies, there are some limitations for the planning of the entire system as follows:

- **System solar multiple**

As mentioned before, solar multiple is a parameter which can control the size of the solar farm. Considering the land usage is directly related to values of PV and CSP solar multiples, the summation of solar multiples for the whole system is limited to a pre-specified range of  $M_{Low}^{Sys}$  and  $M_{High}^{Sys}$  as follows:

$$M_{Low}^{Sys} \leq SM^{CSP} + SM^{PV} \leq M_{High}^{Sys} \quad (23)$$

- **System total investment cost**

Considering the limited budget of the whole project, there is a limitation for total capital investment as follows:

$$TCC_{Low}^{Sys} \leq TCC^{CSP} + TCC^{PV} \leq TCC_{High}^{Sys} \quad (24)$$

Normally, there should be a compromise between capital cost and value of objective functions. Higher investment cost can provide system with less emission and lower values of LCOE.

## 8 SIMULATION AND RESULTS

In this section, three scenarios including the involvement of parabolic trough and central receiver CSP systems as well as the photovoltaic system are developed. In each scenario, the input data related to simulations are firstly provided in detail. Then, the corresponding results are presented. A list of investment options along with their corresponding configurations for PV-battery, parabolic trough CSP-thermal storage and central power CSP-thermal storage obtained in this section are provided in Appendix B. All prices and costs are in Australian Dollars. In this project, meteorological data of NSW Gosford Narara Research is used for system planning. The specifications of the recording station are presented in Table 17.

TABLE 17. SPECIFICATIONS OF NSW GOSFORD NARARA METEOROLOGICAL RESEARCH CENTER

Latitude	Longitude	Time zone	Elevation	Station ID	Source
-33.4	151.333	10	20	947,770	ISD-TMYx

As mentioned in previous sections, the data of TMY has been employed as the meteorological data which cover the most traditional weather condition for the selected location. The data collected from the years 2003-2017 are used for the simulation part. For the solar irradiance, there are two main components including DNI. The radiation which derives directly from the sun with least weakening by atmosphere or obstacles of the earth is called DNI. Diffuse solar radiation (also called DHI) is dispersed, absorbed, and reflected within the atmosphere, regularly by clouds, but also by gas molecules and particulate matter. The global radiation is formed as a factored summation of these two components. As opposed to PV panels which can efficiently work with diffuse irradiance, the DNI is the main component for the effective operation of CSP technology. The TMY record for hourly global irradiance is depicted in Fig. 15. As can be seen, the first and ending months of the year have the highest global irradiance while the value of this parameter is decreased during the months of May to July. It should be mentioned that along with a decrease in the weather temperature, the CFPP may face a seasonal increase in the load demand. In such a situation, the configuration of the CSP plant should be as a compromise between the size and capital investment. As can be seen in Fig. 16, there are fewer variations in the case of DNI which are suitable for the operation of



CSP units. The amount of irradiance recorded for DHI is shown in Fig. 17. However, this parameter is not highly effective for CSP plants, while it is highly important for planning of PV systems.

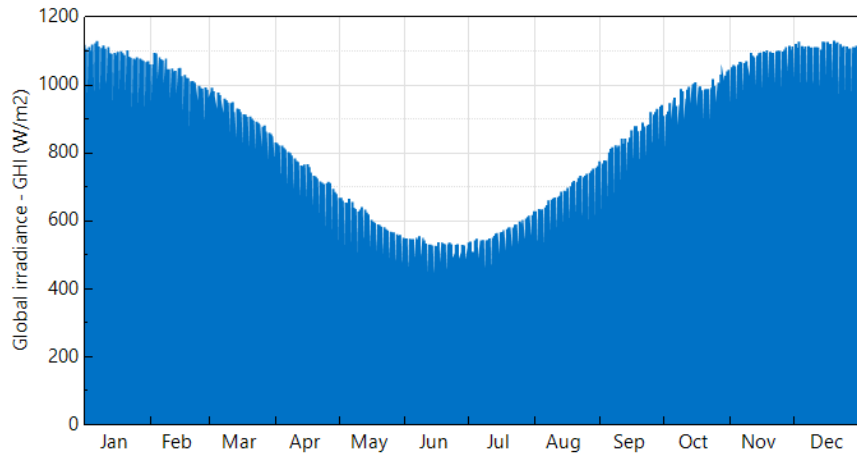


Fig. 15. Hourly global irradiance recorded in the meteorological station

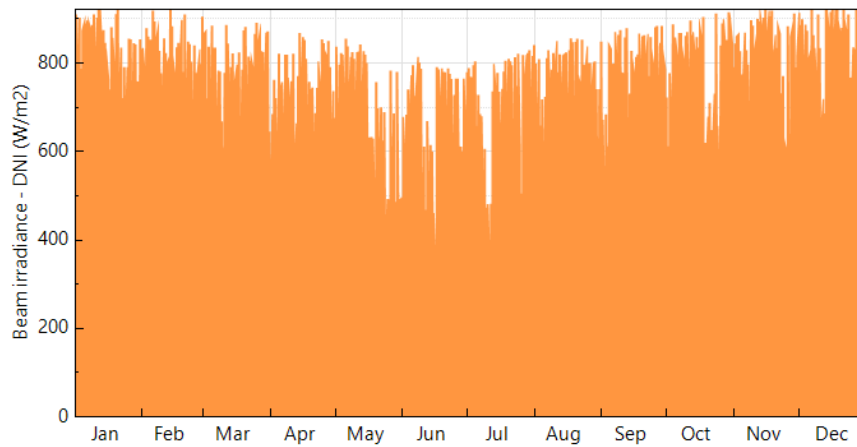


Fig. 16. Hourly beam irradiance recorded in the meteorological station

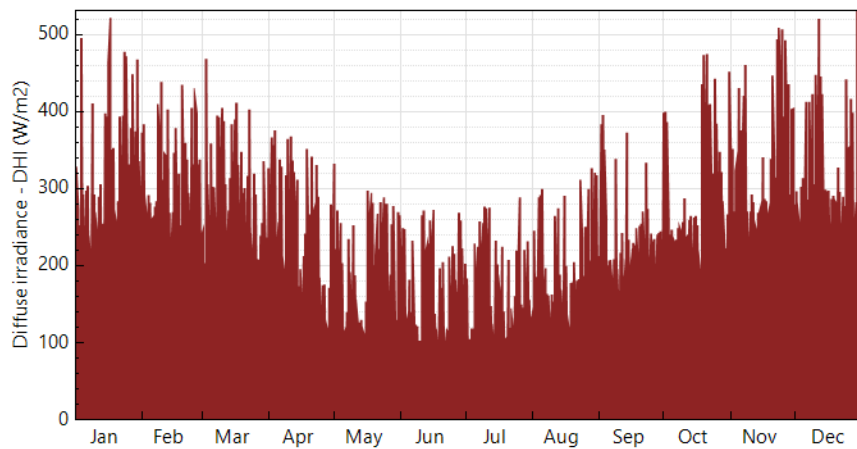


Fig. 17. Hourly diffuse irradiance recorded in the meteorological station

The values of wind speed and dew point temperature are shown in Fig. 18 and Fig. 19.

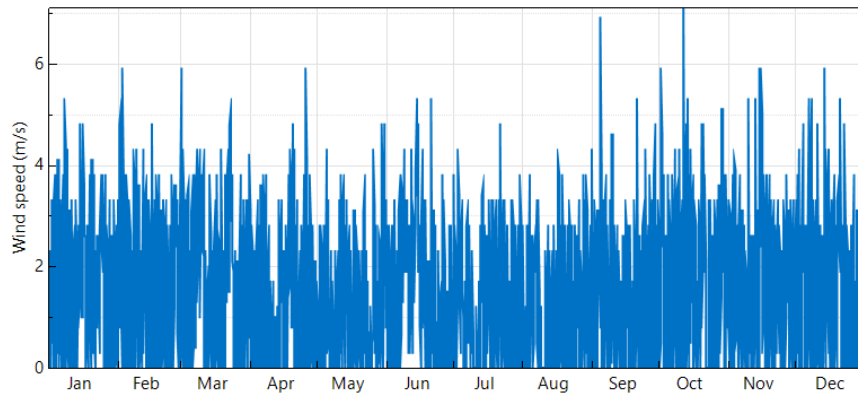


Fig. 18. Hourly wind speed recorded in the meteorological station

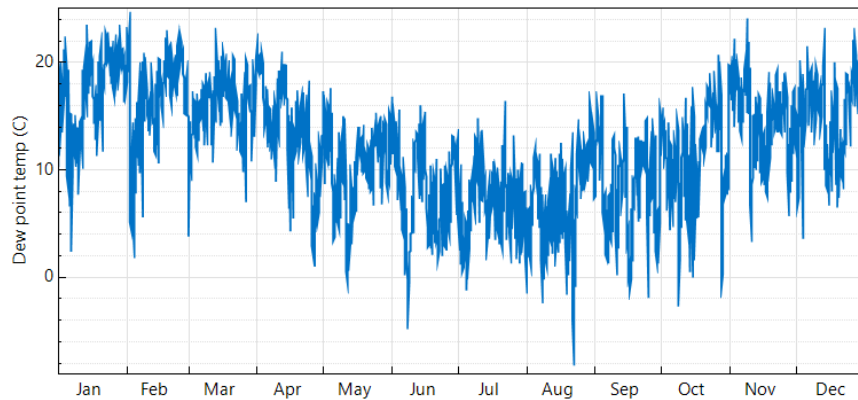


Fig. 19. Hourly dew point temperature recorded in the meteorological station

Both CSP mirrors and PV panels are affected by wind parameters. In addition to the instantaneous solar radiation, the efficiency of PV units is also influenced by module temperature. Although high wind speed may result in a long-term degradation of panels, the cooling effect of the wind can improve the efficiency of PV units. The efficiency of CSP mirrors may also be affected by particles carried in the air during the windy seasons. Such an effect may cause sand-blasting of the surfaces, which leads to less light reaching the semiconductor layer in PV and a lower coefficient of reflection in CSP. The current recorded wind speed may not significantly help PV units through the cooling procedure, it however guarantees fewer negative effects on solar systems. The monthly comparison of different irradiance is shown in Fig. 20. The lowest curve indicates the amount of diffused irradiance. It is important to mention that the values of global irradiance during some months are less than those of direct irradiance. Based on the explanations mentioned

before, a high level of DNI is suitable for the development of a CSP plant while the temperature, as can be seen in Fig. 21, is lower during this season.

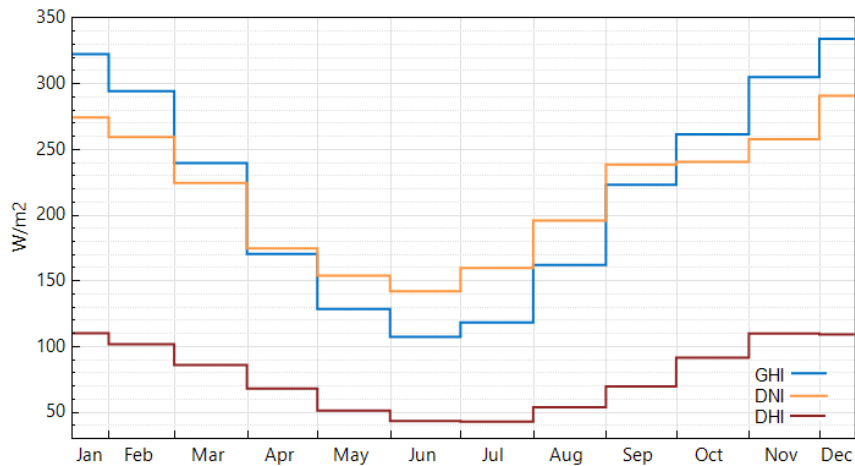


Fig. 20. Monthly irradiance recorded in the meteorological station

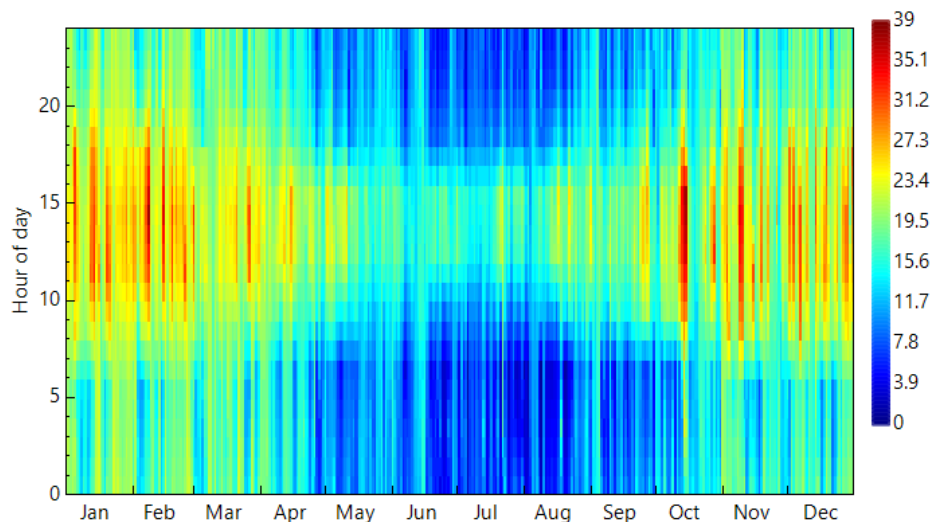


Fig. 21. Monthly heat map of dry-bulb temperature recorded in the meteorological station

The average monthly wind speed and wind direction recorded in the meteorological station is shown in Fig. 22. It shows that during the hot seasons, there also exist more wind that is suitable for PV units. Considering the fact that CFPP in this project is established in a place (i.e., Mannering Park NSW 2259) in which the weather has a low amount of dust to surrounding vegetation and Lake Macquarie, the degrading effect is negligible. Moreover, the highest wind speed (i.e., happening during month Nov) is around 6.48 km/h which will not cause damage to the infrastructure. Wind direction changes are around 25° during a year which demonstrates the nearly stable situation of weather.

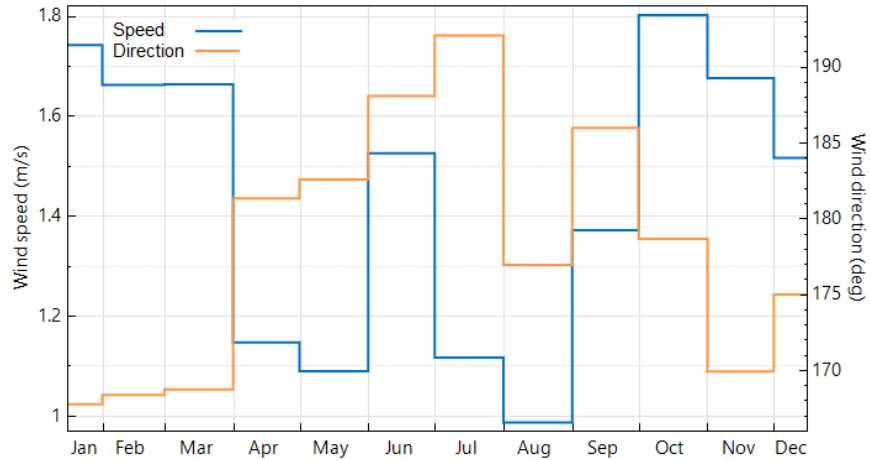


Fig. 22. Monthly wind speed and wind direction recorded in the meteorological station

The profile of irradiance for different months is shown in Fig. 23. Separate from the amount of irradiance which has been discussed in detail in previous figures, another critical point is in the case of the number of hours in which irradiance is available.

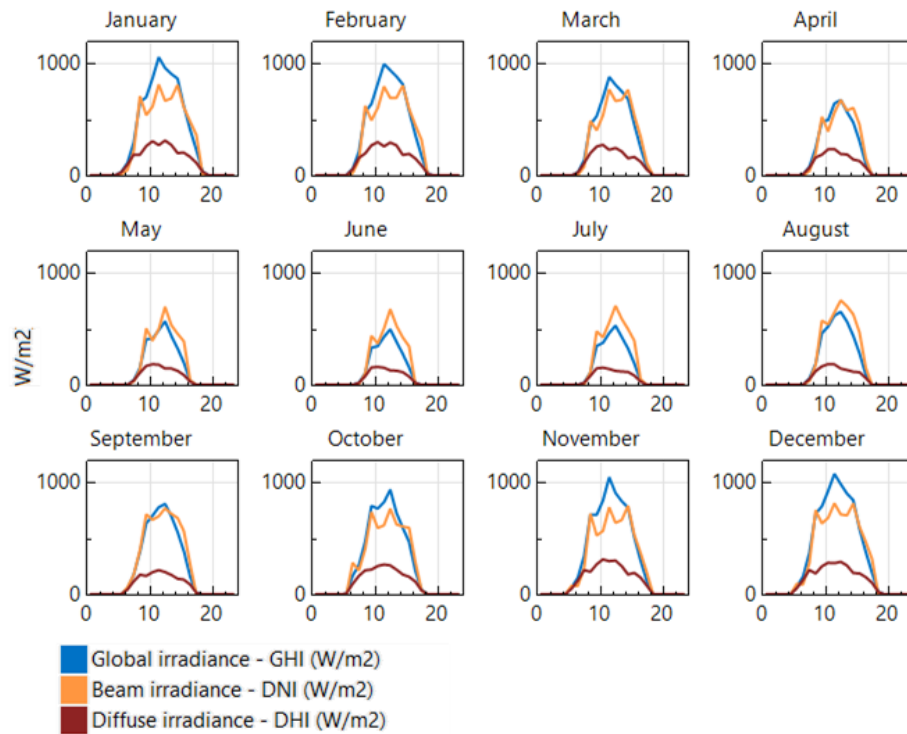


Fig. 23. Monthly profile of different irradiances recorded in the meteorological station

It can be seen that daytime (here it refers to hours with DNI availability) during months May-Aug is around 3-4 hours less than the other months of the year. The duration curve depicted in Fig. 24 shows the limits and frequency of wind speed and solar irradiations.

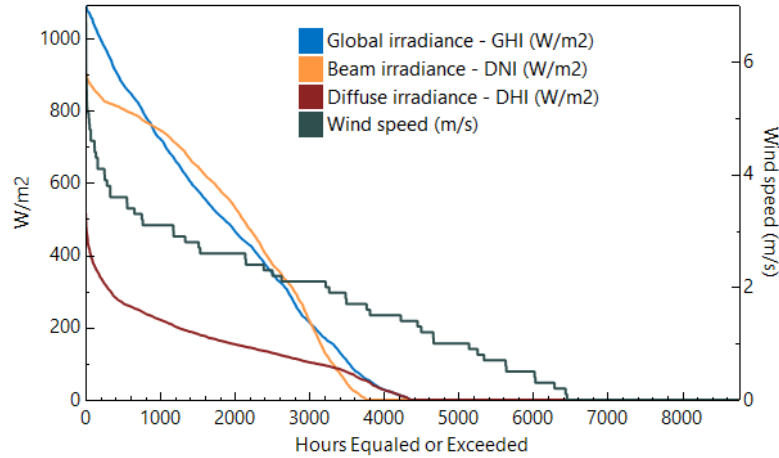


Fig. 24. Duration curve of different irradiances and wind speed in the meteorological station

It can be inferred that the maximum wind speed around 1.8 m/s at low frequency is possible for the targeted location which is not destructive. Alternatively, there is no/very low-speed wind (under 1m/s) for a significant period of the time during the year. Considering the night periods, zero irradiation covers a large number of hours in which solar power (from CSP and PV units) is not available. Finally, the average annual value of some of the most important meteorological parameters is detailed in Table 18.

TABLE 18. AVERAGE ANNUAL VALUE OF METEOROLOGICAL PARAMETERS

Parameter	Unit	Value
Global horizontal	kWh/m <sup>2</sup> /day	5.32
Direct normal (beam)	kWh/m <sup>2</sup> /day	5.21
Diffuse horizontal	kWh/m <sup>2</sup> /day	1.86
Temperature	°C	16.5
Wind speed	m/s	1.4

Low wind speed and temperature are two suitable factors for the development of solar units (both PV and CSP). Based on [74], the minimum suitable DNI for CSP is 2,000 kWh/m<sup>2</sup>/year. Considering the average value of 5.21 kWh/m<sup>2</sup>/day, the selected location is marginally acceptable for the CSP development. Three scenarios with involvement of a parabolic trough, central receiver, and PV farm are considered in this project to obtain the optimal configuration of CSP and PV units. Results of these scenarios demonstrate the type of CSP plant which is suitable for integration with CFPP and the optimal technical and financial parameters which are also determined.

## 8.1 Scenario 1: Parabolic trough CSP

The first scenario investigates the application of PTC for integration into the NSW Vales Point CFPP. This section aims to find an optimal value for technical CSP parameters including solar multiple (i.e., previously explained in CSP system formulation), electrical CSP capacity, CSP thermal storage capacity, full load hours of TES, fluid type, solar collector assembly type, CSP receiver type, and CSP injection point. The point of connecting CSP into the Rankine cycle is adopted based on HTF outlet temperature. Since the power block is available by employing the capability of the CFPP, the investigation on integration point is done when the optimal financial and technical parameters of the CSP unit are determined. The constraint related to land area limitation is modeled in the form of solar multiple. The range decision variables are selected as detailed in Table 19.

TABLE 19. OBJECTIVE PARAMETERS FOR PARABOLIC TROUGH COLLECTOR OPTIMISATION

Parameter	Min	Max	Steps
Solar multiple	1.2	1.7	0.05
CSP capacity (MWe)	80	110	5
CSP thermal storage capacity (MWt)	20	30	2
Full load hours of TES [h]	6	10	2
Fluid type	-	-	Hitec XL, Caloria HT 43, Therminol VP-1
Receiver type	-	-	Solel UVAC 3, Schott PTR80

Total capital cost, LCOE, and emission are considered as output variables. The emission of CFPP is defined as a linear function of the annual energy production of the power plant. Based on [75], the energy intensity rate of Vales Point CFPP is 0.86 Tonne of CO<sub>2eq</sub>/MWh. In this regard, the emission production of this power plant for the year 2017-2018 is 7,015,626 Tonne of CO<sub>2eq</sub>/year.

### 8.1.1 Specifications of the solar field

This section provides the specification of the solar field. As detailed in Table 20, a system including several parallel rows is developed for the solar field in which the number of rows depends on the selected solar multiple.

TABLE 20. SPECIFICATIONS OF SOLAR FIELD (PARABOLIC TROUGH COLLECTOR)

Parameter	Unit	Value	Parameter	Unit	Value
Row spacing	m	15	Header pipe roughness	m	4.57e-5
Stow angle	Degree	170	HTF pump efficiency	%	85
Deploy angle	Degree	10	Freeze protection temp	°C	150
Number of field subsections	-	2	Irradiation at design	W/m <sup>2</sup>	950

Besides, specifications of HTFs are provided in Table 21. In this case, three different commercial HTFs are considered for the joint operation modelling. Not only should the optimal HTF output temperature be suitable for the integration into the CFPP, but also the minimum operating temperature of HTF should be appropriate based on the weather conditions of the CFPP.

TABLE 21. SPECIFICATIONS OF SELECTED HEAT TRANSFER FLUIDS (PARABOLIC TROUGH COLLECTOR)

Name	Type	Min Optimal Operating Temp (°C)	Max Optimal Operating Temp (°C)	Freeze Point (°C)
Hitec XL	Nitrate salt	120	500	120
Caloria HT 43	Mineral hydrocarbon	-12	385	-12 (pour point)
Therminol VP-1	A mixture of Biphenyl and Diphenyl Oxide	12	400	12 (crystallisation point)

The design point variables of the solar field such as the aperture area of a single loop of collectors, optical efficiency, and aperture reflective area are calculated automatically in SAM software. The design parameters of the solar field are provided in Table 22. It should be noted that the inlet and outlet temperatures of the solar field may vary during the operation period.

TABLE 22. GENERAL SPECIFICATION OF SOLAR FIELD (PARABOLIC TROUGH COLLECTOR)

Parameter	Unit	Value	Parameter	Unit	Value
Design loop inlet temp	°C	293	Water usage per wash	L/m <sup>2</sup> , aper	0.7
Design loop outlet temp	°C	391	Washes per year	-	63
Min single loop flow rate	kg/s	1	Non-solar field land area multiplier	-	1.2
Max single loop flow rate	kg/s	12			

### 8.1.2 Specifications of collector

The specifications of the collector are shown in Table 23. As can be seen, SkyFuel SkyTrough (with 80-mm OD receiver) is selected as a receiver type which is one of the proven industrial types. However, it is

possible to select other types of collector provided in SAM software as well. There is also the option in SAM software either to use a combination of different collector types or adding a new collector type when extending solar farm.

TABLE 23. DETAILED TECHNICAL CHARACTERISTICS OF SELECTED COLLECTOR TYPES (PARABOLIC TROUGH COLLECTOR)

Collector Type

Collector name from library

Collector Geometry			
Reflective aperture area	<input type="text" value="656"/> m <sup>2</sup>	Number of modules per assembly	<input type="text" value="8"/>
Aperture width, total structure	<input type="text" value="6"/> m	Average surface-to-focus path length	<input type="text" value="2.15"/> m
Length of collector assembly	<input type="text" value="115"/> m	Piping distance between assemblies	<input type="text" value="1"/> m

Optical Parameters			
Incidence angle modifier coefficients		Geometry effects	<input type="text" value="0.952"/>
Tracking error	<input type="text" value="0.988"/>	Mirror reflectance	<input type="text" value="0.93"/>
General optical error	<input type="text" value="1"/>	Dirt on mirror	<input type="text" value="0.97"/>

Optical Calculations			
Length of single module	<input type="text" value="14.375"/> m	End loss at summer solstice	<input type="text" value="0.998602"/>
IAM at summer solstice	<input type="text" value="0.816056"/>	Optical efficiency at design	<input type="text" value="0.848494"/>

The parameters highlighted in blue colour are calculated by SAM based on data provided in the solar field. Although other parameters can be tuned and optimised within the planning procedure, it is preferred not to involve them as decision variables to avoid making the modeling part highly extensive.

### 8.1.3 Specifications of receiver

As mentioned before, two different types of the receiver including Solel UVAC 3 and Schott PTR80 are considered in this project. The specifications of potential receivers are detailed in Table 24 and Table 25. In the case of the receiver, heat loss and optical derate are the vital issues that are determined based on the physical features of the receiver. We consider different options for selecting components to reach the most optimal configuration. Different CSP manufacturers prefer to use their own optimised configuration which may be less optimised than those results obtained in this project.

### 8.1.4 Power cycle specifications

The thermal energy produced by CSP is converted to the electric energy in the power cycle. Considering the fact that the CSP block will provide steam for CFPP, the pressure and temperature of steam for the



TABLE 24. DETAILED TECHNICAL CHARACTERISTICS OF SELECTED RECEIVER TYPES (PART 1) - (PARABOLIC TROUGH)

Receiver Type

Receiver name from library: Solel UVAC 3

**Receiver Geometry**

Absorber tube inner diameter	0.066 m	Absorber flow plug diameter	0 m
Absorber tube outer diameter	0.07 m	Internal surface roughness	4.5e-05
Glass envelope inner diameter	0.115 m	Absorber flow pattern	Tube flow
Glass envelope outer diameter	0.121 m	Absorber material type	304L

**Parameters and Variations**

	Variation 1	Variation 2	Variation 3	Variation 4*
Variant weighting fraction*	0.985	0.01	0.005	0
<b>Absorber Parameters:</b>				
Absorber absorptance	0.96	0.96	0.9	0
Absorber emittance	Table...	0.65	0.65	0
<b>Envelope Parameters:</b>				
Envelope absorptance	0.02	0.02	0	0
Envelope emittance	0.86	0.86	1	0
Envelope transmittance	0.96	0.96	1	0
	<input type="checkbox"/> Broken Glass	<input type="checkbox"/> Broken Glass	<input checked="" type="checkbox"/> Broken Glass	<input type="checkbox"/> Broken Glass
<b>Gas Parameters:</b>				
Annulus gas type	Hydrogen	Air	Air	Hydrogen
Annulus pressure (torr)	0.0001	750	750	0
<b>Heat Loss at Design:</b>				
Estimated avg. heat loss (W/m)	175	1100	1500	0
<b>Optical Effects:</b>				
Bellows shadowing	0.971	0.971	0.971	0.963
Dirt on receiver	0.98	0.98	1	0.98

\* The variant weighting fractions and Variation 4 inputs are not part of the library.

**Total Weighted Losses**

Heat loss at design: 190.875 W/m

Optical derate: 0.876961

TABLE 25. DETAILED TECHNICAL CHARACTERISTICS OF SELECTED RECEIVER TYPES (PART 2) – (PARABOLIC TROUGH)

Receiver Type

Receiver name from library: Schott PTR80

**Receiver Geometry**

Absorber tube inner diameter	0.076 m	Absorber flow plug diameter	0 m
Absorber tube outer diameter	0.08 m	Internal surface roughness	4.5e-05
Glass envelope inner diameter	0.115 m	Absorber flow pattern	Annular flow
Glass envelope outer diameter	0.12 m	Absorber material type	304L

**Parameters and Variations**

	Variation 1	Variation 2	Variation 3	Variation 4*
Variant weighting fraction*	1	0	0	0
<b>Absorber Parameters:</b>				
Absorber absorptance	0.963	0.963	0.8	0
Absorber emittance	Table...	0.65	0.65	0
<b>Envelope Parameters:</b>				
Envelope absorptance	0.02	0.02	0	0
Envelope emittance	0.86	0.86	1	0
Envelope transmittance	0.964	0.964	1	0
	<input type="checkbox"/> Broken Glass	<input type="checkbox"/> Broken Glass	<input checked="" type="checkbox"/> Broken Glass	<input type="checkbox"/> Broken Glass
<b>Gas Parameters:</b>				
Annulus gas type	Hydrogen	Air	Hydrogen	Hydrogen
Annulus pressure (torr)	0.0001	750	750	0
<b>Heat Loss at Design:</b>				
Estimated avg. heat loss (W/m)	190	1270	1500	0
<b>Optical Effects:</b>				
Bellows shadowing	0.935	0.935	0.935	0.963
Dirt on receiver	0.98	0.98	1	0.98

\* The variant weighting fractions and Variation 4 inputs are not part of the library.

**Total Weighted Losses**

Heat loss at design: 190 W/m

Optical derate: 0.850631

Rankine cycle are selected based on those of the CSP connecting point into CFPP. Additionally, the costs related to the power block are neglected in this project.

### 8.1.5 Storage system specifications

Two storage tanks (one hot and one cold) have been considered in this project. The size of both tanks is considered to be identical. The height of tanks is considered to be fixed while the other parameters of size are defined based on the required volume of TES (i.e., a function of full load hours of TES and electrical capacity of the tank). The dispatch of TES can be run based on predefined scheduling or be optimised by SAM software. The second option has been selected in this project. Specifications of TES are provided in Table 26.

TABLE 26. GENERAL SPECIFICATION OF THERMAL STORAGE (PARABOLIC TROUGH COLLECTOR)

Parameter	Unit	Value	Parameter	Unit	Value
Parallel tank pairs	-	1	Cold tank heater set point	°C	250
Tank height	m	12	Hot tank heater set point	°C	365
Tank fluid min height	m	1	Initial TES fluid temp	°C	300
Tank loss coefficient	W/m <sup>2</sup> -K	0.4	Tank heater efficiency	%	98

### 8.1.6 System costs

The detailed cost of different parameters of the systems is shown in Table 27. Obviously, the cost of the power plant and fossil backup are neglected in this study because of using the generation block of CFPP.

TABLE 27. COSTS OF SYSTEM (PARABOLIC TROUGH COLLECTOR)

Parameter	Unit	Value	Parameter	Unit	Value
Site improvements	\$/m <sup>2</sup>	25	Fossil backup	\$/kWe	0
Solar field	\$/m <sup>2</sup>	150	Power plant	\$/kWe	0
HTF system	\$/m <sup>2</sup>	60	Balance of plant	\$/kWe	0
Storage	\$/kWh	45	Contingency	%	7
Land	\$/Acre	10,000			

### 8.1.7 Multi-objective analysis

In this section, a multi-objective analysis has been done for the scenario involving the PTC technology. This investigation assists generation system planners and operators of the CFPP to reach a deeper sense of the investment range required for generation development, possible operating points, and combinations of

options available for integration of the thermal solar system into the CFPP. Pareto front of planning possibilities for LCOE and annual emission reduction is depicted in Fig. 25. As can be seen, a wide range of publications [14-28] have covered the design points corresponding to annual emission reduction. Obviously, lower values of LCOE refer to higher investment costs (as can be seen in Fig. 26), which results in higher amounts of emission reduction. However, it is worth mentioning that the LOCE values higher than 17.25 (cents/kWh) seem not to be optimal from the financial point of view based on Fig. 26. Pareto front solutions for capital cost and annual emission reduction of PTC technology are shown in Fig. 27. As can be seen in this figure, there is a semi-linear relation between investment cost and emission reduction. Obviously, higher investments can provide generation planners the opportunity to increase the number of PTCs to reach lower levels of CFPP emission. Besides, it can be deduced that adoption of PTC with an investment cost of higher than \$ 240 million is more efficient since the emission reduction slope in this part is higher than the part with investment lower than \$ 240 million.

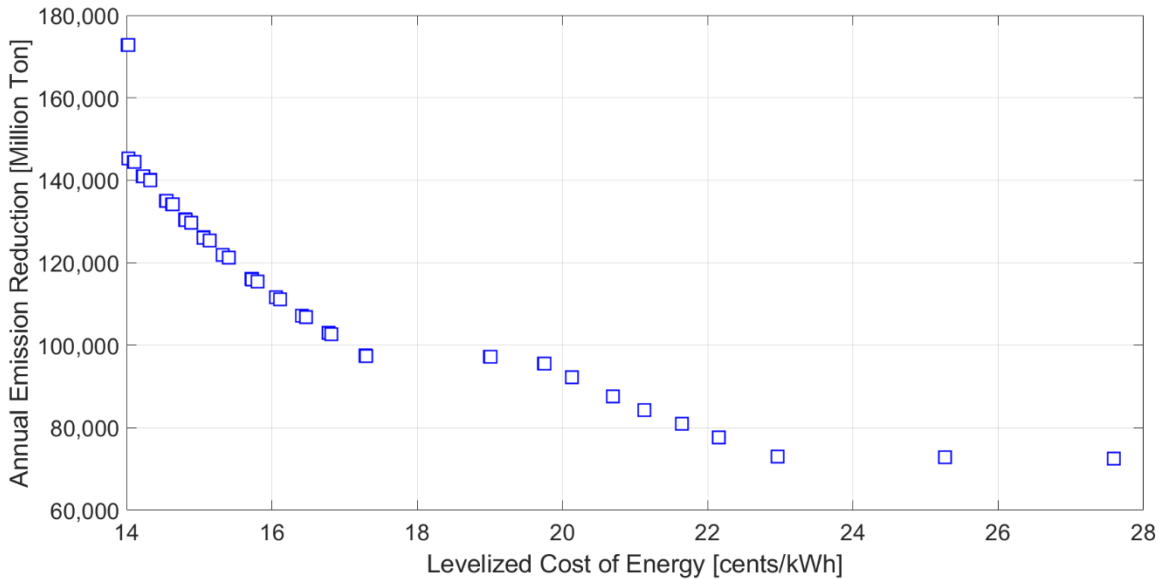


Fig. 25. Bi-objective Pareto front solutions for levelised cost of energy and annual emission reduction (parabolic trough CSP)

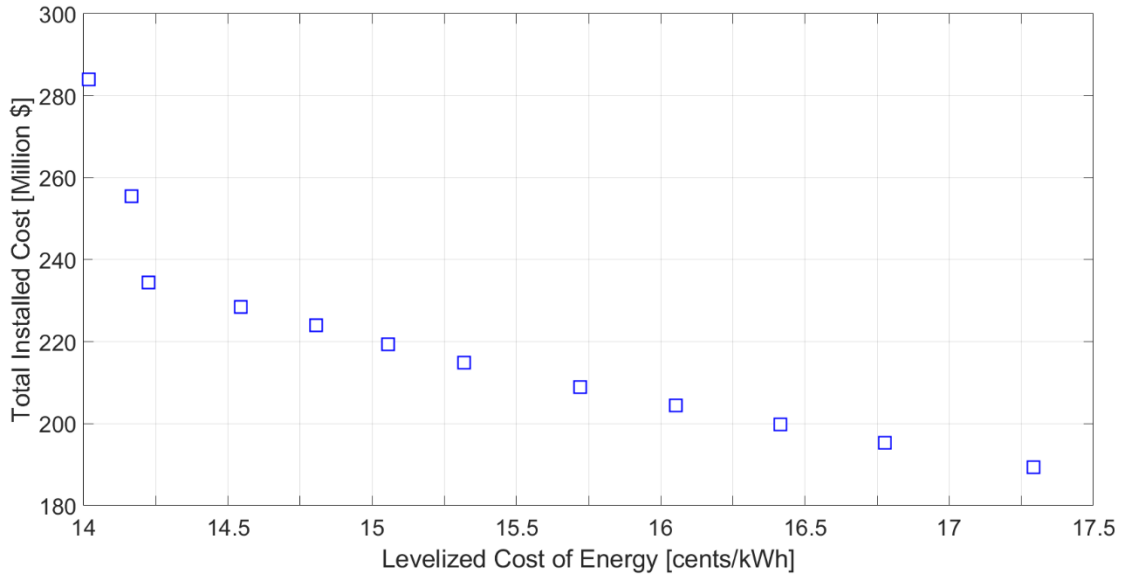


Fig. 26. Bi-objective Pareto front solutions for levelised cost of energy and capital cost (parabolic trough CSP)

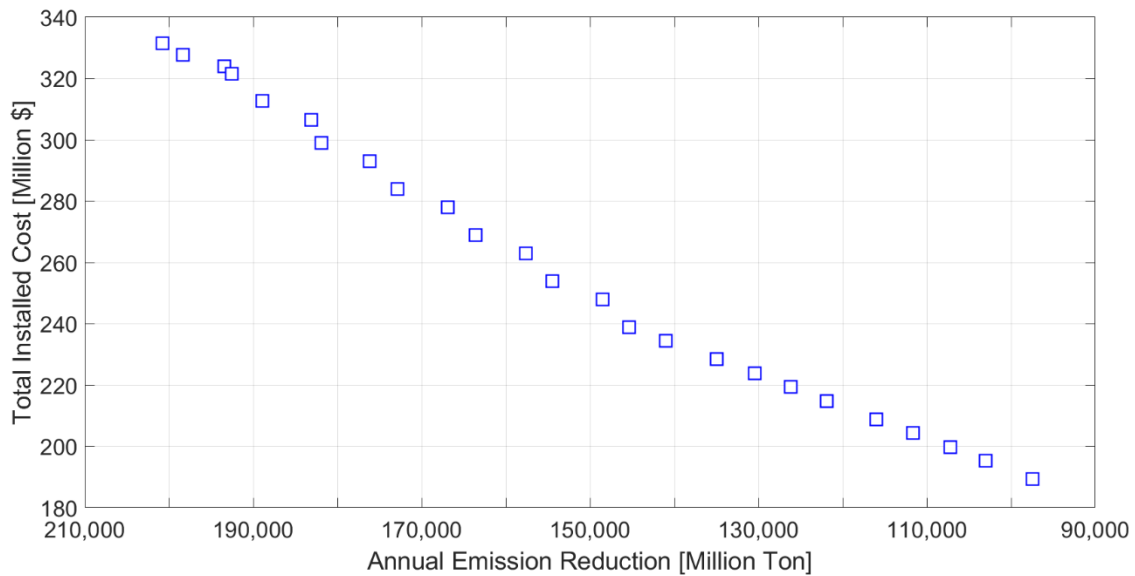


Fig. 27. Bi-objective Pareto front solutions for capital cost and annual emission reduction (parabolic trough CSP)

### 8.1.8 Results

As mentioned before, the SAM software has been utilised to implement the planning task. Considering the fact that SAM does not run any optimisation algorithm, the results are obtained from a parametric procedure. This means the potential range for decision parameters is discretised to several steps and a comprehensive calculation is done for each possibility. In terms of simulation time, this approach is highly time-consuming compared to employing commercial or evolutionary optimisation algorithms; however,

this approach guarantees that the most optimal solution is obtained since every possibility is considered in the calculation procedure. Then, the most optimal solutions in the case of emission reduction, energy provision or other intended parameters are obtained. Moreover, a non-dominated sorting algorithm implemented in the MATLAB software is employed to provide a Pareto-front of bi-objective solutions. In the case of using parabolic trough based CSP, the results show that an approximate 3% emission reduction (200,773.88 Tonne of CO<sub>2eq</sub>/year) is expected for a CSP plant with the electrical capacity around 100 MW. Such a configuration can produce an annual energy of 233,458,000 kWh while it needs a total investment of \$ 331,552,000. Considering an average yearly energy price of \$ 88.56/MWh in NSW, a total saving of \$ 20,675,040.48 per year is expected from the power generation of the CSP plant. Therefore, without considering any inflation rate in the energy price or accounting for interest payments on the capital expenditure, an undiscounted payback period of 16.03 years (i.e., years for payback (yr) = investment cost (\$)/ yearly net profit (\$/yr)) can be expected for the CSP plant; the power plant can still operate for at least 9 additional years, considering 25 years as the project lifespan. It is worth mentioning that higher solar multiples are not efficient based on pre-assessments and current results because of the following two reasons. The most important point is the practical constraint related to the space needed for the development of the solar field as the result of solar multiple increments. Currently, there is limited space for constructing the solar field (CSP and PV) around the Vales Point power plant. The proximity to Lake Macquarie and urban areas are other factors which make extra limitations in this regard and need more investigations. Additionally, as can be seen in Fig. 25 and Fig. 26, further increase in CSP capacity by enlarging the solar farm cannot offer a significant improvement in the power generation of the solar plant because of limited solar irradiation capacity of the CFPP site.

## **8.2 Scenario 2: Power tower CSP-molten salt**

The implementation procedure of the second scenario follows the same methodology as the first scenario. The range decision variables are selected as detailed in Table 28. In this scenario, the range of solar multiple has changed to [1.7-2.2] because the scale of SPT based CSPs is basically larger than PTC

ones. Based on the configuration of SPTs, the type of fluid should be the same for tower and collector.

TABLE 28. POSSIBLE RANGE OF OPERATING FOR SOLAR POWER TOWER

Parameter	Min	Max	Steps
Solar multiple	1.7	2.2	0.05
CSP capacity (MWe)	80	110	5
CSP thermal storage capacity (MWt)	20	30	2
Full load hours of TES [h]	6	10	2
Tower and receiver fluid type	-	-	Salt (60% NaNO <sub>3</sub> and 40% KNO <sub>3</sub> ) and salt (46% LiF, 11.5% NaF and 42% KF)

### 8.2.1 Design point parameters

The key design parameters of the configuration are detailed in Table 29. It can be seen that the operating temperature of HTF in the SPT systems is much higher than that of PTC technology. The value of design point DNI is considered to be the same for both CSP scenarios.

TABLE 29. PARAMETERS OF SOLAR POWER TOWER DESIGN POINT

Parameter	Unit	Value
Design point DNI	W/m <sup>2</sup>	950
HTF hot temperature	°C	574
HTF cold temperature	°C	290
Estimated gross-to-net conversion factor of power cycle *	-	0.9
Cycle thermal efficiency *	-	0.412

\*Parameters are based on the specifications of Vales Point CFPP

### 8.2.2 Heliostat field

This section defines the variables that determine the heliostats position in the solar field as well as the heliostat optical properties and geometry.

One of the most important points about the implementation of the SPT system is to reach an optimal design for the heliostat field. In fact, solar field geometry optimisation calculates the number of mirrors, tower height, receiver height, and diameter of the tower and receiver. This optimisation task is implemented by SAM software for each parametric candidate solution. Other specifications of heliostats are shown in Table 30. The reflectance and availability of mirrors are considered to be 0.9 and 0.99, respectively.

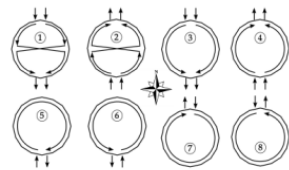
TABLE 30. SPECIFICATIONS OF HELIOSTATS (SOLAR POWER TOWER)

<b>Optimization Settings</b>		<b>Atmospheric Attenuation</b>	
Initial optimization step size	0.06	Polynomial coefficient 0	0.006789
Maximum optimization iterations	200	Polynomial coefficient 1	0.1046 1/km
Optimization convergence tolerance	0.001	Polynomial coefficient 2	-0.017 1/km <sup>2</sup>
		Polynomial coefficient 3	0.002845 1/km <sup>3</sup>
<b>Heliostat Operation</b>		<b>Solar Field Layout Constraints</b>	
Heliostat stow/deploy angle	8 deg	Max. heliostat distance to tower height ratio	9.5
Wind stow speed	15 m/s	Min. heliostat distance to tower height ratio	0.75
Heliostat startup energy	0.025 kWe-hr		
Heliostat tracking power	0.055 kWe		
Design point DNI	950 W/m <sup>2</sup>		
		<b>Mirror Washing</b>	
		Water usage per wash	0.70 L/m <sup>2</sup> .aper.
		Washes per year	63

### 8.2.3 Tower and receiver

As mentioned, the physical dimensions of the tower and receiver are optimised in the SAM software, while other specifications are shown in Table 31.

TABLE 31. DETAILED SPECIFICATION AND PARAMETERS OF TOWER AND RECEIVER (SOLAR POWER TOWER)

<b>Receiver Heat Transfer Properties</b>		<b>Materials and Flow</b>	
Tube outer diameter	40 mm	HTF type	Salt (60% NaNO <sub>3</sub> 40% KNO <sub>3</sub> )
Tube wall thickness	1.25 mm	Material type	Stainless AISI316
Coating emittance	0.88	Flow pattern	2
Coating absorptance	0.94		
Heat loss factor	1		
<b>Design and Operation</b>		<b>Receiver Flux Modeling Parameters</b>	
Minimum receiver turndown fraction	0.25	Maximum receiver flux	1000 kWt/m <sup>2</sup>
Maximum receiver operation fraction	1.2	Estimated receiver heat loss	30.0 kWt/m <sup>2</sup>
Receiver startup delay time	0.2 hr	Receiver flux map resolution	20
Receiver startup delay energy fraction	0.25	Number of days in flux map lookup	8
Receiver HTF pump efficiency	0.850	Hourly frequency in flux map lookup	2 hours
Maximum flow rate to receiver	1572.45 kg/s		
<b>Piping Losses</b>			
Piping heat loss coefficient	10200 Wt/m		
Piping length constant	0 m		
Piping length multiplier	2.6		
Piping length	468.591 m		
Total piping loss	4779.63 kWt		

Airflow patterns are based on the southern hemisphere and the HTF type is considered a decision variable with two options of Salt (60% NaNO<sub>3</sub> and 40% KNO<sub>3</sub>) and Salt (46% LiF, 11.5% NaF and 42% KF).

### 8.2.4 Power cycle specifications

Similar to the PTC technology, the solar power system will be joined into the power block system. Therefore, parameters of the Rankine cycle (e.g. boiler operating pressure and steam temperature) are

considered as the same as the CFPP operation parameters. The control system of inlet pressure is adjusted to have a fixed value. The power consumption of HTF pumping is 0.55 kW/kg/s.

### 8.2.5 Storage system specifications

Similar to the first scenario, one hot and one cold tank have been modeled for SPT. The size of both tanks is considered to be the same. The parameters, tank height, tank fluid min-height, and tank loss coefficient, are the same for both scenarios. However, the operating temperatures for SPT technology are higher than for PTC. These parameters are shown in Table 32. The dispatch scheduling of the TES system is based on that optimised and offered by SAM software.

TABLE 32. GENERAL SPECIFICATION OF THERMAL STORAGE (SOLAR POWER TOWER)

Parameter	Unit	Value	Parameter	Unit	Value
Parallel tank pairs	-	1	Cold tank heater set point	°C	280
Tank height	m	12	Hot tank heater set point	°C	500
Tank fluid min height	m	1	Initial hot HTF percent	%	30
Tank loss coefficient	W/m <sup>2</sup> -K	0.4	Tank heater efficiency	%	99

### 8.2.6 System costs

The detailed cost of different parameters of the systems is shown in Table 33. The cost of the power plant and fossil fuel backup is neglected in this study because of using the generation block of CFPP.

TABLE 33. COSTS OF SYSTEM (SOLAR POWER TOWER)

Parameter	Unit	Value	Parameter	Unit	Value
Site improvements	\$/m <sup>2</sup>	20	Storage	\$/kWh	45
Heliostat field	\$/m <sup>2</sup>	140	Land	\$/Acre	10,000
Fixed tower cost	\$	3,000,000	Fossil backup	\$/kWe	0
Tower cost scaling exponent	%	1.13	Power plant	\$/kWe	0
Receiver reference cost	\$	103,000,000	Balance of plant	\$/kWe	0
Receiver cost scaling exponent	%	7%	Contingency	%	7

### 8.2.7 Multi-objective analysis

The bi-objective analysis for SPT technology development is accomplished in this section. Fig. 28 shows the possible optimal design points for LCOE and annual emission reduction. Similar to the PTC scenario,



the range available for LCOE is a wide range of [11-14.5] cents/kWh based on Fig. 28 to reach an emission level between [180,000, 360,000] million ton/ per year, while the range is limited by Fig. 28 to [11.2, 12.7] cents/kWh if the generation expansion planner intends to design within the optimal range of the investment. Similar to PTC, there is a semi-linear relation between the total capital cost of SPT development and emission reduction as can be seen from Fig. 30. Scaling up the SPT solar farm can increase the emission reduction of CFPP. Comparing Fig. 25 and Fig. 28, it can be deduced that the design range of emission reduction for SPT technology (i.e., between [189,000-365,000 million ton/year]) is located on the top range of PTC technology (i.e., between [72,000-172,000 million ton/year]). It means that in the case of large-scale CFPP like Vales Point, SPT is more practical if a considerable amount of emission reduction is expected. Based on the literature, the reason for this is that the net efficiency of tower-based CSP is generally close to the twice that of the parabolic system. However, it should be noted that the efficiency of CSP technology (both PTC and SPT) greatly depends on the site location and meteorological data (specifically irradiation level).

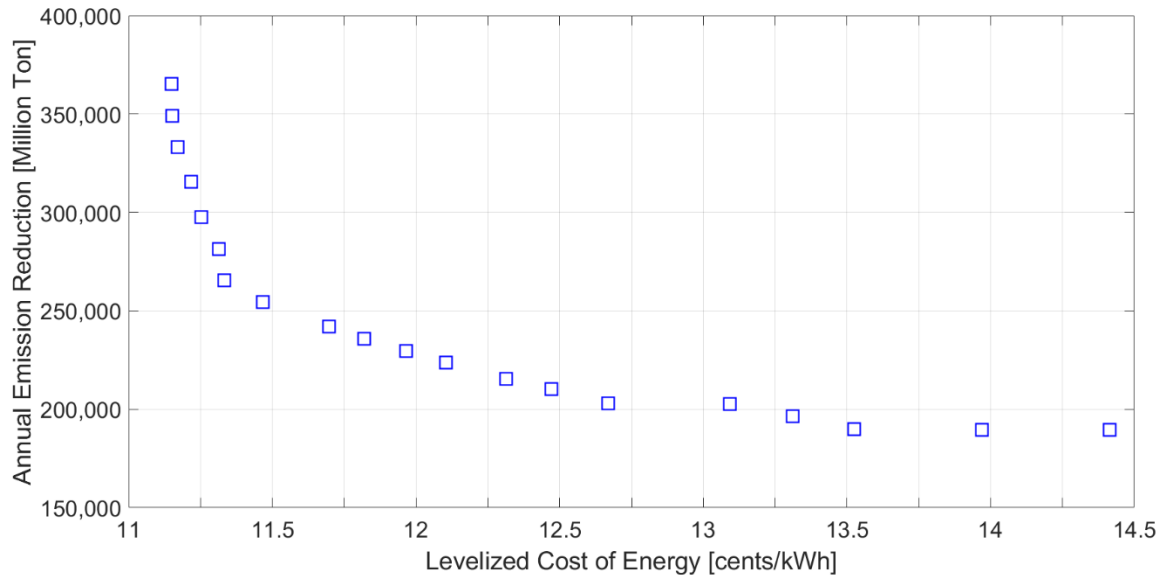


Fig. 28. Bi-objective Pareto front solutions for levelised cost of energy and annual emission reduction (polar tower CSP)

Similarly, there is a small coverage between the capital cost range of SPT (i.e., illustrated in Fig. 29) and that of PTC technology (i.e., depicted in Fig. 26); however at the same range, SPT can provide a lower LCOE than PTC considering the same amount of installation cost (e.g., around \$ 280 million). Besides,

there exists a semi-linear relation between the total capital cost and annual emission reduction of SPT technology, as can be seen in Fig. 30.

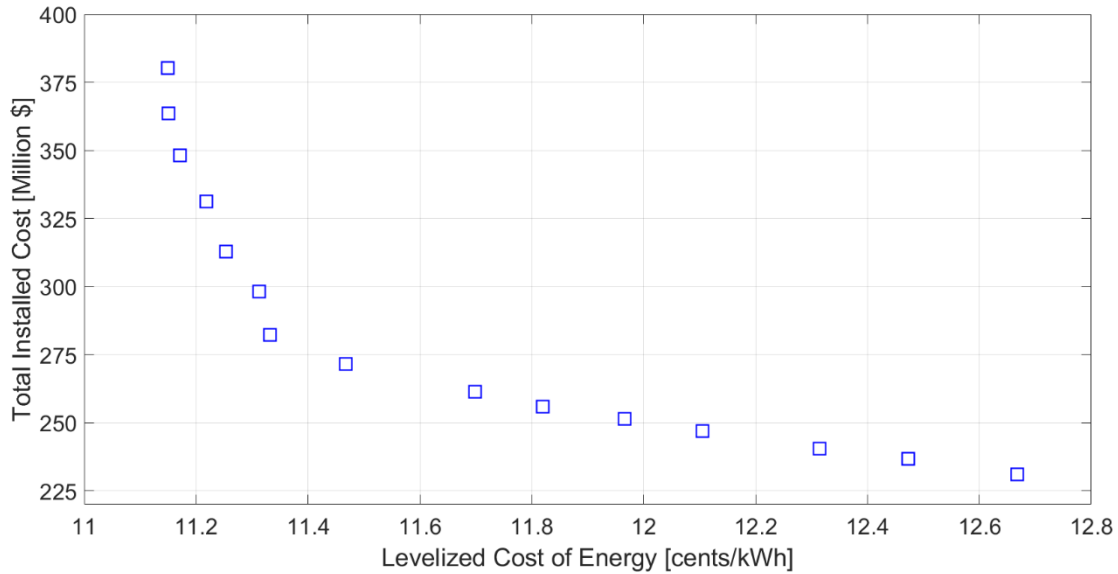


Fig. 29. Bi-objective Pareto front solutions for levelised cost of energy and capital cost (polar tower CSP)

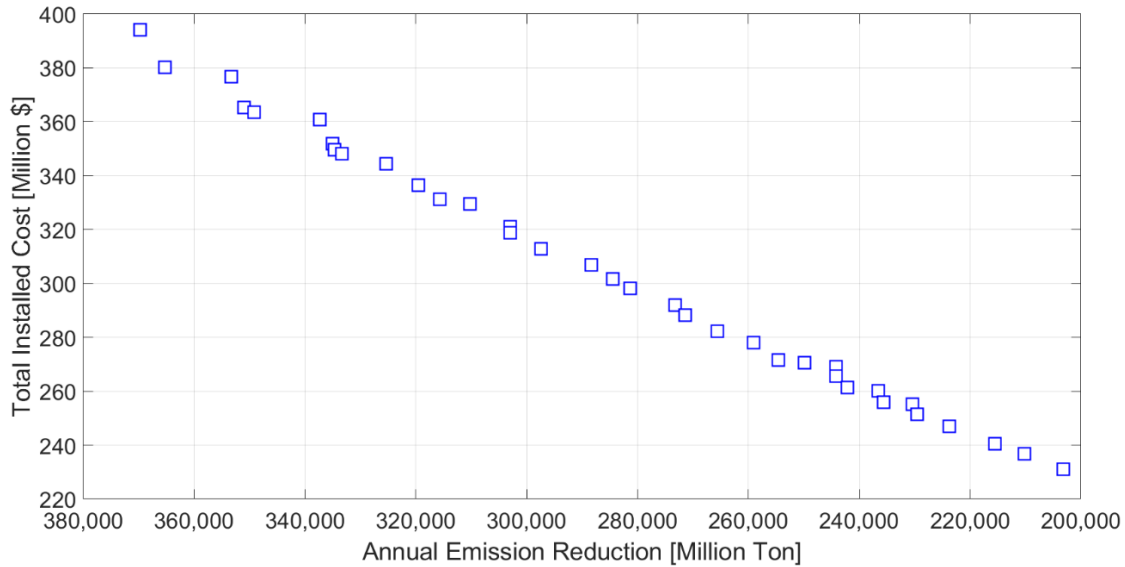


Fig. 30. Bi-objective Pareto front solutions for total capital cost and annual emission reduction (polar tower CSP)

### 8.2.8 Results

Similar to the first scenario, a parametric simulation has been done using SAM software. Then, the non-dominate algorithm has been applied to offer a set of Pareto solutions. In the case of using central tower-based CSP, the results show that an approximate 5% emission reduction (i.e., 369,745.82 Tonne of

CO<sub>2eq</sub>/year) is expected for a CSP plant with the electrical capacity around 100 MW. Such a configuration can produce the annual energy of 429,937,000 kWh while it needs a total investment of \$ 394,107,000. Using the steam provided by SPT for preheating seems to be a waste of investment because of the high capacity of this technology, while PTC technology can be used to join in with as preheating and also to boost boilers' performance as high-pressure steam. Considering an average yearly energy price of \$ 88.56/MWh in NSW, a total saving of \$ 37,834,456 per year is expected from the power generation of the CSP plant. Therefore, without considering any inflation rate in the energy price, or accounting for interest payments on the capital expenditure, an undiscounted payback period of 10.42 years can be expected for CSP plant; while the power plant can still operate for at least 15 additional years, considering 25 years as the project lifespan. Similar to the parabolic trough CSP, restrictions on land should be considered for this type of CSP as well in the case of Vales Point CFPP. Obviously, since power tower CSP needs more space compared to parabolic trough, reaching solar multiple 2.2 (i.e., upper bound) for this CSP type will definitely necessitate some de-vegetation around the CFPP.

### **8.3 Scenario 3: Photovoltaic integration**

The third scenario models the integration of a PV farm into Vales Point CFPP for reserve and internal usage purposes. Type of module and inverter, size of PV farm, and type/size of battery are considered as decision variables. The proposed range of simulation for PV planning is shown in Table 34.

#### **8.3.1 Module type**

The module section permits the operator to select a model for the photovoltaic module's performance. Within each simulation step, based on the incident solar radiation received from weather data and the design parameters, the model computes the electrical DC output of each module. It is assumed that the configuration is made up of an array of identical modules, that is wired into up to four DC subarrays. Three detailed modules with the specifications as indicated in Table 35 -Table 37 are used for simulations.

TABLE 34. POSSIBLE RANGE OF OPERATING FOR PHOTOVOLTAIC FARM

Parameter	Min	Max	Steps
Module type	-	-	Sunpower SPR-X22-480-COM, Solaria Corporation Solaria PowerXT-440C-PD, Hansol Technics Co. Ltd HS415UE-AN1
Inverter type	-	-	ABB: TRIO-20.0-TL-OUTD-S-US-480 [480V], AEG Power Solutions: Protect PV.500-UL, Advanced Energy Industries: AE 250NX (3159200-XXXX) [480V]
Battery type	-	-	Lithium Ion: Nickel Manganese Cobalt Oxide (NMC), Lead Acid: VRLA AGM, Lithium Ion: Lithium Titanate (LTO), Flow Battery: Vanadium
AC PV farm capacity [MW]	20	30	2
Battery bank capacity [MWh]	2	6	1
Battery bank power [MW]	1	3	1

TABLE 35. MODULE SPECIFICATIONS (TYPE 1) – PHOTOVOLTAIC

**Module Characteristics at Reference Conditions** – Sunpower SPR-X22-480-COM

Reference conditions: Total Irradiance = 1000 W/m<sup>2</sup>, Cell temp = 25 C

Nominal efficiency	22.237 %	Temperature coefficients	
Maximum power (Pmp)	480.320 Wdc		-0.352 %/°C
Max power voltage (Vmp)	79.0 Vdc		-1.691 W/°C
Max power current (Imp)	6.1 Adc		
Open circuit voltage (Voc)	92.9 Vdc		-0.293 V/°C
Short circuit current (Isc)	6.5 Adc		-0.272 V/°C
			0.031 %/°C
			0.002 A/°C

**Bifacial Specifications**

Module is bifacial

Transmission fraction: 0.013 0-1

Bifaciality: 0.65 0-1

Ground clearance height: 1 m

**Temperature Correction**

Nominal operating cell temperature (NOCT) method

Heat transfer method

See Help for more information about CEC cell temperature models.

NOCT method parameters

Mounting standoff: Ground or rack mounted

Array height: One story building height or lower

Heat transfer method parameters

Mounting configuration: Rack

Heat transfer dimensions: Module Dimensions

Mounting structure orientation: Structures do not impede flow underneath module

Module width: 1 m

Module length: 2.16 m

Rows of modules in array: 1

Columns of modules in array: 10

Temperature behind the module: 20 °C

Space between module back and roof surface: 0.05 m

**Physical Characteristics**

Material: Mono-c-Si

Module area: 2.160 m<sup>2</sup>

Number of cells: 128

**Additional Parameters**

T<sub>noct</sub>: 45.7 °C

I<sub>L\_ref</sub>: 6.48506 A

R<sub>s</sub>: 0.484263 Ohm

A<sub>ref</sub>: 3.48365 V

I<sub>o\_ref</sub>: 1.66048e-11 A

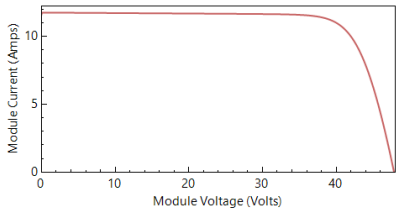
R<sub>sh\_ref</sub>: 619.877 Ohm

The model assumes a reference bandgap voltage Eg\_ref = 1.121 eV, and temperature coefficient for bandgap of -0.0002677 eV/K.

TABLE 36. MODULE SPECIFICATIONS (TYPE 2) – PHOTOVOLTAIC

**Module Characteristics at Reference Conditions** - Solaria Corporation Solaria PowerXT-440C-PD

Reference conditions: Total Irradiance = 1000 W/m<sup>2</sup>, Cell temp = 25 °C



Nominal efficiency	20.9424 %	Temperature coefficients	
Maximum power (Pmp)	439.790 Wdc	-0.359 %/°C	-1.579 W/°C
Max power voltage (Vmp)	39.8 Vdc		
Max power current (Imp)	11.1 Adc		
Open circuit voltage (Voc)	47.9 Vdc	-0.282 %/°C	-0.135 V/°C
Short circuit current (Isc)	11.5 Adc	0.050 %/°C	0.006 A/°C

**Bifacial Specifications**

Module is bifacial

Transmission fraction	0.013	0-1
Bifaciality	0.65	0-1
Ground clearance height	1	m

**Temperature Correction**

Nominal operating cell temperature (NOCT) method  
 Heat transfer method

See Help for more information about CEC cell temperature models.

NOCT method parameters

Mounting standoff: Ground or rack mounted  
 Array height: One story building height or lower

Heat transfer method parameters

Mounting configuration	Rack	Rows of modules in array	1
Heat transfer dimensions	Module Dimensions	Columns of modules in array	10
Mounting structure orientation	Structures do not impede flow underneath module	Temperature behind the module	20 °C
Module width	1 m	Space between module back and roof surface	0.05 m
Module length	2.10 m		

**Physical Characteristics**

Material: Mono-c-Si      Module area: 2.100 m<sup>2</sup>      Number of cells: 432

**Additional Parameters**

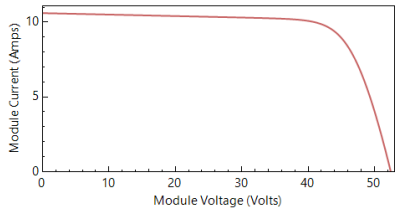
T <sub>noct</sub>	47.9 °C	I <sub>L_ref</sub>	11.7302 A	R <sub>s</sub>	0.226491 Ohm
A <sub>ref</sub>	1.81834 V	I <sub>o_ref</sub>	4.19373e-11 A	R <sub>sh_ref</sub>	286.089 Ohm

The model assumes a reference bandgap voltage Eg\_ref = 1.121 eV, and temperature coefficient for bandgap of -0.0002677 eV/K.

TABLE 37. MODULE SPECIFICATIONS (TYPE 3) – PHOTOVOLTAIC

**Module Characteristics at Reference Conditions** - Hansol Technics Co., Ltd HS415UE-AN1

Reference conditions: Total Irradiance = 1000 W/m<sup>2</sup>, Cell temp = 25 °C



Nominal efficiency	19.8695 %	Temperature coefficients	
Maximum power (Pmp)	415.272 Wdc	-0.379 %/°C	-1.574 W/°C
Max power voltage (Vmp)	42.9 Vdc		
Max power current (Imp)	9.7 Adc		
Open circuit voltage (Voc)	52.5 Vdc	-0.281 %/°C	-0.148 V/°C
Short circuit current (Isc)	10.6 Adc	0.042 %/°C	0.004 A/°C

**Bifacial Specifications**

Module is bifacial

Transmission fraction	0.013	0-1
Bifaciality	0.65	0-1
Ground clearance height	1	m

**Temperature Correction**

Nominal operating cell temperature (NOCT) method  
 Heat transfer method

See Help for more information about CEC cell temperature models.

NOCT method parameters

Mounting standoff: Ground or rack mounted  
 Array height: One story building height or lower

Heat transfer method parameters

Mounting configuration	Rack	Rows of modules in array	1
Heat transfer dimensions	Module Dimensions	Columns of modules in array	10
Mounting structure orientation	Structures do not impede flow underneath module	Temperature behind the module	20 °C
Module width	1 m	Space between module back and roof surface	0.05 m
Module length	2.09 m		

**Physical Characteristics**

Material: Mono-c-Si      Module area: 2.090 m<sup>2</sup>      Number of cells: 78

**Additional Parameters**

T <sub>noct</sub>	45.8 °C	I <sub>L_ref</sub>	10.6166 A	R <sub>s</sub>	0.350245 Ohm
A <sub>ref</sub>	2.03693 V	I <sub>o_ref</sub>	6.46629e-11 A	R <sub>sh_ref</sub>	101.131 Ohm

The model assumes a reference bandgap voltage Eg\_ref = 1.121 eV, and temperature coefficient for bandgap of -0.0002677 eV/K.

### 8.3.2 Inverter type

This section is to select a potential type of inverter based on their performance. Specifications of all inverters are presented based on the datasheet of manufacturers. A single type of inverter is modeled for the PV system in this project. Assuming that the DC output of the PV is equal to the DC power input to the inverter, an estimation for DC to AC conversion efficiency is done for each of the three inverter models. Three types of high-efficiency inverters with specifications in Table 38-Table 40 are modeled in this project.

### 8.3.3 PV farm sizing

The option of PV farm sizing allows the operator to determine the desired value for the system-rated capacity and the desired DC to AC ratio. The size of the PV farm is considered as a decision variable and is optimised within the simulation procedure. The software SAM calculates the number of modules and

TABLE 38. INVERTER SPECIFICATIONS (TYPE 1) – PHOTOVOLTAIC

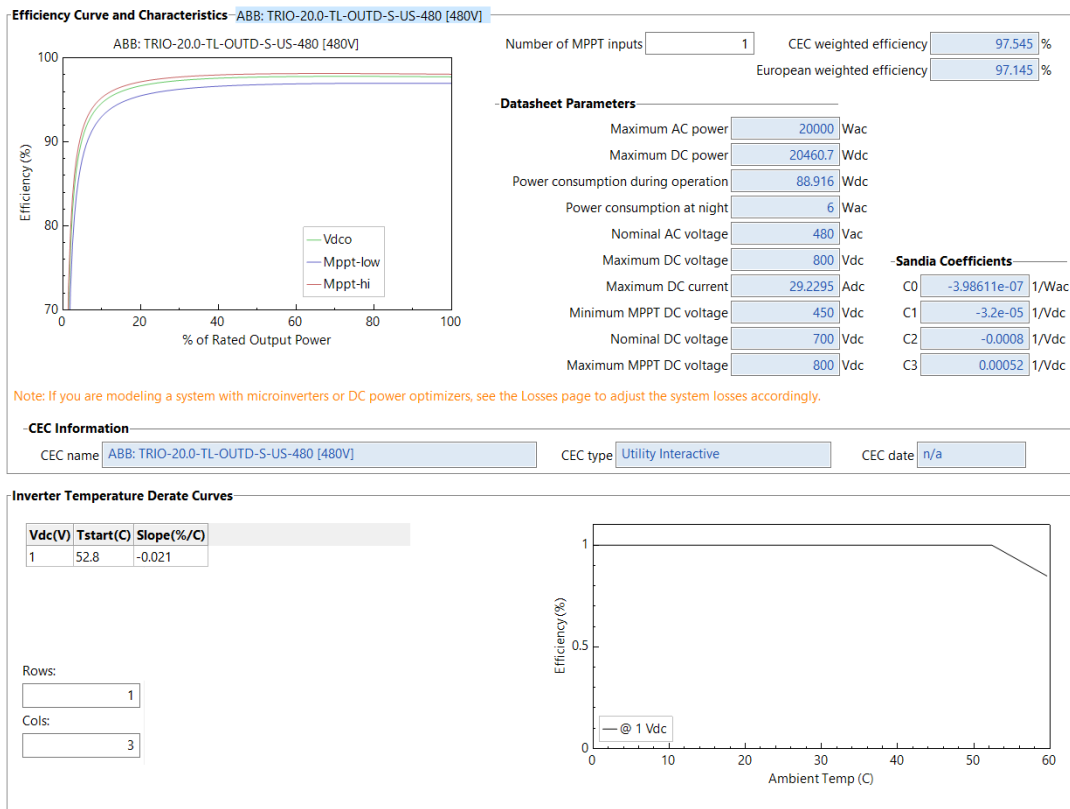


TABLE 39. INVERTER SPECIFICATIONS (TYPE 2) – PHOTOVOLTAIC

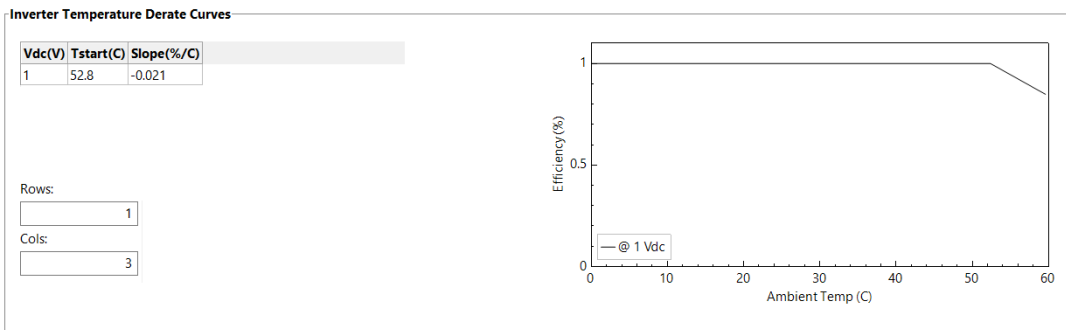
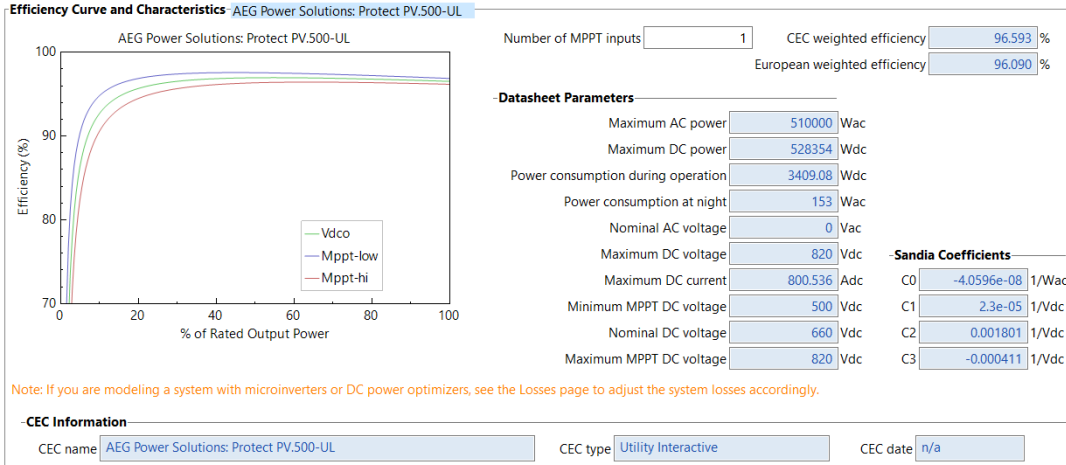
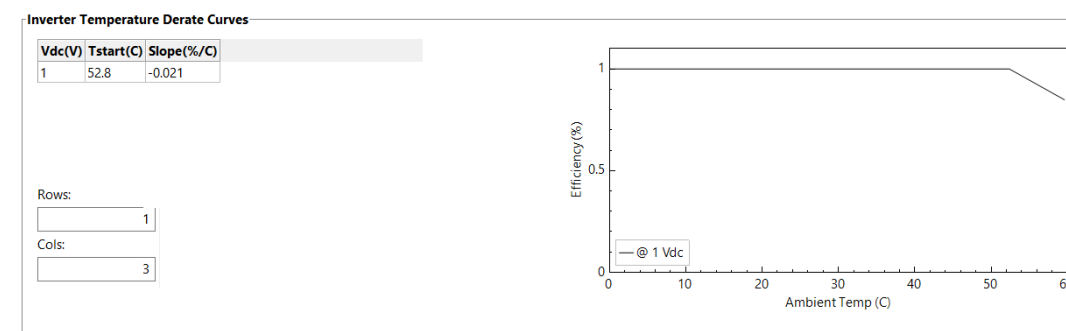
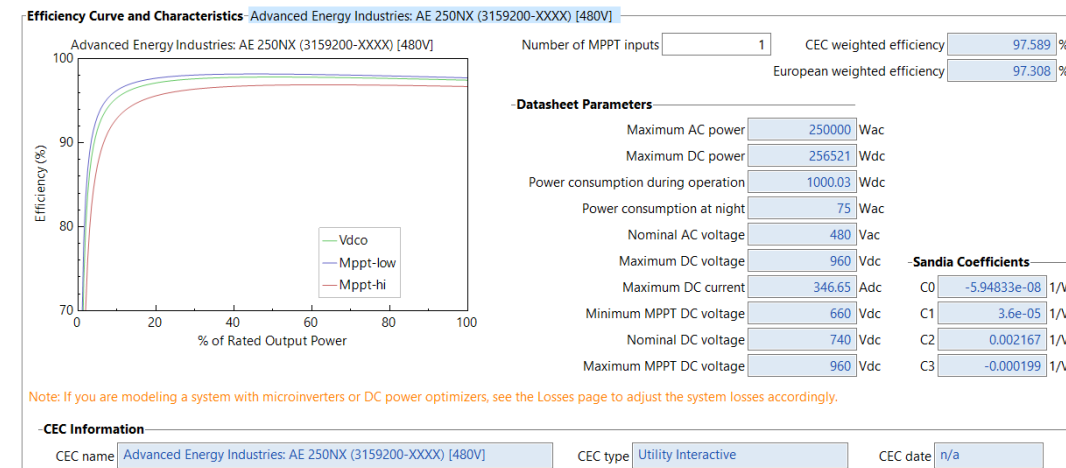


TABLE 40. INVERTER SPECIFICATIONS (TYPE 3) – PHOTOVOLTAIC



inverters to get as close as possible to the desired size. A DC-AC ratio of 1.18 is considered for PV units. Not including space between modules, the total area needed for an array of modules equals the module area (m<sup>2</sup>) multiplied by the number of modules. A fixed structure is considered for solar panels, in which the subarray is fixed at the operator-defined azimuth and tilt angles and does not follow the sun's movement. No shedding effect and a 0.5% degradation rate/year are considered for the PV farm.

### 8.3.4 Battery system

In the presented model, the performance of three battery storage (including lead-acid, lithium-ion, and vanadium redox flow) models are analysed. The battery system is connected to the AC side of the PV system, as indicated in Fig. 31.

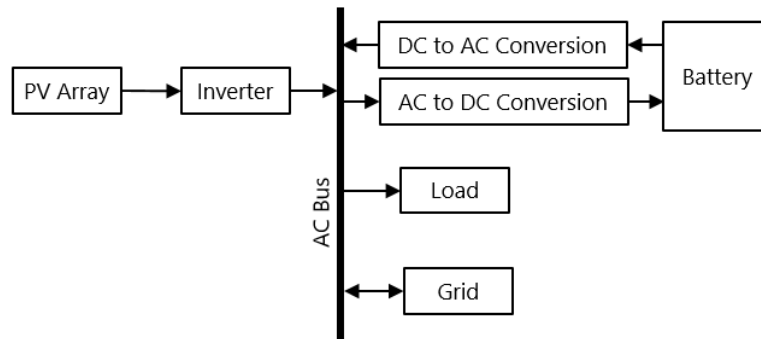


Fig. 31. Battery connected to AC side of photovoltaic system

The proposed model in SAM software automatically sizes for the battery based on the desired size of the PV farm. Conversion efficiency 98%, 96%, and 96% are assumed for DC-DC, AC-DC, and DC-AC converters, respectively. The initial state-of-charge for simulation is 50%, while the minimum and maximum state-of-charge are 15% and 95%. The dispatch of units is accomplished automatically in SAM software. The battery is only charged through a PV farm, not from the grid.

### 8.3.5 Capital costs

This section calculates the direct capital cost. A direct capital cost denotes an expenditure for an installation service or piece of equipment that applies in year zero of the cash flow. The costs of the system are detailed in Table 41.



TABLE 41. COSTS OF PV SYSTEM – PHOTOVOLTAIC

Parameter	Unit	Value	Parameter	Unit	Value
PV module	\$/Wdc	0.35	Environmental studies	\$/Wdc	0.01
Inverter	\$/m <sup>2</sup>	0.06	Engineering	\$/Wdc	0.08
Battery pack	\$/kWh dc	300	Grid interconnection	\$/Wdc	0.03
Balance of system equipment	\$/Wdc	0.2	Land purchase	\$/Wdc	0.03
Installation labor	\$/Wdc	0.13	Land preparation	\$/Wdc	0.02
Contingency	%	3			

### 8.3.6 Multi-objective analysis

The multi-objective results for the PV system with the application for spinning reserve and/or to supply the internal usage of CFPP are presented in this section. Bi-objective Pareto solutions for LCOE versus emission reduction and capital cost are shown in Fig. 32 and Fig. 33, respectively. It can be deduced that for a capital cost around \$ 28 million, some small changes in investment can provide significant changes in LCOE, while the capital cost will be increased to 1.5 times this figure if the expansion planner needs to reduce LOCE from 12.35 to 12.15 cents/kWh. On the other side, a small increase in the investment to values more than \$ 28 million can increase LCOE, and consequently the emission is reduced remarkably.

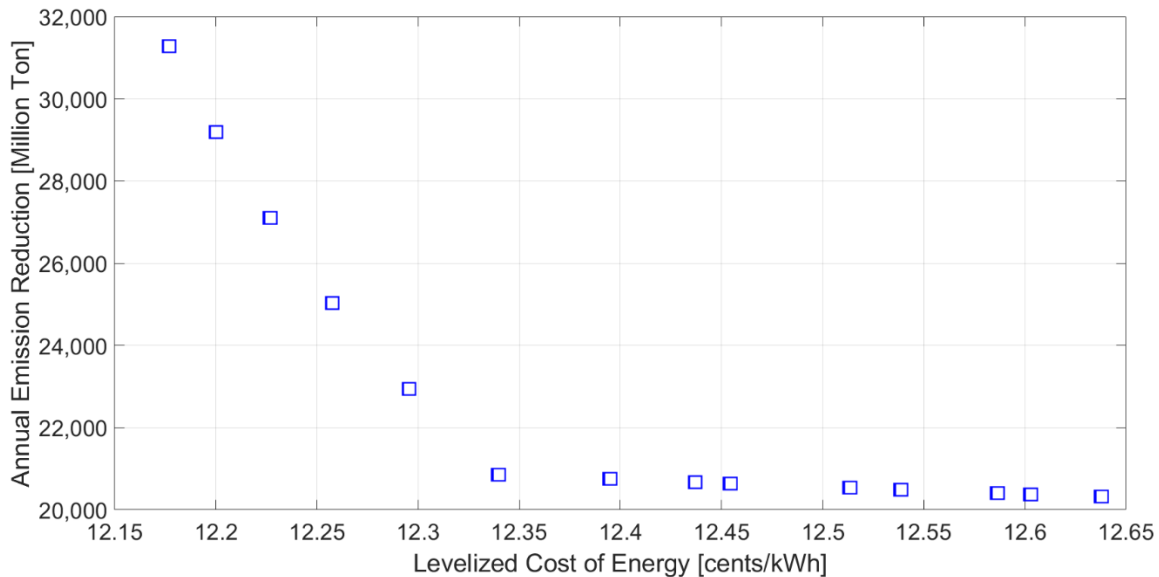


Fig. 32. Bi-objective Pareto front solutions for levelised cost of energy and annual emission reduction (photovoltaic)

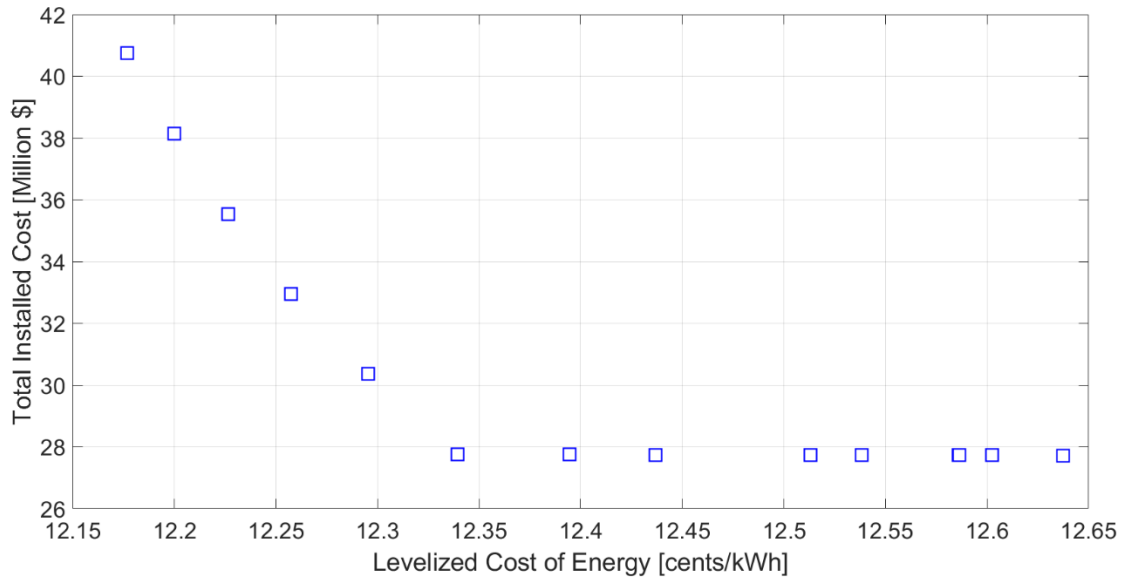


Fig. 33. Bi-objective Pareto front solutions for levelised cost of energy and capital cost (photovoltaic)

Possible design points for capital cost versus annual emission reduction is illustrated in Fig. 34. The stepped shape of changes is the most highlighted point about Fig. 34. Such a discrete figure shows that a change in configurations (including module type, inverter, and PV size) can provide some considerable changes in the efficiency and energy provision of the PV unit. In other words, the adoption of the optimal configuration of the PV units can transfer the system from one operation point to another operating point, which is significantly higher or lower in terms of efficiency, emission, and cost. However, as magnified in

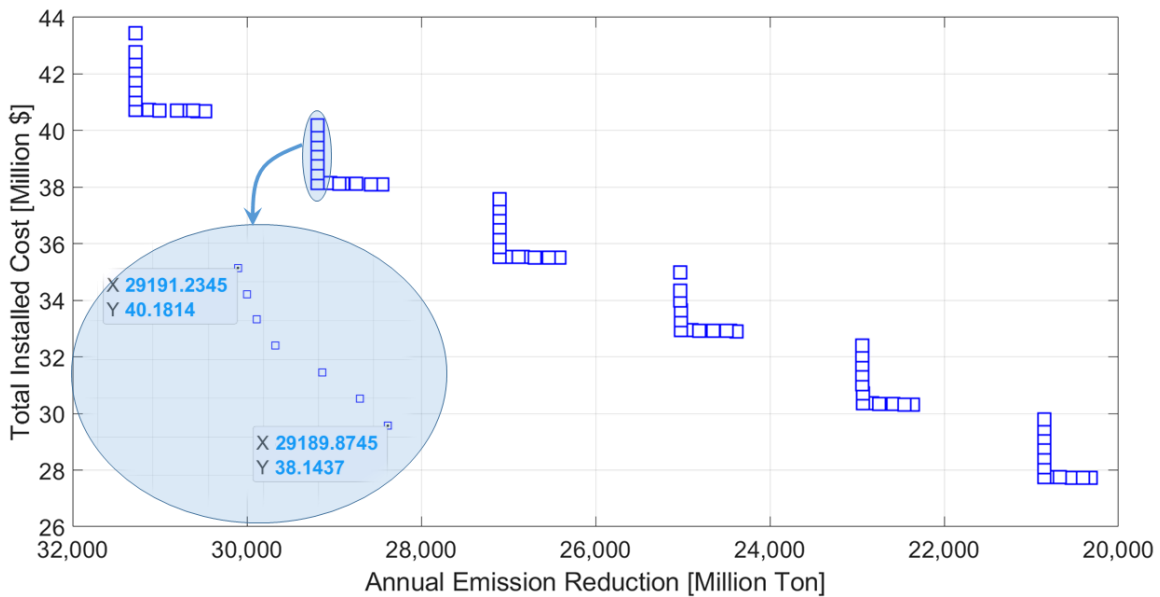


Fig. 34. Bi-objective Pareto front solutions for capital cost and annual emission reduction (photovoltaic)

this figure, while a \$ 2 million change of investment cannot make a major change in emission reduction, an accurate optimisation of the investment cost around \$ 38 million may provide a sizable decline in emissions.

### **8.3.7 Results**

The allocation of the PV farm for a reserve service has been done in this section. The results have been obtained using a parametric approach while a non-dominated sorting algorithm was used to find a set of possible operating points. In this scenario, the results show that an approximate emission reduction of 31,681.62 Tonne of CO<sub>2eq</sub>/year is expected for a PV plant with the electrical capacity around 30 MW. Such a configuration can produce an annual energy of 36,839,100 kWh while it needs a total investment of \$ 43,440,600. Considering the average yearly energy price of \$ 88.56/MWh in NSW, a total saving of \$ 3,262,461.84 per year (i.e., 0.88%) is expected from the power generation of the PV plant. Therefore, without considering any inflation rate in the price of energy, or accounting for interest payments on the capital expenditure, an undiscounted payback period of 13.35 years is expected for the PV plant, while the power plant can still operate for at least 12 additional years with only small operating costs, considering 25 years as the project lifespan.

Worthy of mention is that the annual energy for this PV plant equals to total yearly energy produced by the PV unit, which is evaluated based on TMY data. However, some of the energy is wasted due to power loss of PV converters and also in the charge/discharge cycle of the batteries. In our dispatch optimisation algorithm, the energy generated is not intentionally prioritised, but because buying price is lower than the selling wholesale price, the algorithm automatically leads to the prioritised dispatch, i.e., it is dedicated to firstly charging the battery and then any surplus is exported to the grid at the wholesale price.

Additionally, the first intention of the PV-Battery configuration is to save coal for the CFPP, and it can be used in both wholesale and ancillary markets. The reasons for considering the energy price of the wholesale market for monetary savings of PV-battery configuration are as follows:

- While the pattern of energy price in the wholesale market is predictable, the energy price in the ancillary markets significantly depends on different market factors, including the number of

participants in the reserve market, time of day, type of participant generators, type of contingency, amount of required power. Therefore, it is challenging and prone to inaccuracies to consider an estimation for energy prices in the ancillary market.

- Basically, PV system is used in the wholesale market, not ancillary market. Battery energy storage can be used for ancillary market, but because of the small capacity of BESS in this project, it is still dedicated to participating in the wholesale market.
- Due to the above-mentioned modelling complexity of financial parameters, it would be a substantial challenge to determine the capacity of a battery storage unit based on both PV farm specifications and ancillary market participation.

Additionally, using the average yearly energy price for the PV output may result in a rather optimistic total savings, because of 1) the time of PV dispatch into the wholesale market, which would likely be sold at a price lower than the average wholesale price; and 2) the duration for which the battery can discharge at the peak and thus obtain greater revenues. However, this method can be extended by using the average daily or historic yearly data of prices.

## 9 CONCLUSIONS

In this project, potential applications of a joint operation of solar system with a traditional thermal power station was investigated. In this regard, both CSP and PV systems were applied to a CFPP (i.e., a case study of Vales Point Power plant) in NSW. As illustrated in the literature review, PTC and SPT are two potential CSP types (considering maturity and technical specifications) suitable for integration with CFPP. Therefore, after a detailed investigation of the thermodynamic Rankine cycle of the power plant, the application of these two CSP technologies was simulated. The detailed allocation of the PV farm was also accomplished. SAM software was employed because of its detailed and valid models for the planning task of renewable energy. Moreover, accurate financial models of SAM are another superior feature of this software which are capable of providing a realistic estimation of the required investment cost. Results obtained from three scenarios shows that both CSP technologies (i.e., PTC and SPT) show high potential for being integrated with NSW CFPP. Results show that the total investment cost of power tower technology is higher than that of parabolic trough technology (i.e., around 20%), while its energy production is 84% higher than PTC. An expected 5% emission reduction is highly promising for such a large CFPP like Vales Point station. Moreover, steam temperature and pressure provided by both technologies seem to be suitable for them to be integrated at defined points of the Rankine cycle. In addition, a comparison of the estimated undiscounted payback periods for PTC and SPT shows that solar tower technology can highly benefit the CFPP operator for around 15 years after the first 10 years (i.e., payback period) with a small operating cost. In the case of the PV farm, the obtained results show that a 30 MW system with a battery storage capacity of 6 MWh is appropriate for a reserve task. Comparison of the investment cost of the PV system with the CSP technology of similar size demonstrated that the CSP system can be more suitable for the hybrid system since the existence of the CFPP power block may cut costs through utilisation of the existing turbine. However, including electrical battery units in the PV system as a reserve unit can provide a very fast response for CFPP and prevent generation variations because of load demand changes. Finally, integration of power tower CSP and a PV farm with a total capacity of 130 MW seems to be highly

promising in NSW as it has the potential to cut approximate 6% of power plant emissions per year. Table 42 summarises the results obtained from the three considered scenarios.

TABLE 42. COMPARISON OF SCENARIOS

Technology	Max capacity [MW]	Investment [\$]	Emission reduction [t CO <sub>2eq</sub> /year]	Annual energy production [kWh]	Saving from energy production [\$]	Payback period [year, undiscounted]
PTC	100	331,552,000	200,773.88 [3%]	233,458,000	20,675,040	16.03
SPT	100	394,107,000	369,745.82 [5%]	429,937,000	37,834,456	10.42
PV	30	43,440,600	31,681.62 [0.88 %]	36,839,100	3,262,461	13.35

The recommended practice is the joint operation of CSP and PV technologies integrated with CFPP. In this regard, two options are available based on the type of CSP (i.e., PTC or SPT). Since the technologies are independent, simultaneous adoption of both CSP and PV can be obtained by a direct summation of benefits provided by these individual systems. Table 43 shows the two possible options of the recommended practice. In the case of payback period, as noted in Table 42, this period is not the same for both technologies. Therefore, the worst case for both options is around 16 years for the joint PCT and PV technologies. It is expected to provide a profit of \$ 225,224,892 for PTC+PV and a profit of \$ 606,666,372 for SPT+PV after the payback period when the system reaches 25 years of service.

TABLE 43. RECOMMENDED JOINT PV-CSP PRACTICE

Technology	Max capacity [MW]	Investment [\$]	Emission reduction [t CO <sub>2eq</sub> /year]	Annual energy production [kWh]	Average yearly energy price [\$/MWh]	Saving from energy production [\$]	Percentage of saving [%]
PTC+PV	130	374,992,600	232,455.5	270,297,100	88.56	23,937,501	3.31%
SPT+PV	130	437,547,600	401,427.44	466,776,100	88.56	41,096,917	5.72%

It is worth mentioning that the current proposed 100 MW capacity for CSPs is around 7.57% of the total capacity of Vales Point power plant (i.e., 1,320 MW), due to the practical site constraints of Vales Point. In fact, this value can be the maximum emission reduction possible for a system with 100% efficiency, which is not feasible in practice. Therefore, considering the low operation efficiency of solar thermal units, the current results are highly promising for the joint operation of CFPP and CSP units. One of the reasons for such an efficiency increase is that the high-temperature steam provided by CSP systems is directly fed

into the power block of Vales Point instead of feeding it into a separate turbine or being stored in thermal tanks. Additionally, this approach cuts several losses of traditional CSP power plants. For example, during the hours in which the temperature of the steam provided by CSP systems is higher or lower than the range of normal operation for a standalone CSP system, this steam can still be valuable for the joint operation of Vales Point power plant (either for high-pressure turbine if the temperature is very high or for preheating if the temperature is very low).

In terms of cost, based on the report issued by the International Renewable Energy Agency (IRENA) [18], the current cost of CSP systems is around \$ 4,930/kW to \$ 9,800/kW, depending on the project location and storage duration. The results of this study show that the current cost of CSP systems is less than \$ 4,000/kW while having up to 10 hours of storage units (i.e., currently, the thermal storage system is considered as a major part of investment costs). Not having a separate electric power block for CSP systems could provide a significant reduction in the total capital cost.

Finally, one solution to reaching a higher emission reduction is to increase the capacity of the CSP plant. However, it should be noted that the typical size for a single CSP power plant located in a place with the yearly solar irradiation in the range of 2,000-2,300 kWh/m<sup>2</sup>/year is around 100 MW considering several other meteorological factors, although the yearly solar irradiation is lower than 2,000 kWh/m<sup>2</sup>/year for the location of Vales Point CFPP. It means that, since the number and specifications of mirrors as well as size and specifications of receivers are optimised for this amount of radiation, an increase in the number of mirrors or size of the solar receiver cannot offer a linear increase in the amount of CSP steam provision (or reaching higher temperatures). Moreover, a higher number of receivers in solar farms results in a higher steam temperature, which may not be necessary based on the required specifications of the CFPP turbine. In other words, it is not efficient to have bigger sizes of the CSP plant having the current available methodological situation. In this regard, as an applicable solution, the generation system planner may need to construct several identical CSP systems with the same capital cost to obtain more steam and subsequently, a higher amount of emission reduction. Basically, it is the same approach adopted in several large-scale CSP power plants in the world in which instead of establishing one very large CSP system,

several identical optimised scale CSP units in the form of a solar power plant are constructed. This approach prevents hardships related to the design of huge receiver systems as well.



## References

- [1] D. T. Ton and W. P. Wang, "A more resilient grid: The U.S. department of energy joins with stakeholders in an R&D plan," *IEEE Power and Energy Magazine*, vol. 13, no. 3, pp. 26-34, 2015.
- [2] M. J. Ghadi, A. Rajabi, S. Ghavidel, A. Azizivahed, L. Li, and J. Zhang, "From active distribution systems to decentralized microgrids: a review on regulations and planning approaches based on operational factors," *Applied Energy*, vol. 253, p. 113543, 2019.
- [3] Corporate Finance Institute. Levelized Cost of Energy (LCOE) [Online]. Available: <https://corporatefinanceinstitute.com/resources/knowledge/finance/levelized-cost-of-energy-lcoe/>
- [4] U.S. Energy Information Administration. Levelized cost and levelized avoided cost of new generation resources in the annual energy outlook 2019 [Online]. Available: [https://www.eia.gov/outlooks/aeo/pdf/electricity\\_generation.pdf](https://www.eia.gov/outlooks/aeo/pdf/electricity_generation.pdf)
- [5] M. J. Ghadi, S. Ghavidel, A. Rajabi, A. Azizivahed, L. Li, and J. Zhang, "A review on economic and technical operation of active distribution systems," *Renewable and Sustainable Energy Reviews*, vol. 104, pp. 38-53, 2019.
- [6] Department of the Environment and Energy, Australian Energy Statistics. Table O - Electricity generation by fuel type 2017-18 and 2018 [Online]. Available: <https://www.energy.gov.au/publications/australian-energy-statistics-table-o-electricity-generation-fuel-type-2017-18-and-2018>
- [7] W. Li, *Risk assessment of power systems: Models, methods, and applications*. John Wiley & Sons, 2014.
- [8] Department of Industry, Science, Energy and Resources, Australian Government. Quarterly update of Australia's national greenhouse gas inventory for March 2019 [Online]. Available: <http://www.environment.gov.au/climate-change/climate-science-data/greenhouse-gas-measurement/publications/quarterly-update-australias-nggi-mar-2019>
- [9] X. Liu, M. Shahidehpour, Z. Li, X. Liu, Y. Cao, and Z. Bie, "Microgrids for enhancing the power grid resilience in extreme conditions," *IEEE Transactions on Smart Grid*, vol. 8, no. 2, pp. 589-597, 2017.
- [10] R. Neches and A. M. Madni, "Towards affordably adaptable and effective systems," *Systems Engineering*, vol. 16, no. 2, pp. 224-234, 2013.
- [11] C. S. Holling, "Resilience and stability of ecological systems," *Annual review of ecology and systematics*, vol. 4, no. 1, pp. 1-23, 1973.
- [12] C. Folke, "Resilience: The emergence of a perspective for social-ecological systems analyses," *Global environmental change*, vol. 16, no. 3, pp. 253-267, 2006.
- [13] L. Seeliger and I. Turok, "Towards sustainable cities: Extending resilience with insights from vulnerability and transition theory," *Sustainability*, vol. 5, no. 5, pp. 2108-2128, 2013.
- [14] M. Panteli and P. Mancarella, "The grid: Stronger bigger smarter?: Presenting a conceptual framework of power system resilience," *IEEE Power Energy Mag*, vol. 13, no. 3, pp. 58-66, 2015.
- [15] M. Van der Hoeven and D. Houssin, "Energy technology perspectives 2015: Mobilising innovation to accelerate climate action," *International Energy Agency: Paris, France*, 2015.
- [16] M. T. Islam, N. Huda, A. Abdullah, and R. Saidur, "A comprehensive review of state-of-the-art concentrating solar power (CSP) technologies: Current status and research trends," *Renewable and Sustainable Energy Reviews*, vol. 91, pp. 987-1018, 2018.
- [17] H. Müller-Steinhagen and F. Trieb, "Concentrating solar power," *A review of the technology. Ingenia Inform QR Acad Eng*, vol. 18, pp. 43-50, 2004.
- [18] International Renewable Energy Agency (IRENA), "Renewable power generation costs in 2018," *Report, International Renewable Energy Agency, Abu Dhabi*, 2018.
- [19] F. Santos-Alamillos, D. Pozo-Vázquez, J. Ruiz-Arias, L. Von Bremen, and J. Tovar-Pescador, "Combining wind farms with concentrating solar plants to provide stable renewable power," *Renewable Energy*, vol. 76, pp. 539-550, 2015.
- [20] T. M. Pavlović, I. S. Radonjić, D. D. Milosavljević, and L. S. Pantić, "A review of concentrating solar power plants in the world and their potential use in Serbia," *Renewable and Sustainable Energy Reviews*, vol. 16, no. 6, pp. 3891-3902, 2012.
- [21] A. Ummadisingu and M. Soni, "Concentrating solar power-technology, potential and policy in India," *Renewable and sustainable energy reviews*, vol. 15, no. 9, pp. 5169-5175, 2011.
- [22] First Green Consulting Private Limited. Comparison of CSP technologies [Online]. Available: <https://firstgreenconsulting.wordpress.com/2012/06/04/comparison-of-csp-technologies/comparison-of-csp-technologies/>

- [23] M. Z. A. Ab Kadir, Y. Rafeeu, and N. M. Adam, "Prospective scenarios for the full solar energy development in Malaysia," *Renewable and Sustainable Energy Reviews*, vol. 14, no. 9, pp. 3023-3031, 2010.
- [24] A. Sharma, "A comprehensive study of solar power in India and World," *Renewable and Sustainable Energy Reviews*, vol. 15, no. 4, pp. 1767-1776, 2011.
- [25] K. Kaygusuz, "Prospect of concentrating solar power in Turkey: the sustainable future," *Renewable and Sustainable Energy Reviews*, vol. 15, no. 1, pp. 808-814, 2011.
- [26] A. Poullikkas, G. Kourtis, and I. Hadjipaschalis, "Parametric analysis for the installation of solar dish technologies in Mediterranean regions," *Renewable and Sustainable Energy Reviews*, vol. 14, no. 9, pp. 2772-2783, 2010.
- [27] F. Cavallaro, "Multi-criteria decision aid to assess concentrated solar thermal technologies," *Renewable Energy*, vol. 34, no. 7, pp. 1678-1685, 2009.
- [28] S. A. Kalogirou, "Solar thermal collectors and applications," *Progress in energy and combustion science*, vol. 30, no. 3, pp. 231-295, 2004.
- [29] K. Lovegrove *et al.*, "Paraboloidal dish solar concentrators for multi-megawatt power generation," in *Proceedings of ISES*, 2003, pp. 14-19.
- [30] R. Affandi, C. K. Gan, A. Ghani, and M. Ruddin, "Performance comparison for parabolic dish concentrating solar power in high level DNI locations with George Town, Malaysia," in *Applied Mechanics and Materials*, 2015, vol. 699, pp. 570-576: Trans Tech Publ.
- [31] O. Behar, A. Khellaf, and K. Mohammedi, "A review of studies on central receiver solar thermal power plants," *Renewable and sustainable energy reviews*, vol. 23, pp. 12-39, 2013.
- [32] A. Mohamad, J. Orfi, and H. Alansary, "Heat losses from parabolic trough solar collectors," *International journal of energy research*, vol. 38, no. 1, pp. 20-28, 2014.
- [33] A. Fernández-García, E. Zarza, L. Valenzuela, and M. Pérez, "Parabolic-trough solar collectors and their applications," *Renewable and Sustainable Energy Reviews*, vol. 14, no. 7, pp. 1695-1721, 2010.
- [34] G. Manzolini, A. Giotri, C. Saccolotto, P. Silva, and E. Macchi, "Development of an innovative code for the design of thermodynamic solar power plants part A: Code description and test case," *Renewable Energy*, vol. 36, no. 7, pp. 1993-2003, 2011.
- [35] G. Machinda, S. Chowdhury, R. Arscott, S. Chowdhury, and S. Kibaara, "Concentrating solar thermal power technologies: A review," in *India Conference (INDICON), 2011 Annual IEEE*, 2011, pp. 1-6: IEEE.
- [36] J. D. Nixon, P. K. Dey, and P. A. Davies, "Which is the best solar thermal collection technology for electricity generation in north-west India? Evaluation of options using the analytical hierarchy process," *Energy*, vol. 35, no. 12, pp. 5230-5240, 2010.
- [37] S. Alexopoulos and B. Hoffschmidt, "Solar tower power plant in Germany and future perspectives of the development of the technology in Greece and Cyprus," *Renewable Energy*, vol. 35, no. 7, pp. 1352-1356, 2010.
- [38] A. Gottschalk and U. Ramamoorthi, "Parametric simulation and economic estimation of thermal energy storage in solar power tower," *Materials Today: Proceedings*, vol. 5, no. 1, Part 1, pp. 1571-1577, 2018.
- [39] Y. Luo, T. Lu, and X. Du, "Novel optimization design strategy for solar power tower plants," *Energy Conversion and Management*, vol. 177, pp. 682-692, 2018.
- [40] R. Chen, Z. Rao, and S. Liao, "Determination of key parameters for sizing the heliostat field and thermal energy storage in solar tower power plants," *Energy Conversion and Management*, vol. 177, pp. 385-394, 2018.
- [41] G. Manente, S. Rech, and A. Lazzaretto, "Optimum choice and placement of concentrating solar power technologies in integrated solar combined cycle systems," *Renewable Energy*, vol. 96, pp. 172-189, 2016.
- [42] N. El Gharbi, H. Derbal, S. Bouaichaoui, and N. Said, "A comparative study between parabolic trough collector and linear Fresnel reflector technologies," *Energy Procedia*, vol. 6, pp. 565-572, 2011.
- [43] H. Zhang, J. Baeyens, J. Degrève, and G. Cacères, "Concentrated solar power plants: review and design methodology," *Renewable and sustainable energy reviews*, vol. 22, pp. 466-481, 2013.
- [44] M. J. Ghadi, L. Li, J. Zhang, L. Chen, Q. Huang, "A Review on the development of concentrated solar power and its Integration in coal-fired power plants," presented at the 11th Asia-Pacific Power and Energy Engineering Conference, China, 2019.
- [45] A. W. Dowling, T. Zheng, and V. M. Zavala, "Economic assessment of concentrated solar power technologies: A review," *Renewable and Sustainable Energy Reviews*, vol. 72, pp. 1019-1032, 2017.
- [46] P. Zhou, R. Y. Jin, and L. W. Fan, "Reliability and economic evaluation of power system with renewables: A review," *Renewable and Sustainable Energy Reviews*, vol. 58, pp. 537-547, 2016.
- [47] M. Cooper, "Renewable and distributed resources in a post-Paris low carbon future: The key role and political

- economy of sustainable electricity," *Energy Research & Social Science*, vol. 19, pp. 66-93, 2016.
- [48] L. Bretschger, M. Meulemann, and A. Stünzi, "Climate policy based on the paris agreement," in *Reference Module in Earth Systems and Environmental Sciences*: Elsevier, 2018.
- [49] G. J. Nathan *et al.*, "Solar thermal hybrids for combustion power plant: A growing opportunity," *Progress in Energy and Combustion Science*, vol. 64, pp. 4-28, 2018.
- [50] R. Mena, R. Escobar, Á. Lorca, M. Negrete-Pincetic, and D. Olivares, "The impact of concentrated solar power in electric power systems: A Chilean case study," *Applied Energy*, vol. 235, pp. 258-283, 2019.
- [51] B. Belgasim, Y. Aldali, M. J. R. Abdunnabi, G. Hashem, and K. Hossin, "The potential of concentrating solar power (CSP) for electricity generation in Libya," *Renewable and Sustainable Energy Reviews*, vol. 90, pp. 1-15, 2018.
- [52] R. Ling-zhi, Z. Xin-gang, Z. Yu-zhuo, and L. Yan-bin, "The economic performance of concentrated solar power industry in China," *Journal of Cleaner Production*, vol. 205, pp. 799-813, 2018.
- [53] O. Ogunmodimu and E. C. Okoroigwe, "Concentrating solar power technologies for solar thermal grid electricity in Nigeria: A review," *Renewable and Sustainable Energy Reviews*, vol. 90, pp. 104-119, 2018.
- [54] A. Ummadisingu and M. S. Soni, "Concentrating solar power – Technology, potential and policy in India," *Renewable and Sustainable Energy Reviews*, vol. 15, no. 9, pp. 5169-5175, 2011.
- [55] A. Kumar, O. Prakash, and A. Dube, "A review on progress of concentrated solar power in India," *Renewable and Sustainable Energy Reviews*, vol. 79, pp. 304-307, 2017.
- [56] W. Zhang, "Concentrating solar power—State of the art, cost analysis and pre-feasibility study for the implementation in China," *Diplomado Energía y Medio ambiente II. Universität Stuttgart Institut für energiewirtschaft und rationelle energianwendung*, 2009.
- [57] J. Zou, "Review of concentrating solar thermal power industry in China: Status quo, problems, trend and countermeasures," in *IOP Conference Series: Earth and Environmental Science*, 2018, vol. 108, no. 5, p. 052119: IOP Publishing.
- [58] S. Gorjian and B. Ghobadian, "Solar thermal power plants: progress and prospects in Iran," *Energy Procedia*, vol. 75, pp. 533-539, 2015.
- [59] C. Murphy, Y. Sun, W. J. Cole, G. J. Maclaurin, M. S. Mehos, and C. S. Turchi, "The potential role of concentrating solar power within the context of DOE's 2030 solar cost targets," National Renewable Energy Laboratory, Golden, CO (United States), 2019.
- [60] P. Kurup and C. Turchi, "Initial investigation into the potential of CSP industrial process heat for the southwest united states," NREL/TP-6A20-64709, National Renewable Energy Laboratory, 2015.
- [61] G. San Miguel and B. Corona, "Economic viability of concentrated solar power under different regulatory frameworks in Spain," *Renewable and Sustainable Energy Reviews*, vol. 91, pp. 205-218, 2018.
- [62] S. W. Channon and P. C. Eames, "The cost of balancing a parabolic trough concentrated solar power plant in the Spanish electricity spot markets," *Solar Energy*, vol. 110, pp. 83-95, 2014.
- [63] K. Lovegrove, M. Watt, R. Passey, G. Pollock, and J. Wyder, *Realising the Potential of Concentrating Solar Power in Australia: Summary for Stakeholders*. Australian Solar Institute Pty, Limited, 2012.
- [64] M. Panteli, D. N. Trakas, P. Mancarella, and N. D. Hatziargyriou, "Boosting the power grid resilience to extreme weather events using defensive islanding," *IEEE Transactions on Smart Grid*, vol. 7, no. 6, pp. 2913-2922, 2016.
- [65] Y. Xu, C.-C. Liu, K. P. Schneider, F. K. Tuffner, and D. T. Ton, "Microgrids for service restoration to critical load in a resilient distribution system," *IEEE Transactions on Smart Grid*, vol. 9, no. 1, pp. 426-437, 2016.
- [66] B. Simon, C. Coffrin, and P. Van Hentenryck, "Randomized adaptive vehicle decomposition for large-scale power restoration," in *Lecture Notes in Computer Science (including subseries Lecture Notes in Artificial Intelligence and Lecture Notes in Bioinformatics)* vol. 7298 LNCS, ed, 2012, pp. 379-394.
- [67] The National Renewable Energy Laboratory. Concentrating solar power projects in Australia, [Online]. Available: <https://solarpaces.nrel.gov/by-country/AU>
- [68] C. A. Pan and F. Dinter, "Combination of PV and central receiver CSP plants for base load power generation in South Africa," *Solar Energy*, vol. 146, pp. 379-388, 2017.
- [69] R. Bravo and D. Friedrich, "Two-stage optimisation of hybrid solar power plants," *Solar Energy*, vol. 164, pp. 187-199, 2018.
- [70] P. del Río, C. Peñasco, and P. Mir-Artigues, "An overview of drivers and barriers to concentrated solar power in the European Union," *Renewable and Sustainable Energy Reviews*, vol. 81, pp. 1019-1029, 2018.
- [71] R. Figueiredo, P. Nunes, M. Meireles, M. Madaleno, and M. C. Brito, "Replacing coal-fired power plants by photovoltaics in the Portuguese electricity system," *Journal of Cleaner Production*, 2019.
- [72] M. Mehos, C. Turchi, J. Jorgenson, P. Denholm, C. Ho, and K. Armijo, "On the path to SunShot-advancing

- concentrating solar power technology, performance, and dispatchability," EERE Publication and Product Library, 2016.
- [73] J. H. Peterseim, S. White, A. Tadros, and U. Hellwig, "Concentrated solar power hybrid plants, which technologies are best suited for hybridisation?," *Renewable Energy*, vol. 57, pp. 520-532, 2013.
- [74] K. M. Powell, K. Rashid, K. Ellingwood, J. Tuttle, and B. D. Iverson, "Hybrid concentrated solar thermal power systems: A review," *Renewable and Sustainable Energy Reviews*, vol. 80, pp. 215-237, 2017.
- [75] M. T. Islam, N. Huda, A. B. Abdullah, and R. Saidur, "A comprehensive review of state-of-the-art concentrating solar power (CSP) technologies: Current status and research trends," *Renewable and Sustainable Energy Reviews*, vol. 91, pp. 987-1018, 2018.
- [76] S. Pramanik and R. V. Ravikrishna, "A review of concentrated solar power hybrid technologies," *Applied Thermal Engineering*, vol. 127, pp. 602-637, 2017.
- [77] J. H. Peterseim, S. White, A. Tadros, and U. Hellwig, "Concentrating solar power hybrid plants – Enabling cost effective synergies," *Renewable Energy*, vol. 67, pp. 178-185, 2014.
- [78] O. Behar, "Solar thermal power plants – A review of configurations and performance comparison," *Renewable and Sustainable Energy Reviews*, vol. 92, pp. 608-627, 2018.
- [79] G. Năstase, A. Șerban, G. Dragomir, A. I. Brezeanu, and I. Bucur, "Photovoltaic development in Romania. Reviewing what has been done," *Renewable and Sustainable Energy Reviews*, vol. 94, pp. 523-535, 2018.
- [80] Y. Li, Q. Zhang, G. Wang, B. McLellan, X. F. Liu, and L. Wang, "A review of photovoltaic poverty alleviation projects in China: Current status, challenge and policy recommendations," *Renewable and Sustainable Energy Reviews*, vol. 94, pp. 214-223, 2018.
- [81] M. Lee, "Economic feasibility analysis and policy implication for photovoltaic system at cohousing in KOREA," *Renewable Energy*, 2018.
- [82] E. Rosales-Asensio, M. de Simón-Martín, D. Borge-Diez, A. Pérez-Hoyos, and A. Comenar Santos, "An expert judgement approach to determine measures to remove institutional barriers and economic non-market failures that restrict photovoltaic self-consumption deployment in Spain," *Solar Energy*, vol. 180, pp. 307-323, 2019.
- [83] S. Martín-Martínez, M. Cañas-Carretón, A. Honrubia-Escribano, and E. Gómez-Lázaro, "Performance evaluation of large solar photovoltaic power plants in Spain," *Energy Conversion and Management*, vol. 183, pp. 515-528, 2019.
- [84] K. Janda, "Slovak electricity market and the price merit order effect of photovoltaics," *Energy Policy*, vol. 122, pp. 551-562, 2018.
- [85] D. D. d. S. Carstens and S. K. d. Cunha, "Challenges and opportunities for the growth of solar photovoltaic energy in Brazil," *Energy Policy*, vol. 125, pp. 396-404, 2019.
- [86] A. Ferreira *et al.*, "Economic overview of the use and production of photovoltaic solar energy in Brazil," *Renewable and Sustainable Energy Reviews*, vol. 81, pp. 181-191, 2018.
- [87] J. Khoury, R. Mbayed, G. Salloum, E. Monmasson, and J. Guerrero, "Review on the integration of photovoltaic renewable energy in developing countries—Special attention to the Lebanese case," *Renewable and Sustainable Energy Reviews*, vol. 57, pp. 562-575, 2016.
- [88] C. Brunet, O. Savadogo, P. Baptiste, and M. A. Bouchard, "Shedding some light on photovoltaic solar energy in Africa – A literature review," *Renewable and Sustainable Energy Reviews*, vol. 96, pp. 325-342, 2018.
- [89] A. Abubakar Mas'ud *et al.*, "A review on the recent progress made on solar photovoltaic in selected countries of sub-Saharan Africa," *Renewable and Sustainable Energy Reviews*, vol. 62, pp. 441-452, 2016.
- [90] S. Seme, K. Sredenšek, B. Štumberger, and M. Hadžiselimović, "Analysis of the performance of photovoltaic systems in Slovenia," *Solar Energy*, vol. 180, pp. 550-558, 2019.
- [91] P. A. Basore and W. J. Cole, "Comparing supply and demand models for future photovoltaic power generation in the USA," *Progress in Photovoltaics: Research and Applications*, vol. 26, no. 6, pp. 414-418, 2018.
- [92] A. Bahadori and C. Nwaoha, "A review on solar energy utilisation in Australia," *Renewable and Sustainable Energy Reviews*, vol. 18, pp. 1-5, 2013.
- [93] A. J. Chapman, B. McLellan, and T. Tezuka, "Residential solar PV policy: An analysis of impacts, successes and failures in the Australian case," *Renewable energy*, vol. 86, pp. 1265-1279, 2016.
- [94] M. Yu and A. Halog, "Solar photovoltaic development in Australia—a life cycle sustainability assessment study," *Sustainability*, vol. 7, no. 2, pp. 1213-1247, 2015.
- [95] U. Desideri and P. E. Campana, "Analysis and comparison between a concentrating solar and a photovoltaic power plant," *Applied Energy*, vol. 113, pp. 422-433, 2014.
- [96] F. Magrassi, E. Rocco, S. Barberis, M. Gallo, and A. Del Borghi, "Hybrid solar power system versus

- photovoltaic plant: A comparative analysis through a life cycle approach," *Renewable Energy*, vol. 130, pp. 290-304, 2019.
- [97] A. Borisova and D. Popov, "An option for the integration of solar photovoltaics into small nuclear power plant with thermal energy storage," *Sustainable Energy Technologies and Assessments*, vol. 18, pp. 119-126, 2016.
- [98] S. Sadeghi and I. B. Askari, "Prefeasibility techno-economic assessment of a hybrid power plant with photovoltaic, fuel cell and Compressed Air Energy Storage (CAES)," *Energy*, vol. 168, pp. 409-424, 2019.
- [99] B. Ming, P. Liu, L. Cheng, Y. Zhou, and X. Wang, "Optimal daily generation scheduling of large hydro-photovoltaic hybrid power plants," *Energy Conversion and Management*, vol. 171, pp. 528-540, 2018.
- [100] Z. Yang, P. Liu, L. Cheng, H. Wang, B. Ming, and W. Gong, "Deriving operating rules for a large-scale hydro-photovoltaic power system using implicit stochastic optimization," *Journal of Cleaner Production*, vol. 195, pp. 562-572, 2018.
- [101] A. Beluco, P. Kroeff de Souza, and A. Krenzinger, "A method to evaluate the effect of complementarity in time between hydro and solar energy on the performance of hybrid hydro PV generating plants," *Renewable Energy*, vol. 45, pp. 24-30, 2012.
- [102] W. Fang, Q. Huang, S. Huang, J. Yang, E. Meng, and Y. Li, "Optimal sizing of utility-scale photovoltaic power generation complementarily operating with hydropower: A case study of the world's largest hydro-photovoltaic plant," *Energy Conversion and Management*, vol. 136, pp. 161-172, 2017.
- [103] A. Woyte and S. Goy, "Large grid-connected photovoltaic power plants: Best practices for the design and operation of large photovoltaic power plants," in *The Performance of Photovoltaic (PV) Systems*, N. Pearsall, Ed.: Woodhead Publishing, pp. 321-337, 2017.
- [104] R. Zhai, J. Qi, Y. Zhu, M. Zhao, and Y. Yang, "Novel system integrations of 1000MW coal-fired power plant retrofitted with solar energy and CO<sub>2</sub> capture system," *Applied Thermal Engineering*, vol. 125, pp. 1133-1145, 2017.
- [105] S. Suojanen, E. Hakkarainen, M. Tähtinen, and T. Sihvonen, "Modeling and analysis of process configurations for hybrid concentrated solar power and conventional steam power plants," *Energy Conversion and Management*, vol. 134, pp. 327-339, 2017.
- [106] Y. Yang, Q. Yan, R. Zhai, A. Kouzani, and E. Hu, "An efficient way to use medium-or-low temperature solar heat for power generation – integration into conventional power plant," *Applied Thermal Engineering*, vol. 31, no. 2, pp. 157-162, 2011.
- [107] Y. Zhao, H. Hong, and H. Jin, "Mid and low-temperature solar-coal hybridization mechanism and validation," *Energy*, vol. 74, pp. 78-87, 2014.
- [108] Y. Zhao, H. Hong, and H. Jin, "Appropriate feed-in tariff of solar-coal hybrid power plant for China's Inner Mongolia Region," *Applied Thermal Engineering*, vol. 108, pp. 378-387, 2016.
- [109] J. Wu, H. Hou, Y. Yang, and E. Hu, "Annual performance of a solar aided coal-fired power generation system (SACPG) with various solar field areas and thermal energy storage capacity," *Applied Energy*, vol. 157, pp. 123-133, 2015.
- [110] J. Li, X. Yu, J. Wang, and S. Huang, "Coupling performance analysis of a solar aided coal-fired power plant," *Applied Thermal Engineering*, vol. 106, pp. 613-624, 2016.
- [111] A. Narimani, A. Abeygunawardana, G. Nourbakhsh, G. F. Ledwich, and G. R. Walker, "Comparing operational value of CSP with TES to PV with battery storage in Australian national electricity market," in *2017 Australasian Universities Power Engineering Conference (AUPEC)*, 2017, pp. 1-5: IEEE.
- [112] C. Li, R. Zhai, Y. Yang, K. Patchigolla, J. E. Oakey, and P. Turner, "Annual performance analysis and optimization of a solar tower aided coal-fired power plant," *Applied Energy*, vol. 237, pp. 440-456, 2019.
- [113] J. Wu, H. Hou, and Y. Yang, "Annual economic performance of a solar-aided 600MW coal-fired power generation system under different tracking modes, aperture areas, and storage capacities," *Applied Thermal Engineering*, vol. 104, pp. 319-332, 2016.
- [114] S. J. Mills, "Integrating intermittent renewable energy technologies with coal-fired power plant," *CCC/189. London: IEA Clean Coal Centre*, 2011.
- [115] Q. Yan, E. Hu, Y. Yang, and R. Zhai, "Evaluation of solar aided thermal power generation with various power plants," *International Journal of Energy Research*, vol. 35, no. 10, pp. 909-922, 2011.
- [116] D. Renné, "Resource assessment and site selection for solar heating and cooling systems," in *Advances in Solar Heating and Cooling*: Elsevier, 2016, pp. 13-41.
- [117] S. Wilcox and W. Marion, *Users manual for TMY3 data sets*. National Renewable Energy Laboratory, Golden, CO, 2008.
- [118] N. Blair *et al.*, "System advisor model, SAM 2014.1.14: General description," National Renewable Energy

- Laboratory, Golden, CO (United States), 2014.
- [119] W. Short, D. J. Packey, and T. Holt, "A manual for the economic evaluation of energy efficiency and renewable energy technologies," National Renewable Energy Laboratory, Golden, CO (United States), 1995.
- [120] P. Gilman, N. Blair, M. Mehos, C. Christensen, S. Janzou, and C. Cameron, "Solar advisor model user guide for version 2.0," National Renewable Energy Laboratory, Golden, CO (United States), 2008.

## Appendices

### Appendix A:

#### List of publication:

- [1] M. J. Ghadi, L. Li, J. Zhang, L. Chen, Q. Huang, and C. Li, "A Review on the Development of Concentrated Solar Power and its Integration in Coal-Fired Power Plants," in *2019 IEEE Innovative Smart Grid Technologies-Asia (ISGT Asia)*, 2019, pp. 1106-1111: IEEE.

#### List of all staff that have been engaged on the Project:

Name	Position in the project	Affiliation
Mr. Peter Loneragan	Research Engagement Manager	University Technology Sydney
A/Prof. Jiangfeng (Jeff) Zhang	Chief Investigator	Previously with University Technology Sydney, and now with Clemson University
A/Prof. Li Li	Chief Investigator	University Technology Sydney
Mr. Mojtaba Jabbari Ghadi	Research Assistant	University Technology Sydney

### Appendix B:

In the appendix B, a list of investment options along with their corresponding configurations for PV-battery, parabolic trough CSP-thermal storage and central power CSP-thermal storage obtained in Section 8 are attached to this report.

**Sign off**

I, the undersigned, being a person duly authorised by the Grantee, certify that:

- (a) the above information is true and complete;
- (b) the expenditure of the Funding received to date has been used solely on the Project; and
- (c) there is no matter or circumstances of which I am aware that would constitute a breach by the Grantee or, if applicable the End Recipient and Subcontractors', of any term of the Funding Deed.

Signature: 

Position: Associate Professor

School of Electrical and Data Engineering

Faculty of Engineering and IT

University of Technology Sydney

Name: Li Li

Date: 04/09/2020



## Appendix B1: Solutions for PV-battery configuration

### Pareto solutions for LCOE-Emission objective

Battery type	Battery bank size (kWh)	Battery bank power (kW)	Inverter Type	Module type	Desired size (kWdc)	Annual energy (kWh)	Total Cost (\$)	LCOE (cents/kWh)	Emission (M ton)
Lithium Ion: NMC	2,000	1,000	ABB: TRIO-20.0	Sunpower X22-480-COM	23,600	24,004,900	27,727,900	12.6025	20,380.73645
Lead Acid: VRLA AGM	2,000	1,000	ABB: TRIO-20.0	Sunpower X22-480-COM	23,600	23,933,600	27,723,600	12.6375	20,319.78057
Lithium Ion: NMC	2,000	1,000	Advanced Energy Industries	Sunpower X22-480-COM	23,600	24,134,500	27,732,800	12.5384	20,490.81468
Flow Battery: Vanadium	2,000	1,000	Advanced Energy Industries	Sunpower X22-480-COM	23,600	24,134,400	27,734,600	12.539	20,490.72968
Lithium Ion: NMC	2,000	1,000	ABB: TRIO-20.0	Hansol HS415UE-AN1	23,600	24,440,900	27,755,300	12.3945	20,751.35609
Lithium Ion: NMC	2,000	1,000	AEG Power Solutions	Hansol HS415UE-AN1	23,600	24,314,900	27,747,700	12.4542	20,643.89067
Lithium Ion: NMC	2,000	1,000	Advanced Energy Industries	Hansol HS415UE-AN1	23,600	24,554,900	27,758,300	12.3395	20,848.16488
Flow Battery: Vanadium	2,000	1,000	Advanced Energy Industries	Hansol HS415UE-AN1	23,600	24,554,800	27,760,200	12.3401	20,848.07988
Lithium Ion: NMC	2,000	1,000	ABB: TRIO-20.0	Solaria XT-440C-PD	23,600	24,189,300	27,739,000	12.5134	20,537.48997
Lithium Ion: NMC	2,000	1,000	AEG Power Solutions	Solaria XT-440C-PD	23,600	24,040,800	27,732,200	12.5862	20,410.89029
Lead Acid: VRLA AGM	2,000	1,000	Advanced Energy Industries	Solaria XT-440C-PD	23,600	24,346,500	27,744,800	12.4369	20,671.0299
Lithium Ion: NMC	2,000	1,000	Advanced Energy Industries	Hansol HS415UE-AN1	25,960	27,012,500	30,356,700	12.2953	22,934.74505
Lithium Ion: NMC	2,000	1,000	Advanced Energy Industries	Hansol HS415UE-AN1	30,680	31,921,600	35,545,300	12.2267	27,103.02461
Lithium Ion: NMC	2,000	1,000	Advanced Energy Industries	Hansol HS415UE-AN1	33,040	34,379,200	38,143,700	12.2	29,189.60537
Lead Acid: VRLA AGM	2,000	1,000	Advanced Energy Industries	Hansol HS415UE-AN1	33,040	34,379,500	38,143,700	12.1999	29,189.87448
Lithium Ion: NMC	2,000	1,000	Advanced Energy Industries	Hansol HS415UE-AN1	35,400	36,836,800	40,742,000	12.1768	31,276.18614

### Pareto solutions for LCOE-Cost objective

Lithium Ion: NMC	2,000	1,000	ABB: TRIO-20.0	Sunpower X22-480-COM	23,600	24,004,900	27,727,900	12.6025	20,380.73645
Lead Acid: VRLA AGM	2,000	1,000	ABB: TRIO-20.0	Sunpower X22-480-COM	23,600	24,005,200	27,728,000	12.6023	20,381.00157
Lead Acid: VRLA AGM	2,000	1,000	AEG Power Solutions	Sunpower X22-480-COM	23,600	23,933,600	27,723,600	12.6375	20,319.78057
Lead Acid: VRLA AGM	2,000	1,000	Advanced Energy Industries	Sunpower X22-480-COM	23,600	24,134,800	27,732,800	12.5383	20,491.07988
Lead Acid: VRLA AGM	2,000	1,000	ABB: TRIO-20.0	Hansol HS415UE-AN1	23,600	24,441,200	27,755,300	12.3944	20,751.62129
Lithium Ion: NMC	2,000	1,000	Advanced Energy Industries	Hansol HS415UE-AN1	23,600	24,554,900	27,758,300	12.3395	20,848.16488
Lead Acid: VRLA AGM	2,000	1,000	Advanced Energy Industries	Hansol HS415UE-AN1	23,600	24,555,200	27,758,400	12.3394	20,848.4300
Lead Acid: VRLA AGM	2,000	1,000	ABB: TRIO-20.0	Solaria XT-440C-PD	23,600	24,189,500	27,739,000	12.5132	20,537.67008
Lithium Ion: NMC	2,000	1,000	AEG Power Solutions	Solaria XT-440C-PD	23,600	24,040,800	27,732,200	12.5862	20,410.89029

Lead Acid: VRLA AGM	2,000	1,000	AEG Power Solutions	Solaria XT-440C-PD	23,600	24,041,100	27,732,300	12.586	20,411.15557
Lead Acid: VRLA AGM	2,000	1,000	Advanced Energy Industries	Solaria XT-440C-PD	23,600	24,346,500	27,744,800	12.4369	20,671.02996
Lead Acid: VRLA AGM	2,000	1,000	Advanced Energy Industries	Hansol HS415UE-AN1	25,960	27,012,800	30,356,700	12.2952	22,935.01127
Lead Acid: VRLA AGM	2,000	1,000	Advanced Energy Industries	Hansol HS415UE-AN1	28,320	29,472,100	32,955,200	12.2575	25,023.34100
Lead Acid: VRLA AGM	2,000	1,000	Advanced Energy Industries	Hansol HS415UE-AN1	30,680	31,921,900	35,545,300	12.2265	27,103.29278
Lead Acid: VRLA AGM	2,000	1,000	Advanced Energy Industries	Hansol HS415UE-AN1	33,040	34,379,500	38,143,700	12.1999	29,189.87448
Lithium Ion: NMC	2,000	1,000	Advanced Energy Industries	Hansol HS415UE-AN1	35,400	36,836,800	40,742,000	12.1768	31,276.18614
Lithium Ion: TO	2,000	1,000	Advanced Energy Industries	Hansol HS415UE-AN1	35,400	36,836,800	40,742,000	12.1768	31,276.18614

**Pareto solutions for Emission-Cost objective**

Lithium Ion: NMC	2,000	1,000	Advanced Energy Industries	Hansol HS415UE-AN1	35,400	36,836,800	40,742,000	12.1768	31,276.18614
Flow Battery: Vanadium	2,000	1,000	Advanced Energy Industries	Hansol HS415UE-AN1	33,040	34,379,100	38,145,600	12.2004	29,189.52037
Lithium Ion: TO	2,000	1,000	Advanced Energy Industries	Hansol HS415UE-AN1	30,680	31,921,600	35,545,300	12.2267	27,103.02461
Lithium Ion: TO	2,000	1,000	Advanced Energy Industries	Hansol HS415UE-AN1	28,320	29,471,800	32,955,200	12.2577	25,023.07384
Lead Acid: VRLA AGM	2,000	1,000	Advanced Energy Industries	Hansol HS415UE-AN1	25,960	27,012,800	30,356,700	12.2952	22,935.01127
Flow Battery: Vanadium	2,000	1,000	Advanced Energy Industries	Hansol HS415UE-AN1	23,600	24,554,800	27,760,200	12.3401	20,848.07988

## Appendix B2- Solutions for Parabolic trough configuration

### Pareto solutions for LCOE-Emission objective

Solar multiple	P_ref (MWe)	Tank max heat (MWe)	Thermal storage hours (hr)	HTF type	Receiver Type	LCOE (cents/kWh)	Annual energy (kWh)	Total cost (\$)	Emission (M Ton)
1.7	95	20	6	Caloria HT 43	Solel UVAC 3	14.017	284,059,000	200,958,000	172,823.88
1.7	95	22	6	Caloria HT 43	Solel UVAC 3	14.0177	284,059,000	200,948,000	172,815.28
1.7	95	24	6	Caloria HT 43	Solel UVAC 3	14.0182	284,059,000	200,940,000	172,808.40
1.7	95	26	6	Caloria HT 43	Solel UVAC 3	14.019	284,059,000	200,929,000	172,798.94
1.7	95	28	6	Caloria HT 43	Solel UVAC 3	14.0196	284,059,000	200,920,000	172,791.20
1.7	95	30	6	Caloria HT 43	Solel UVAC 3	14.0202	284,059,000	200,911,000	172,783.46
1.7	80	20	6	Caloria HT 43	Solel UVAC 3	14.0237	238,970,000	169,008,000	145,346.88
1.7	80	22	6	Caloria HT 43	Solel UVAC 3	14.0244	238,970,000	169,000,000	145,340.01
1.7	80	24	6	Caloria HT 43	Solel UVAC 3	14.0249	238,970,000	168,993,000	145,333.98
1.7	80	26	6	Caloria HT 43	Solel UVAC 3	14.0254	238,970,000	168,987,000	145,328.82
1.7	80	28	6	Caloria HT 43	Solel UVAC 3	14.0258	238,970,000	168,982,000	145,324.52
1.7	80	30	6	Caloria HT 43	Solel UVAC 3	14.0263	238,970,000	168,976,000	145,319.36
1.7	80	20	6	Hitec XL	Solel UVAC 3	14.102	238,970,000	168,044,000	144,517.84
1.7	80	22	6	Hitec XL	Solel UVAC 3	14.1028	238,970,000	168,035,000	144,510.10
1.7	80	24	6	Hitec XL	Solel UVAC 3	14.1036	238,970,000	168,025,000	144,501.50
1.7	80	26	6	Hitec XL	Solel UVAC 3	14.1042	238,970,000	168,018,000	144,495.48
1.7	80	28	6	Hitec XL	Solel UVAC 3	14.1047	238,970,000	168,012,000	144,490.32
1.7	80	30	6	Hitec XL	Solel UVAC 3	14.1051	238,970,000	168,008,000	144,486.88
1.65	80	20	6	Caloria HT 43	Solel UVAC 3	14.2257	234,459,000	163,986,000	141,027.96
1.65	80	22	6	Caloria HT 43	Solel UVAC 3	14.2266	234,459,000	163,976,000	141,019.36
1.65	80	24	6	Caloria HT 43	Solel UVAC 3	14.2274	234,459,000	163,966,000	141,010.76
1.65	80	26	6	Caloria HT 43	Solel UVAC 3	14.2282	234,459,000	163,957,000	141,003.02
1.65	80	28	6	Caloria HT 43	Solel UVAC 3	14.2291	234,459,000	163,946,000	140,993.56
1.65	80	30	6	Caloria HT 43	Solel UVAC 3	14.2298	234,459,000	163,938,000	140,986.68
1.65	80	20	6	Hitec XL	Solel UVAC 3	14.3205	234,459,000	162,873,000	140,070.78
1.65	80	22	6	Hitec XL	Solel UVAC 3	14.3213	234,459,000	162,863,000	140,062.18
1.65	80	24	6	Hitec XL	Solel UVAC 3	14.3238	234,459,000	162,833,000	140,036.38
1.65	80	26	6	Hitec XL	Solel UVAC 3	14.3243	234,459,000	162,827,000	140,031.22
1.65	80	28	6	Hitec XL	Solel UVAC 3	14.3249	234,459,000	162,821,000	140,026.06
1.65	80	30	6	Hitec XL	Solel UVAC 3	14.3253	234,459,000	162,816,000	140,021.76
1.6	80	20	6	Caloria HT 43	Solel UVAC 3	14.544	228,444,000	156,969,000	134,993.34
1.6	80	22	6	Caloria HT 43	Solel UVAC 3	14.5448	228,444,000	156,960,000	134,985.60
1.6	80	24	6	Caloria HT 43	Solel UVAC 3	14.5456	228,444,000	156,952,000	134,978.72
1.6	80	26	6	Caloria HT 43	Solel UVAC 3	14.5464	228,444,000	156,943,000	134,970.98
1.6	80	28	6	Caloria HT 43	Solel UVAC 3	14.5471	228,444,000	156,935,000	134,964.10
1.6	80	30	6	Caloria HT 43	Solel UVAC 3	14.5477	228,444,000	156,928,000	134,958.08
1.6	80	22	6	Hitec XL	Solel UVAC 3	14.6284	228,444,000	156,040,000	134,194.40
1.6	80	24	6	Hitec XL	Solel UVAC 3	14.629	228,444,000	156,034,000	134,189.24
1.6	80	20	6	Hitec XL	Solel UVAC 3	14.6291	228,444,000	156,033,000	134,188.38
1.6	80	26	6	Hitec XL	Solel UVAC 3	14.6296	228,444,000	156,028,000	134,184.08
1.6	80	28	6	Hitec XL	Solel UVAC 3	14.6301	228,444,000	156,022,000	134,178.92
1.6	80	30	6	Hitec XL	Solel UVAC 3	14.6305	228,444,000	156,017,000	134,174.62
1.55	80	20	6	Caloria HT 43	Solel UVAC 3	14.8046	223,933,000	151,680,000	130,444.80
1.55	80	22	6	Caloria HT 43	Solel UVAC 3	14.8056	223,933,000	151,669,000	130,435.34
1.55	80	24	6	Caloria HT 43	Solel UVAC 3	14.8067	223,933,000	151,657,000	130,425.02
1.55	80	26	6	Caloria HT 43	Solel UVAC 3	14.8078	223,933,000	151,646,000	130,415.56
1.55	80	28	6	Caloria HT 43	Solel UVAC 3	14.8085	223,933,000	151,639,000	130,409.54
1.55	80	30	6	Caloria HT 43	Solel UVAC 3	14.8092	223,933,000	151,632,000	130,403.52
1.55	80	20	6	Hitec XL	Solel UVAC 3	14.8902	223,933,000	150,786,000	129,675.96
1.55	80	22	6	Hitec XL	Solel UVAC 3	14.8912	223,933,000	150,776,000	129,667.36
1.55	80	24	6	Hitec XL	Solel UVAC 3	14.8918	223,933,000	150,770,000	129,662.20
1.55	80	26	6	Hitec XL	Solel UVAC 3	14.8924	223,933,000	150,764,000	129,657.04
1.55	80	28	6	Hitec XL	Solel UVAC 3	14.893	223,933,000	150,757,000	129,651.02
1.55	80	30	6	Hitec XL	Solel UVAC 3	14.8935	223,933,000	150,752,000	129,646.72
1.5	80	20	6	Caloria HT 43	Solel UVAC 3	15.0551	219,422,000	146,679,000	126,143.94
1.5	80	22	6	Caloria HT 43	Solel UVAC 3	15.0561	219,422,000	146,669,000	126,135.34
1.5	80	24	6	Caloria HT 43	Solel UVAC 3	15.0573	219,422,000	146,657,000	126,125.02
1.5	80	26	6	Caloria HT 43	Solel UVAC 3	15.0585	219,422,000	146,645,000	126,114.70
1.5	80	28	6	Caloria HT 43	Solel UVAC 3	15.0591	219,422,000	146,639,000	126,109.54
1.5	80	30	6	Caloria HT 43	Solel UVAC 3	15.0594	219,422,000	146,636,000	126,106.96
1.5	80	20	6	Hitec XL	Solel UVAC 3	15.1394	219,422,000	145,842,000	125,424.12
1.5	80	22	6	Hitec XL	Solel UVAC 3	15.1402	219,422,000	145,834,000	125,417.24
1.5	80	24	6	Hitec XL	Solel UVAC 3	15.1409	219,422,000	145,827,000	125,411.22
1.5	80	26	6	Hitec XL	Solel UVAC 3	15.1415	219,422,000	145,821,000	125,406.06
1.5	80	28	6	Hitec XL	Solel UVAC 3	15.142	219,422,000	145,817,000	125,402.62
1.5	80	30	6	Hitec XL	Solel UVAC 3	15.1424	219,422,000	145,813,000	125,399.18
1.45	80	20	6	Caloria HT 43	Solel UVAC 3	15.318	214,911,000	141,728,000	121,886.08
1.45	80	22	6	Caloria HT 43	Solel UVAC 3	15.3192	214,911,000	141,717,000	121,876.62

1.45	80	24	6	Caloria HT 43	Solel UVAC 3	15.3193	214,911,000	141,716,000	121,875.76
1.45	80	26	6	Caloria HT 43	Solel UVAC 3	15.32	214,911,000	141,708,000	121,868.88
1.45	80	28	6	Caloria HT 43	Solel UVAC 3	15.3207	214,911,000	141,702,000	121,863.72
1.45	80	30	6	Caloria HT 43	Solel UVAC 3	15.3214	214,911,000	141,696,000	121,858.56
1.45	80	20	6	Hitec XL	Solel UVAC 3	15.4024	214,911,000	140,932,000	121,201.52
1.45	80	22	6	Hitec XL	Solel UVAC 3	15.4032	214,911,000	140,925,000	121,195.50
1.45	80	24	6	Hitec XL	Solel UVAC 3	15.4039	214,911,000	140,919,000	121,190.34
1.45	80	26	6	Hitec XL	Solel UVAC 3	15.4044	214,911,000	140,914,000	121,186.04
1.45	80	28	6	Hitec XL	Solel UVAC 3	15.4048	214,911,000	140,910,000	121,182.60
1.45	80	30	6	Hitec XL	Solel UVAC 3	15.4051	214,911,000	140,907,000	121,180.02
1.4	80	20	6	Caloria HT 43	Solel UVAC 3	15.7214	208,897,000	134,925,000	116,035.50
1.4	80	22	6	Caloria HT 43	Solel UVAC 3	15.7222	208,897,000	134,918,000	116,029.48
1.4	80	24	6	Caloria HT 43	Solel UVAC 3	15.723	208,897,000	134,911,000	116,023.46
1.4	80	26	6	Caloria HT 43	Solel UVAC 3	15.7238	208,897,000	134,904,000	116,017.44
1.4	80	30	6	Caloria HT 43	Solel UVAC 3	15.7241	208,897,000	134,901,000	116,014.86
1.4	80	28	6	Caloria HT 43	Solel UVAC 3	15.7244	208,897,000	134,898,000	116,012.28
1.4	80	20	6	Hitec XL	Solel UVAC 3	15.8005	208,897,000	134,233,000	115,440.38
1.4	80	22	6	Hitec XL	Solel UVAC 3	15.8009	208,897,000	134,230,000	115,437.80
1.4	80	24	6	Hitec XL	Solel UVAC 3	15.8018	208,897,000	134,223,000	115,431.78
1.4	80	26	6	Hitec XL	Solel UVAC 3	15.8023	208,897,000	134,218,000	115,427.48
1.4	80	28	6	Hitec XL	Solel UVAC 3	15.8025	208,897,000	134,216,000	115,425.76
1.35	80	20	6	Caloria HT 43	Solel UVAC 3	16.0518	204,386,000	129,822,000	111,646.92
1.35	80	22	6	Caloria HT 43	Solel UVAC 3	16.053	204,386,000	129,812,000	111,638.32
1.35	80	24	6	Caloria HT 43	Solel UVAC 3	16.0537	204,386,000	129,806,000	111,633.16
1.35	80	26	6	Caloria HT 43	Solel UVAC 3	16.0545	204,386,000	129,799,000	111,627.14
1.35	80	28	6	Caloria HT 43	Solel UVAC 3	16.0552	204,386,000	129,794,000	111,622.84
1.35	80	30	6	Caloria HT 43	Solel UVAC 3	16.0557	204,386,000	129,790,000	111,619.40
1.35	80	20	6	Hitec XL	Solel UVAC 3	16.1145	204,386,000	129,305,000	111,202.30
1.35	80	22	6	Hitec XL	Solel UVAC 3	16.1153	204,386,000	129,299,000	111,197.14
1.3	80	22	6	Caloria HT 43	Solel UVAC 3	16.4135	199,875,000	124,686,000	107,229.96
1.3	80	20	6	Caloria HT 43	Solel UVAC 3	16.4138	199,875,000	124,684,000	107,228.24
1.3	80	24	6	Caloria HT 43	Solel UVAC 3	16.4141	199,875,000	124,681,000	107,225.66
1.3	80	28	6	Caloria HT 43	Solel UVAC 3	16.4144	199,875,000	124,679,000	107,223.94
1.3	80	30	6	Caloria HT 43	Solel UVAC 3	16.4148	199,875,000	124,676,000	107,221.36
1.3	80	20	6	Hitec XL	Solel UVAC 3	16.4675	199,875,000	124,268,000	106,870.48
1.3	80	22	6	Hitec XL	Solel UVAC 3	16.4682	199,875,000	124,262,000	106,865.32
1.3	80	24	6	Hitec XL	Solel UVAC 3	16.4688	199,875,000	124,258,000	106,861.88
1.3	80	28	6	Hitec XL	Solel UVAC 3	16.469	199,875,000	124,256,000	106,860.16
1.3	80	26	6	Hitec XL	Solel UVAC 3	16.4692	199,875,000	124,255,000	106,859.30
1.25	80	20	6	Caloria HT 43	Solel UVAC 3	16.7776	195,364,000	119,759,000	102,992.74
1.25	80	22	6	Caloria HT 43	Solel UVAC 3	16.7785	195,364,000	119,752,000	102,986.72
1.25	80	24	6	Caloria HT 43	Solel UVAC 3	16.7793	195,364,000	119,746,000	102,981.56
1.25	80	26	6	Caloria HT 43	Solel UVAC 3	16.7801	195,364,000	119,741,000	102,977.26
1.25	80	28	6	Caloria HT 43	Solel UVAC 3	16.7804	195,364,000	119,738,000	102,974.68
1.25	80	20	6	Hitec XL	Solel UVAC 3	16.8177	195,364,000	119,467,000	102,741.62
1.25	80	22	6	Hitec XL	Solel UVAC 3	16.8183	195,364,000	119,462,000	102,737.32
1.2	80	20	6	Caloria HT 43	Solel UVAC 3	17.2921	189,349,000	113,324,000	97,458.64
1.2	80	22	6	Caloria HT 43	Solel UVAC 3	17.293	189,349,000	113,318,000	97,453.48
1.2	80	24	6	Caloria HT 43	Solel UVAC 3	17.2939	189,349,000	113,313,000	97,449.18
1.2	80	26	6	Caloria HT 43	Solel UVAC 3	17.2944	189,349,000	113,309,000	97,445.74
1.2	80	28	6	Caloria HT 43	Solel UVAC 3	17.2946	189,349,000	113,308,000	97,444.88
1.2	80	20	6	Hitec XL	Solel UVAC 3	17.2953	189,349,000	113,303,000	97,440.58
1.2	80	22	6	Hitec XL	Solel UVAC 3	17.2954	189,349,000	113,302,000	97,439.72
1.2	80	20	8	Hitec XL	Solel UVAC 3	18.9974	213,370,000	113,095,000	97,261.70
1.2	80	22	8	Hitec XL	Solel UVAC 3	18.9976	213,370,000	113,094,000	97,260.84
1.2	80	20	8	Caloria HT 43	Solel UVAC 3	19.0078	213,370,000	113,032,000	97,207.52
1.2	80	22	8	Caloria HT 43	Solel UVAC 3	19.0085	213,370,000	113,028,000	97,204.08
1.2	80	24	8	Caloria HT 43	Solel UVAC 3	19.0094	213,370,000	113,023,000	97,199.78
1.2	80	26	8	Caloria HT 43	Solel UVAC 3	19.0104	213,370,000	113,017,000	97,194.62
1.2	80	28	8	Caloria HT 43	Solel UVAC 3	19.0106	213,370,000	113,016,000	97,193.76
1.5	80	20	6	Therminol VP-1	Solel UVAC 3	19.7478	219,422,000	111,174,000	95,609.64
1.5	80	22	6	Therminol VP-1	Solel UVAC 3	19.7483	219,422,000	111,171,000	95,607.06
1.5	80	24	6	Therminol VP-1	Solel UVAC 3	19.7485	219,422,000	111,170,000	95,606.20
1.5	80	26	6	Therminol VP-1	Solel UVAC 3	19.7488	219,422,000	111,168,000	95,604.48
1.5	80	28	6	Therminol VP-1	Solel UVAC 3	19.749	219,422,000	111,167,000	95,603.62
1.5	80	30	6	Therminol VP-1	Solel UVAC 3	19.7492	219,422,000	111,166,000	95,602.76
1.45	80	20	6	Therminol VP-1	Solel UVAC 3	20.1302	214,911,000	107,228,000	92,216.08
1.45	80	22	6	Therminol VP-1	Solel UVAC 3	20.1304	214,911,000	107,227,000	92,215.22
1.4	80	20	6	Therminol VP-1	Solel UVAC 3	20.6911	208,897,000	101,942,000	87,670.12
1.4	80	24	6	Therminol VP-1	Solel UVAC 3	20.6913	208,897,000	101,941,000	87,669.26
1.35	80	20	6	Therminol VP-1	Solel UVAC 3	21.1278	204,386,000	98,089,000	84,357.23
1.3	80	20	6	Therminol VP-1	Solel UVAC 3	21.6411	199,875,000	94,055,700	80,887.90
1.25	80	20	6	Therminol VP-1	Solel UVAC 3	22.1531	195,364,000	90,217,300	77,586.88
1.2	80	20	6	Therminol VP-1	Solel UVAC 3	22.9651	189,349,000	84,883,000	72,999.38
1.2	80	22	6	Therminol VP-1	Solel UVAC 3	22.9654	189,349,000	84,882,000	72,998.52

1.2	80	24	6	Therminol VP-1	Solel UVAC 3	22.9657	189,349,000	84,880,900	72,997.57
1.2	80	26	6	Therminol VP-1	Solel UVAC 3	22.9658	189,349,000	84,880,300	72,997.06
1.2	80	28	6	Therminol VP-1	Solel UVAC 3	22.966	189,349,000	84,879,700	72,996.54
1.2	80	30	6	Therminol VP-1	Solel UVAC 3	22.9661	189,349,000	84,879,500	72,996.37
1.2	80	20	8	Therminol VP-1	Solel UVAC 3	25.2691	213,370,000	84,618,700	72,772.08
1.2	80	22	8	Therminol VP-1	Solel UVAC 3	25.2694	213,370,000	84,617,700	72,771.22
1.2	80	24	8	Therminol VP-1	Solel UVAC 3	25.2698	213,370,000	84,616,100	72,769.85
1.2	80	26	8	Therminol VP-1	Solel UVAC 3	25.2702	213,370,000	84,615,000	72,768.90
1.2	80	28	8	Therminol VP-1	Solel UVAC 3	25.2703	213,370,000	84,614,600	72,768.56
1.2	80	20	10	Therminol VP-1	Solel UVAC 3	27.5877	237,391,000	84,353,700	72,544.18
1.2	80	22	10	Therminol VP-1	Solel UVAC 3	27.5882	237,391,000	84,352,100	72,542.81
1.2	80	26	10	Therminol VP-1	Solel UVAC 3	27.5889	237,391,000	84,349,900	72,540.91
1.2	80	24	10	Therminol VP-1	Solel UVAC 3	27.589	237,391,000	84,349,800	72,540.83
1.2	80	28	10	Therminol VP-1	Solel UVAC 3	27.5892	237,391,000	84,348,900	72,540.05
1.2	80	30	10	Therminol VP-1	Schott PTR80	27.5892	237,391,000	84,348,900	72,540.05

**Pareto solutions for LCOE-Cost objective**

Solar multiple	P_ref (MWe)	Tank max heat (MWe)	Thermal storage hours (hr)	HTF type	Receiver Type	LCOE (cents/kWh)	Annual energy (kWh)	Total cost (\$)	Emission (M Ton)
1.7	95	20	6	Caloria HT 43	Solel UVAC 3	14.017	284,059,000	200,958,000	172,823.88
1.7	80	20	6	Caloria HT 43	Solel UVAC 3	14.0237	238,970,000	169,008,000	145,346.88
1.65	80	20	6	Caloria HT 43	Solel UVAC 3	14.2257	234,459,000	163,986,000	141,027.96
1.6	80	20	6	Caloria HT 43	Solel UVAC 3	14.544	228,444,000	156,969,000	134,993.34
1.55	80	20	6	Caloria HT 43	Solel UVAC 3	14.8046	223,933,000	151,680,000	130,444.80
1.5	80	20	6	Caloria HT 43	Solel UVAC 3	15.0551	219,422,000	146,679,000	126,143.94
1.45	80	20	6	Caloria HT 43	Solel UVAC 3	15.318	214,911,000	141,728,000	121,886.08
1.4	80	20	6	Caloria HT 43	Solel UVAC 3	15.7214	208,897,000	134,925,000	116,035.50
1.35	80	20	6	Caloria HT 43	Solel UVAC 3	16.0518	204,386,000	129,822,000	111,646.92
1.3	80	22	6	Caloria HT 43	Solel UVAC 3	16.4135	199,875,000	124,686,000	107,229.96
1.25	80	20	6	Caloria HT 43	Solel UVAC 3	16.7776	195,364,000	119,759,000	102,992.74
1.2	80	20	6	Caloria HT 43	Solel UVAC 3	17.2921	189,349,000	113,324,000	97,458.64
1.2	80	20	6	Caloria HT 43	Schott PTR80	17.2921	189,349,000	113,324,000	97,458.64

**Pareto solutions for Emission-Cost objective**

Solar multiple	P_ref (MWe)	Tank max heat (MWe)	Thermal storage hours (hr)	HTF type	Receiver Type	LCOE (cents/kWh)	Annual energy (kWh)	Total cost (\$)	Emission (M Ton)
1.2	80	22	6	Therminol VP-1	Solel UVAC 3	17.2954	189,349,000	113,302,000	97,439.72
1.25	80	22	6	Therminol VP-1	Solel UVAC 3	16.8183	195,364,000	119,462,000	102,737.32
1.3	80	20	6	Caloria HT 43	Solel UVAC 3	16.4138	199,875,000	124,684,000	107,228.24
1.35	80	20	6	Caloria HT 43	Schott PTR80	16.0518	204,386,000	129,822,000	111,646.92
1.4	80	28	6	Therminol VP-1	Solel UVAC 3	15.8025	208,897,000	134,216,000	115,425.76
1.45	80	30	6	Therminol VP-1	Solel UVAC 3	15.4051	214,911,000	140,907,000	121,180.02
1.5	80	30	6	Therminol VP-1	Solel UVAC 3	15.1424	219,422,000	145,813,000	125,399.18
1.55	80	28	6	Caloria HT 43	Solel UVAC 3	14.8085	223,933,000	151,639,000	130,409.54
1.6	80	30	6	Therminol VP-1	Solel UVAC 3	14.6305	228,444,000	156,017,000	134,174.62
1.65	80	20	6	Caloria HT 43	Schott PTR80	14.2257	234,459,000	163,986,000	141,027.96
1.7	80	28	6	Caloria HT 43	Schott PTR80	14.0258	238,970,000	168,982,000	145,324.52
1.65	85	20	6	Caloria HT 43	Solel UVAC 3	14.2974	247,985,000	172,702,000	148,523.72
1.7	85	20	6	Caloria HT 43	Solel UVAC 3	14.0264	254,000,000	179,590,000	154,447.40
1.65	90	22	6	Caloria HT 43	Schott PTR80	14.2821	263,015,000	183,312,000	157,648.32
1.7	90	30	6	Caloria HT 43	Solel UVAC 3	14.0283	269,029,000	190,178,000	163,553.08
1.65	95	20	6	Caloria HT 43	Schott PTR80	14.2581	278,044,000	194,066,000	166,896.76
1.7	95	24	6	Caloria HT 43	Schott PTR80	14.0182	284,059,000	200,940,000	172,808.40
1.65	100	22	6	Caloria HT 43	Solel UVAC 3	14.2384	293,074,000	204,795,000	176,123.70
1.7	100	20	6	Caloria HT 43	Solel UVAC 3	14.0204	299,089,000	211,527,000	181,913.22
1.65	105	20	6	Caloria HT 43	Schott PTR80	14.3329	306,600,000	212,945,000	183,132.70
1.7	105	24	6	Caloria HT 43	Solel UVAC 3	14.1219	312,614,000	219,650,000	188,899.00
1.65	110	20	6	Caloria HT 43	Solel UVAC 3	14.2972	321,629,000	223,900,000	192,554.00
1.65	111	22	6	Caloria HT 43	Schott PTR80	14.3427	324,034,000	224,907,000	193,420.02
1.7	110	22	6	Caloria HT 43	Schott PTR80	14.0938	327,644,000	230,662,000	198,369.32
1.7	111	30	6	Caloria HT 43	Schott PTR80	14.0865	331,552,000	233,415,000	200,736.90

## Appendix B3- Solutions for Power tower configuration

### Pareto solutions for LCOE-Emission objective

Solar multiple	P_ref (MWe)	Hot tank max heat (MWe)	Thermal storage hours (hours)	HTF type	LCOE (cents/kWh)	Annual energy (kWh)	Total cost (\$)	Emission (M Ton)
2.2	110	20	6	Salt (60% NaNo3)	11.1491	424,805,000	380,155,000	365,332.30
2.2	105	20	6	Salt (60% NaNo3)	11.1511	406,006,000	363,535,000	349,165.16
2.2	100	20	6	Salt (60% NaNo3)	11.1707	387,580,000	348,070,000	333,318.80
2.2	95	20	6	Salt (60% NaNo3)	11.2182	367,073,000	331,222,000	315,682.78
2.2	90	20	6	Salt (60% NaNo3)	11.2538	345,917,000	312,960,000	297,488.62
2.2	85	20	6	Salt (60% NaNo3)	11.3132	327,138,000	298,156,000	281,338.68
2.2	80	20	6	Salt (60% NaNo3)	11.332	308,798,000	282,278,000	265,566.28
2.1	80	20	6	Salt (60% NaNo3)	11.467	296,001,000	271,570,000	254,560.86
2	80	20	6	Salt (60% NaNo3)	11.6985	281,599,000	261,491,000	242,175.14
1.95	80	20	6	Salt (60% NaNo3)	11.8199	274,002,000	255,860,000	235,641.72
1.9	80	20	6	Salt (60% NaNo3)	11.9656	266,940,000	251,397,000	229,568.40
1.85	80	20	6	Salt (60% NaNo3)	12.105	260,149,000	246,872,000	223,728.14
1.8	80	20	6	Salt (60% NaNo3)	12.3143	250,646,000	240,586,000	215,555.56
1.75	80	20	6	Salt (60% NaNo3)	12.4723	244,472,000	236,848,000	210,245.92
1.7	80	20	6	Salt (60% NaNo3)	12.6677	236,251,000	231,169,000	203,175.86
1.7	80	20	8	Salt (60% NaNo3)	13.0925	235,766,000	241,317,000	202,758.76
1.75	80	20	6	Salt (46.5% Lift)	13.3103	228,551,000	236,848,000	196,553.86
1.7	80	20	6	Salt (46.5% Lift)	13.525	220,770,000	231,169,000	189,862.20
1.7	80	20	8	Salt (46.5% Lift)	13.9695	220,481,000	241,317,000	189,613.66
1.7	80	20	10	Salt (46.5% Lift)	14.4135	220,216,000	251,464,000	189,385.76
1.7	80	30	10	Salt (46.5% Lift)	14.4135	220,216,000	251,464,000	189,385.76

### Pareto solutions for LCOE-Cost objective

Solar multiple	P_ref (MWe)	Hot tank max heat (MWe)	Thermal storage hours (hours)	HTF type	LCOE (cents/kWh)	Annual energy (kWh)	Total cost (\$)	Emission (M Ton)
2.2	110	20	6	Salt (60% NaNo3)	11.1491	424,805,000	380,155,000	365,332.30
2.2	105	20	6	Salt (60% NaNo3)	11.1511	406,006,000	363,535,000	349,165.16
2.2	100	20	6	Salt (60% NaNo3)	11.1707	387,580,000	348,070,000	333,318.80
2.2	95	20	6	Salt (60% NaNo3)	11.2182	367,073,000	331,222,000	315,682.78
2.2	90	20	6	Salt (60% NaNo3)	11.2538	345,917,000	312,960,000	297,488.62
2.2	85	20	6	Salt (60% NaNo3)	11.3132	327,138,000	298,156,000	281,338.68
2.2	80	20	6	Salt (60% NaNo3)	11.332	308,798,000	282,278,000	265,566.28
2.1	80	20	6	Salt (60% NaNo3)	11.467	296,001,000	271,570,000	254,560.86
2	80	20	6	Salt (60% NaNo3)	11.6985	281,599,000	261,491,000	242,175.14
1.95	80	20	6	Salt (60% NaNo3)	11.8199	274,002,000	255,860,000	235,641.72
1.9	80	20	6	Salt (60% NaNo3)	11.9656	266,940,000	251,397,000	229,568.40
1.85	80	20	6	Salt (60% NaNo3)	12.105	260,149,000	246,872,000	223,728.14
1.8	80	20	6	Salt (60% NaNo3)	12.3143	250,646,000	240,586,000	215,555.56
1.75	80	20	6	Salt (60% NaNo3)	12.4723	244,472,000	236,848,000	210,245.92
1.7	80	20	6	Salt (60% NaNo3)	12.6677	236,251,000	231,169,000	203,175.86
1.7	80	30	6	Salt (60% NaNo3)	12.6677	236,251,000	231,169,000	203,175.86

### Pareto solutions for Emission-Cost objective

Solar multiple	P_ref (MWe)	Hot tank max heat (MWe)	Thermal storage hours (hours)	HTF type	LCOE (cents/kWh)	Annual energy (kWh)	Total cost (\$)	Emission (M Ton)
1.7	80	20	6	Salt (60% NaNo3)	12.6677	236,251,000	231,169,000	203,175.86
1.75	80	20	6	Salt (60% NaNo3)	12.4723	244,472,000	236,848,000	210,245.92

1.7	85	20	6	Salt (60% NaNo3)	12.6109	250,160,000	242,981,000	215,137.60
1.85	80	26	6	Salt (60% NaNo3)	12.105	260,149,000	246,872,000	223,728.14
1.9	80	20	6	Salt (60% NaNo3)	11.9656	266,940,000	251,397,000	229,568.40
1.8	85	22	6	Salt (60% NaNo3)	12.224	267,985,000	255,180,000	230,467.10
1.95	80	20	6	Salt (60% NaNo3)	11.8199	274,002,000	255,860,000	235,641.72
1.85	85	20	6	Salt (60% NaNo3)	12.081	275,150,000	260,034,000	236,629.00
1.7	95	20	6	Salt (60% NaNo3)	12.4995	280,414,000	269,330,000	241,156.04
1.9	85	22	6	Salt (60% NaNo3)	11.8989	283,972,000	265,525,000	244,215.92
1.8	90	28	6	Salt (60% NaNo3)	12.1777	283,992,000	269,107,000	244,233.12
1.95	85	26	6	Salt (60% NaNo3)	11.7975	290,635,000	270,572,000	249,946.10
2.1	80	26	6	Salt (60% NaNo3)	11.467	296,001,000	271,570,000	254,560.86
2	85	28	6	Salt (60% NaNo3)	11.625	301,247,000	277,957,000	259,072.42
2.2	80	26	6	Salt (60% NaNo3)	11.332	308,798,000	282,278,000	265,566.28
2.1	85	30	6	Salt (60% NaNo3)	11.4213	315,615,000	288,338,000	271,428.90
1.9	95	22	6	Salt (60% NaNo3)	11.8319	317,237,000	294,343,000	272,823.82
2.2	85	28	6	Salt (60% NaNo3)	11.3132	327,138,000	298,156,000	281,338.68
2.1	90	24	6	Salt (60% NaNo3)	11.435	330,740,000	301,742,000	284,436.40
2	95	20	6	Salt (60% NaNo3)	11.5656	335,328,000	306,919,000	288,382.08
2.2	90	24	6	Salt (60% NaNo3)	11.2538	345,917,000	312,960,000	297,488.62
2	100	20	6	Salt (60% NaNo3)	11.5295	352,399,000	321,032,000	303,063.14
1.95	105	22	6	Salt (60% NaNo3)	11.617	360,800,000	329,491,000	310,288.00
2.2	95	20	6	Salt (60% NaNo3)	11.2182	367,073,000	331,222,000	315,682.78
2.1	100	26	6	Salt (60% NaNo3)	11.3397	371,616,000	336,383,000	319,589.76
1.95	110	20	6	Salt (60% NaNo3)	11.5868	378,341,000	344,403,000	325,373.26
2.2	100	22	6	Salt (60% NaNo3)	11.1707	387,580,000	348,070,000	333,318.80
2.1	105	30	6	Salt (60% NaNo3)	11.2829	389,202,000	349,675,000	334,713.72
2	110	20	6	Salt (60% NaNo3)	11.4423	389,615,000	351,875,000	335,068.90
2.2	100	20	8	Salt (60% NaNo3)	11.3439	392,225,000	360,754,000	337,313.50
2.2	105	22	6	Salt (60% NaNo3)	11.1511	406,006,000	363,535,000	349,165.16
2.1	110	28	6	Salt (60% NaNo3)	11.2495	408,216,000	365,437,000	351,065.76
2.2	105	24	8	Salt (60% NaNo3)	11.3267	410,819,000	376,853,000	353,304.34
2.2	110	30	6	Salt (60% NaNo3)	11.1491	424,805,000	380,155,000	365,332.30
2.2	110	30	8	Salt (60% NaNo3)	11.3226	429,937,000	394,107,000	369,745.82